CHALMERS
UNIVERSITY OF TECHNOLOGY

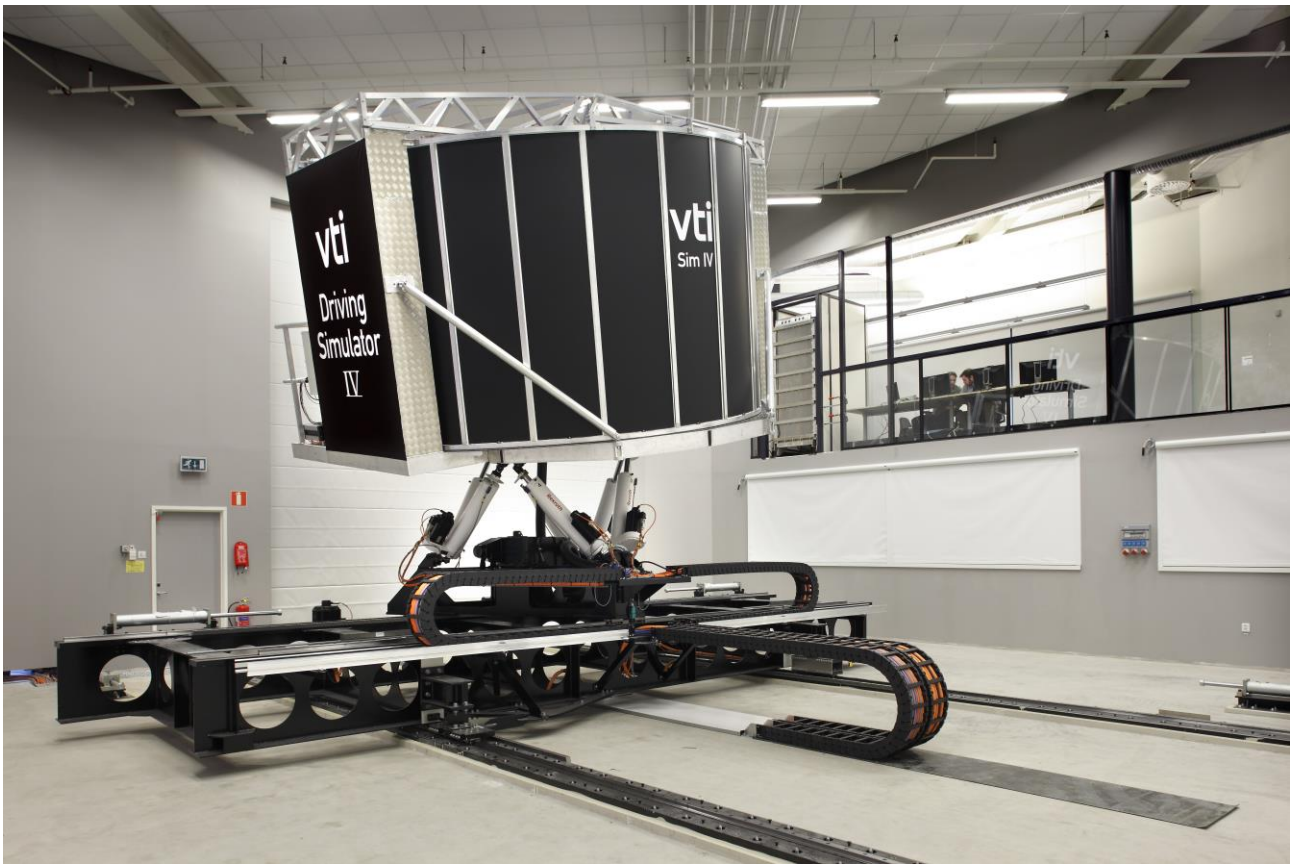

A truck dynamics model for driving simulators

Master's thesis in Automotive Engineering

STEFANO SEDRAN

Department of Applied Mechanics
CHALMERS UNIVERSITY OF TECHNOLOGY
Gothenburg, Sweden 2016

MASTER'S THESIS IN AUTOMOTIVE ENGINEERING

A truck dynamics model for driving simulators

STEFANO SEDRAN

Department of Applied Mechanics
Division of Vehicle Engineering and Autonomous Systems
Vehicle Dynamics group
CHALMERS UNIVERSITY OF TECHNOLOGY
Göteborg, Sweden 2016

A truck dynamics model for driving simulators

STEFANO SEDRAN

Master's Thesis 2016:07
ISSN 1652-8557
Department of Applied Mechanics
Division of Vehicle Engineering and Autonomous Systems
Vehicle Dynamics group
Chalmers University of Technology
SE-412 96 Göteborg
Sweden
Telephone: + 46 (0)31-772 1000

Cover:
View of VTI´s driving simulator Sim IV, located in Göteborg, Sweden.

Name of the printers / Department of Applied Mechanics
Göteborg, Sweden 2016-03-11

A truck dynamics model for driving simulators

Master's thesis in Automotive Engineering

STEFANO SEDRAN
Department of Applied Mechanics
Division of Vehicle Engineering and Autonomous Systems
Vehicle Dynamics group
Chalmers University of Technology

Abstract

Driving simulators provide important opportunities to study interaction between the drivers and vehicle in a wide variety of situations and scenarios. A vehicle dynamics model in the simulator calculates the motion of the simulated vehicle based on the inputs of the driver, in real time. The Swedish National Road and Transport Research Institute (VTI) has a need for an open and in-house developed truck model for its driving simulators. Currently, the truck dynamics models used so far were developed, operated and owned by an OEM. This has obvious restrictions for its use and publicity. This thesis presents the development of a truck dynamics model to be used in the VTI's driving simulators, keeping the OEM model as a reference.

The aim of this project is the development of an open model, with a high level of readability and flexibility for future understanding, modification and use. The model is written in the programming language Modelica in the software Dymola. The chosen strategy is using basic code, even though a library structure is designed. The thesis objective is to investigate the required level of detail for the modelling of trucks for driving simulators. An A-double combination is selected, focusing on the context of normal driving at almost constant speed on dry road. The model complexity is gradually increased, focusing, in each step, on what is believed to be the main contributing phenomena to the trajectory of the vehicle.

The model validation consists of two parts. At first, desktop simulations aim at comparing each step of the developed model with the OEM model, using an ISO lane change maneuver. The importance of roll steer, torsional flexibility of the tractor chassis frame, axle dynamics, friction in the fifth wheel, nonlinearity of tyres is investigated. Afterwards, a further comparison is carried out by performing experiments in the VTI's driving simulator with a few test drivers.

Key words:

Truck vehicle dynamics, A-double, driving simulators, real-time simulations, Modelica, open model.

Contents

Preface

This thesis was performed from September 2015 to March 2016 at the VTI's Göteborg office, within an Erasmus+ programme at the Chalmers University of Technology from the Polytechnic University of Turin. At first, I would like to thank the three institutions for giving me the opportunity to have this experience. It was hard for some aspects, but it gave great results both in terms of thesis work and of personal development. I have also realised how beautiful Sweden and Göteborg are, which made me take the decision to move here.

A huge thank you goes to my thesis supervisor, Fredrik Bruzelius, for his great help and everyday support. Without all the time spent, his suggestions, opinions and guidance, this thesis would not been the same. Finally, his friendliness and confidence in me made the work much more pleasant.

Many gratitudes go to my thesis examiner Bengt Jacobson, for all his time that he spent for his guidance and for providing comments and ideas. I felt that I have received valuable feedbacks throughout my thesis work.

I also acknowledge my thesis examiner from my home university, Nicola Amati.

I highly appreciate the inputs provided by the VTI's researcher Sogol Kharrazi, by Peter Sundström from Modelon AB and by Niklas Fröjd from Volvo Global Trucks Technology.

Many thanks to Bruno Augusto for his availability, for his friendship and positivity and to all VTI's employees. I received a warm welcome and I felt everyday the quiet and friendly environment of the office. Working with them was a great experience.

I also would like to acknowledge the people who participated to the simulator experiment: Georg Tschan, Pär Pettersson, Leo Laine, Niklas Fröjd, Bengt Jacobson, Ivo Batkovic and Björn Persson Mattsson.

Special thanks go to the friends from Vagnhallen CrossFit, who always give their best in sharing this passion.

I also remember all my friends in Italy and in other countries and the new friends met here. They make life more colourful.

Finally, my biggest thanks go the closest people to me. My family, who gave me the biggest support and love. I particularly remember the Christmas holidays spent together. And thanks, Gema, for your infinite help, for believing in me and for the wonderful moments spent together. You gave an amazing light to the whole experience.

Göteborg, March 2016-03-11

STEFANO SEDRAN

Notations

Roman upper case letters

A	Frontal area of a unit
A_{piston}	Area of power piston surface
C	Cornering stiffness of a tyre
C_0	Cornering coefficient of a tyre
C_d	Drag coefficient
C_F	Front cornering stiffness
C_R	Sum of rear cornering stiffnesses
E_r	Roll steer coefficient of steered axle
F_{aero}	Aerodynamic drag
$F_{damp,L}$	Force of left damper of an axle
$F_{damp,R}$	Force of right damper of an axle
$F_{spring,L}$	Force of left spring of an axle
$F_{spring,R}$	Force of right spring of an axle
F_{static}	Static force of a spring
$F_{x,axle}$	Longitudinal force of an axle
$F_{x,axles}$	Longitudinal force from all axles
$F_{x,cab}$	Longitudinal force from cabin
$F_{x,ext}$	External longitudinal force
$F_{x,F}$	Longitudinal force from front articulation joint
$F_{x,j}$	Longitudinal force at cabin-chassis joint
$F_{x,R}$	Longitudinal force from rear articulation joint
$F_{x,tyre}$	Longitudinal force of a tyre
$F_{x,tyreL}$	Longitudinal force of a left tyre
$F_{x,tyreR}$	Longitudinal force of a right tyre
$F_{y,axle}$	Lateral force of an axle
$F_{y,axles}$	Lateral force from all axles
$F_{y,cab}$	Lateral force from cabin
$F_{y,ext}$	External lateral force
$F_{y,F}$	Lateral force from front articulation joint
$F_{y,j}$	Lateral force at cabin-chassis joint
$F_{y,R}$	Lateral force from rear articulation joint
$F_{y,tyre}$	Longitudinal force of a tyre
$F_{y,tyreL}$	Lateral force of a left tyre
$F_{y,tyreR}$	Lateral force of a right tyre
$F_{z,axle}$	Vertical force of an axle
$F_{z,axles}$	Vertical force from all axles
$F_{z,cab}$	Vertical force from cabin
$F_{z,ext}$	External vertical force
$F_{z,F}$	Vertical force from front articulation joint
$F_{z,j}$	Vertical force at cabin-chassis joint
$F_{z,R}$	Vertical force from rear articulation joint
$F_{z,static,tyre}$	Vertical static force of a tyre
$F_{z,tyre}$	Vertical force of a tyre
$F_{z,tyreL}$	Vertical force of a left tyre
$F_{z,tyreR}$	Vertical force of a right tyre
I_x	Roll inertia of a unit
$I_{x,axle}$	Roll inertia of an axle
$I_{x,cab}$	Roll inertia of cabin
I_y	Pitch inertia of a unit
$I_{y,cab}$	Pitch inertia of cabin
I_z	Yaw inertia of a unit
$I_{z,cab}$	Yaw inertia of cabin
L	Distance from front axle to middle point between rear axles
L_F	Distance of front reference point for chassis frame torsion to chassis centre of gravity
L_R	Distance of rear reference point for chassis frame torsion to chassis centre of gravity
L_{tot}	Distance between reference points for chassis frame torsion
M_{damp}	Linear damping torque in
$M_{z,j}$	Yaw moment at cabin-chassis

	fifth wheel
M_{fr}	Dry friction torque in fifth wheel
M_{Fx}	Fraction of kingpin torque due to longitudinal forces
M_{Fy}	Fraction of kingpin torque due to lateral forces
M_{Fz}	Fraction of kingpin torque due to vertical forces
M_{KP}	Kingpin torque
M_{Mz}	Fraction of kingpin torque due to aligning torques
M_{stab}	Moment of stabiliser of an axle
$M_{st,wheel}$	Steering wheel torque
M_{wheel}	Torque at one wheel
$M_{x,axle}$	Roll moment of an axle
$M_{x,axles}$	Roll moment from all axles
$M_{x,cab}$	Roll moment from cabin
$M_{x,ext}$	External roll moment
$M_{x,F}$	Roll moment from front articulation joint
$M_{x,j}$	Roll moment at cabin-chassis joint
$M_{x,R}$	Roll moment from rear articulation joint
$M_{y,axle}$	Pitch moment of an axle
$M_{y,axles}$	Pitch moment from all axles
$M_{y,cab}$	Pitch moment from cabin
$M_{y,ext}$	External pitch moment
$M_{y,F}$	Pitch moment from front articulation joint
$M_{y,j}$	Pitch moment at cabin-chassis joint
$M_{y,R}$	Pitch moment from rear articulation joint
$M_{z,axle}$	Yaw moment of an axle
$M_{z,axles}$	Yaw moment from all axles
$M_{z,cab}$	Yaw moment from cabin
$M_{z,ext}$	External yaw moment
$M_{z,F}$	Yaw moment from front articulation joint
	joint
$M_{z,R}$	Yaw moment from rear articulation joint
$M_{z,tyre}$	Aligning torque of a tyre
$M_{z,tyreL}$	Aligning torque of a left tyre
$M_{z,tyreR}$	Aligning torque of a right tyre
N	Number of rear axles
R	Wheel radius of a wheel
T	Tandem factor
T_{brake}	Braking torque on a wheel
T_{drive}	Drive torque on a wheel
T_{eng}	Engine torque
$T_{eng,max}$	Maximum engine torque
$T_{eng,min}$	Minimum engine torque
TW	Track width of an axle
V_x	Longitudinal velocity of a unit
$V_{x,cab}$	Longitudinal velocity of cabin
$V_{x,F}$	Longitudinal velocity of front articulation joint
$V_{x,j}$	Longitudinal velocity of cabin-chassis joint
$V_{x,R}$	Longitudinal velocity of rear articulation joint
V_y	Lateral velocity of a unit
$V_{y,cab}$	Lateral velocity of cabin
$V_{y,F}$	Lateral velocity of front articulation joint
$V_{y,j}$	Lateral velocity of cabin-chassis joint
$V_{y,R}$	Lateral velocity of rear articulation joint
V_z	Vertical velocity of a unit
$V_{z,cab}$	Vertical velocity of cabin
$V_{z,F}$	Vertical velocity of front articulation joint
$V_{z,j}$	Vertical velocity of cabin-chassis joint
$V_{z,R}$	Vertical velocity of rear articulation joint

Roman lower case letters

a_x	Longitudinal acceleration of a unit
$a_{x,cab}$	Longitudinal acceleration of cabin
a_y	Lateral acceleration of a unit
$a_{y,cab}$	Lateral acceleration of cabin
a_z	Vertical acceleration of a unit
$a_{z,axle}$	Vertical acceleration of an axle
$a_{z,cab}$	Vertical acceleration of cabin
acc_{input}	Input from accelerator pedal
$bank\_road$	Road banking of a unit
$brake_{input}$	Input from brake pedal
$c_{5^{th}w}$	Damping coefficient of fifth wheel
c_d	Damping coefficient of a damper
$c_{p,cab}$	Damping coefficient of cabin suspensions in pitch
$c_{r,cab}$	Damping coefficient of cabin suspensions in roll
c_t	Damping coefficient of frame torsion
$c_{z,cab}$	Damping coefficient of cabin suspensions in heave
d_{axle}	Longitudinal distance of an axle from unit centre of gravity
$d_{axle,S}$	Longitudinal distance of an axle from unit sprung mass centre of gravity
d_{cab}	Longitudinal distance of cabin from unit centre of gravity
$d_{cab,P}$	Longitudinal distance of cabin from pitch axis
d_{damps}	Distance between dampers of an axle
$d_{F,p}$	Longitudinal distance of front articulation joint from pitch axis
d_p	Distance of sprung mass centre of gravity from pitch axis
d_r	Distance of sprung mass centre of gravity from roll axis
$d_{R,p}$	Longitudinal distance of rear articulation joint from pitch axis
$d_{springs}$	Distance between springs of an axle
$d_{x,F}$	Longitudinal distance of front articulation joint from unit centre of gravity
$d_{x,p}$	Longitudinal distance of sprung mass centre of gravity from pitch axis
$d_{x,R}$	Longitudinal distance of front articulation joint from unit centre of gravity
$d_{xS,F}$	Longitudinal distance of front articulation joint from unit sprung mass centre of gravity
$d_{xS,R}$	Longitudinal distance of front articulation joint from unit sprung mass centre of gravity
$d_{z,p}$	Vertical distance of sprung mass centre of gravity from pitch axis
$d_{zS,F}$	Vertical distance of front articulation joint from unit sprung mass centre of gravity
$d_{zS,R}$	Vertical distance of front articulation joint from unit sprung mass centre of gravity
f_r	Coefficient of rolling resistance
g	Gravitational acceleration
h	Distance between cabin centre of gravity and cabin-chassis joint
h_{cabCG}	Height of cabin centre of gravity from ground
$h_{cab,j}$	Height of cabin-chassis joint from ground
h_F	Height of front articulation joint from ground
h_R	Height of rear articulation joint from ground
h_r	Height of roll axis from
$slope\_road$	Road slope of a unit

	ground
h_{rc}	Height of an axle roll centre from ground
i_T	Total transmission ratio
i_{tot}	Overall steering ratio
$k_{5^{th}w}$	Stiffness coefficient of fifth wheel
k_s	Stiffness coefficient of a spring
k_{stab}	Stiffness coefficient of a stabiliser
k_t	Stiffness coefficient of frame torsion
$k_{t,s}$	Specific stiffness coefficient of frame torsion
k_W	Stiffness coefficient of a tyre in heave
$k_{p,cab}$	Stiffness coefficient of cabin suspensions in pitch
$k_{r,cab}$	Stiffness coefficient of cabin suspensions in roll
$k_{z,cab}$	Stiffness coefficient of cabin suspensions in heave
$l_{axle,P}$	Longitudinal distance of an axle from pitch axis
l_{eq}	Equivalent wheelbase
m	Mass of a unit with axles
m_{axle}	Mass of an axle
m_{cab}	Mass of cabin
m_s	Mass of a unit without axles
n_W	Number of wheels per axle side
$offset$	Maximum value of dry friction torque in fifth wheel
p_{servo}	Servo pressure
r_k	Steering-axis offset at ground
r_p	Distance of servo pressure force from sector axis
v_{dampL}	Velocity of a left damper rod
v_{dampR}	Velocity of a left damper rod
$v_{x,W}$	Longitudinal velocity of a wheel centre
$v_{x,WL}$	Longitudinal velocity of a left wheel centre
$v_{x,WR}$	Longitudinal velocity of a right wheel centre
$v_{y,W}$	Lateral velocity of a wheel centre
$v_{y,WL}$	Lateral velocity of a left wheel centre
$v_{y,WR}$	Lateral velocity of a right wheel centre
t	Pneumatic trail of a tyre
z	Vertical position of a unit
z_{axle}	Vertical position of an axle
z_{cab}	Vertical position of cabin
z_j	Vertical position of cabin-chassis joint
z_{road}	Vertical position of tyre-road contact
$z_{springL}$	Length of a left spring of an axle
$z_{springR}$	Length of a right spring of an axle
z_t	Vertical compression of a tyre
z_{wheel}	Vertical position of a wheel centre
z_{wheelL}	Vertical position of a left wheel centre
z_{wheelR}	Vertical position of a right wheel centre

Greek lower case letters

α	Lateral slip angle of a tyre
β	Angle between line joining centre of gravity to pitch axis and x-axis
δ	Mean of left and right wheel steer angles with roll steer contribution
δ_L	Steer angle of left wheel
δ_R	Steer angle of right wheel
$\delta_{st,wheel}$	Steering wheel angle
δ_{wheels}	Mean of left and right wheel steer angles
$\varepsilon_{torsion}$	Torsion angle of steering torsion bar

η_T	Transmission efficiency
θ	Roll angle of a unit
θ_{axle}	Roll angle of an axle
θ_{cab}	Roll angle of cabin
θ_F	Roll angle of front reference point for chassis frame torsion
θ_R	Roll angle of rear reference point for chassis frame torsion
θ_r	Relative roll angle
θ_{rel}	Relative roll angle axle-chassis
ρ_{air}	Air density
σ	Kingpin inclination angle
τ	Torsion angle of chassis frame, caster angle
φ	Pitch angle of a unit
φ_{cab}	Pitch angle of cabin
φ_r	Relative pitch angle
ψ	Yaw angle of a unit
ψ_{cab}	Yaw angle of cabin
ψ_r	Relative yaw angle
ω_{eng}	Engine angular velocity
$\omega_{eng,idle}$	Engine angular velocity at idle
$\omega_{eng,max}$	Maximum engine angular velocity
$\omega_{eng,mean,w}$	Mean of angular velocities of driven wheels
ω_{wheel}	Angular velocity of a wheel

1 Introduction

This report describes the development and validation of a truck dynamics model to be used in an advanced driving simulator at the Swedish National Road and Transport Research Institute, also known as VTI. VTI is an independent and internationally prominent research institute in the transport sector. Its principal task is to conduct research and development related to infrastructure, traffic and transport. The institute has more than forty years of experience using simulators and is a leading authority in conducting simulator experiments and developing simulator technology. The newest VTI's simulator, Sim IV, is located at VTI's Göteborg office and is the simulator used in this project.

1.1 Background

Driving simulators provide important opportunities to study interaction between the drivers and vehicle in a wide variety of situations and scenarios, from the reaction to and acceptance of new technologies related to active safety to the effects of drug, alcohol and tiredness on the driver. Driving simulator experiments need a dynamics model of the vehicle under study, which has the purpose of approximating the behaviour of the vehicle on a real road. More details about the role of the vehicle dynamics model in the driving simulator are given in Section 1.7.

1.2 Project definition

VTI has a need for an open and in-house developed truck model for its driving simulators Sim II and Sim IV. Currently, the truck dynamics models used so far were developed, operated and owned by Volvo Trucks. This had obvious restrictions for its use and publicity. It is often desirable to have an open model, for which a deeper knowledge can be maintained and a flexibility that admits modifications without limitations. A further motivation to develop a truck dynamics model was to investigate which phenomena are of importance with respect to the driving simulator application.
The aim of this project was the development of an open model, utilizing the validated model of the OEM as a reference. The chosen programming language is Modelica (more details about the softwares are given in Section 2.4.1).

1.3 Research question

The thesis research question is to investigate the required level of detail for the modelling of each component and phenomenon for the driving of trucks in driving simulators.
The required level of detail needs to be defined in a context, i.e. a situation or a scenario, which will be specified in Section 2.2. Moreover, the choice of the modelled vehicle combination is illustrated in Section 2.1.

1.4 Deliverables

The thesis work aimed to deliver a vehicle dynamics model of a truck, that is,

- created in the Modelica programming language
- is an open model, that can be simulated in open source tools

- should have a high level of readability and flexibility for future understanding, modification and use
- is able to run in real-time in the driving simulator Sim IV without any real-time performances problem
- is evaluated to be satisfactory with respect to the OEM model in the chosen driving context (see Section 2.2).

1.5 Limitations

The limitations of the developed vehicle dynamics model mainly originate from the choice of the driving context (Section 2.2).
Hence, the longitudinal dynamics has been treated with less detail compared to the lateral and vertical dynamics. Therefore, accelerating and braking maneuvers are represented in a more approximated way.
The tyres are supposed to keep always in the linear region of the tyre characterisitcs and with constant dry high friction conditions. As a consequence, it is not suitable for simulating heavy braking or evasive lateral maneuvers.
The model cannot handle wheel lift phenomenon, hence the wheels are supposed to keep always in contact with the ground.
Parking maneuvers are not suitable test cases, due to the simplicity of the tyre models.
Furthermore, active safety functions such as ABS, ESC and Cruise Control have not been considered in the model.

1.6 Method

The model was developed by gradually increasing the complexity step-by-step (more details are given in Section 2.5). In each step, the increment was determined by focusing on what was believed to be the main contributing phenomena to the trajectory of the vehicle.
The model, and all the gradual steps to the model, have been benchmarked against the validated OEM model by means of desktop simulations to objectively evaluate the performance of the resulting model (Section 10.1). It should kept in mind, however, that the required degree of complexity is ultimately determined by the perception of drivers of the driving simulator. Therefore, only what notably affects the motion of the tractor and the driver's perception in the driving simulator is motivated to be modelled.
The work is concluded with some comparative experiments in the driving simulator Sim IV towards the OEM model (Section 10.2).

1.7 The driving simulator

The driving simulator can be divided into 5 main subsystems, whose interaction is managed by the coordinating software, which thus plays a central role (as shown in Figure 1.1). In fact, these subsystems need to work in synchrony to guarantee the best performance of the simulator and hence the most realistic driving experience.
The vehicle cabin is the main interface of the driver with the simulator. Either a car cabin (Volvo XC-60) or a truck cabin (Volvo FH 16-700) can be fit on Sim IV (see Figure 1.2).

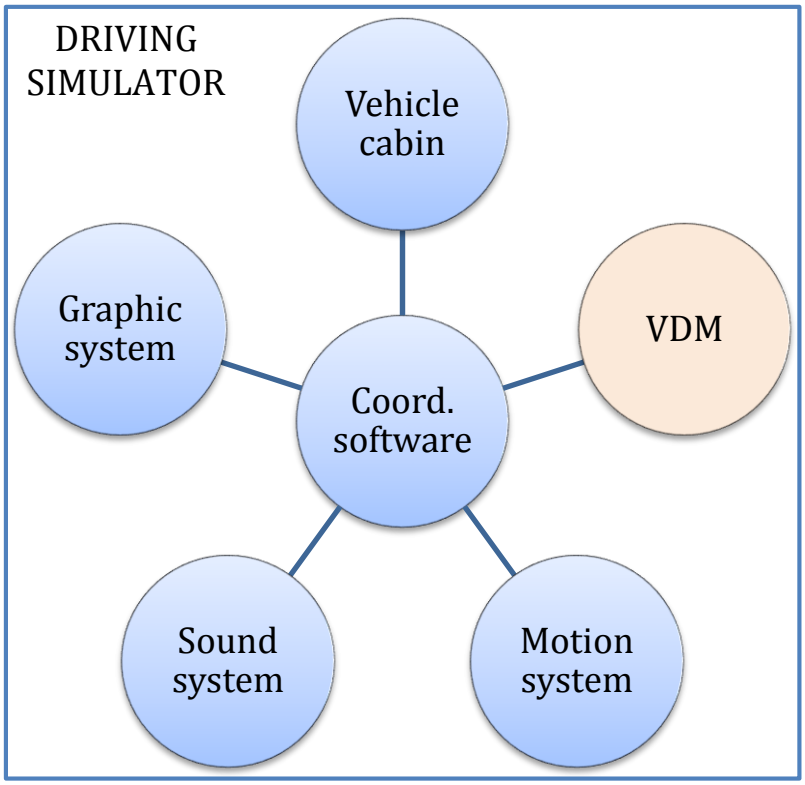

Figure 1.1 Driving simulator divided into its subsystems. The subsystem which development is the aim of this project is in a different colour.

Figure 1.2 Views of truck cabin (Volvo FH 16-700).

The graphic system consists of a 180º screen surrounding the vehicle cabin and covering the entire driver's vision field. The graphics are represented in the screen using several projectors. In addition, the side view mirrors of the cabin have been replaced by LCD screens to represent what the driver would see in reality (the rear part of the vehicle, the environment behind it, other approaching vehicles, etc.). Figure 1.3 illustrates what the drivers sees while driving the truck.

Figure 1.3 View of the screens from the driver's position while driving.

Another relevant part of representing the environment in the simulator is the sound system, which is composed by several speakers in the cabin. The sound reproduced by these speakers is controlled by a sound model that considers several factors, like vehicle velocity, working conditions of the engine and type and characteristics of the road. Furthermore, a microphone allows communication between driver in the simulator and engineers in the control room.
In Sim IV the vehicle cabin is mounted on a motion platform. The movements of the platform are controlled by a complex motion cueing algorithm, developed in-house, see Fischer (2001). The motion platform, shown in Figure 1.4, can be moved over rails in both longitudinal and lateral directions to generate longitudinal and lateral accelerations. In addition, actuators with an hexapod geometry allows generating roll, pitch and yaw angles, as well as some vertical displacement.

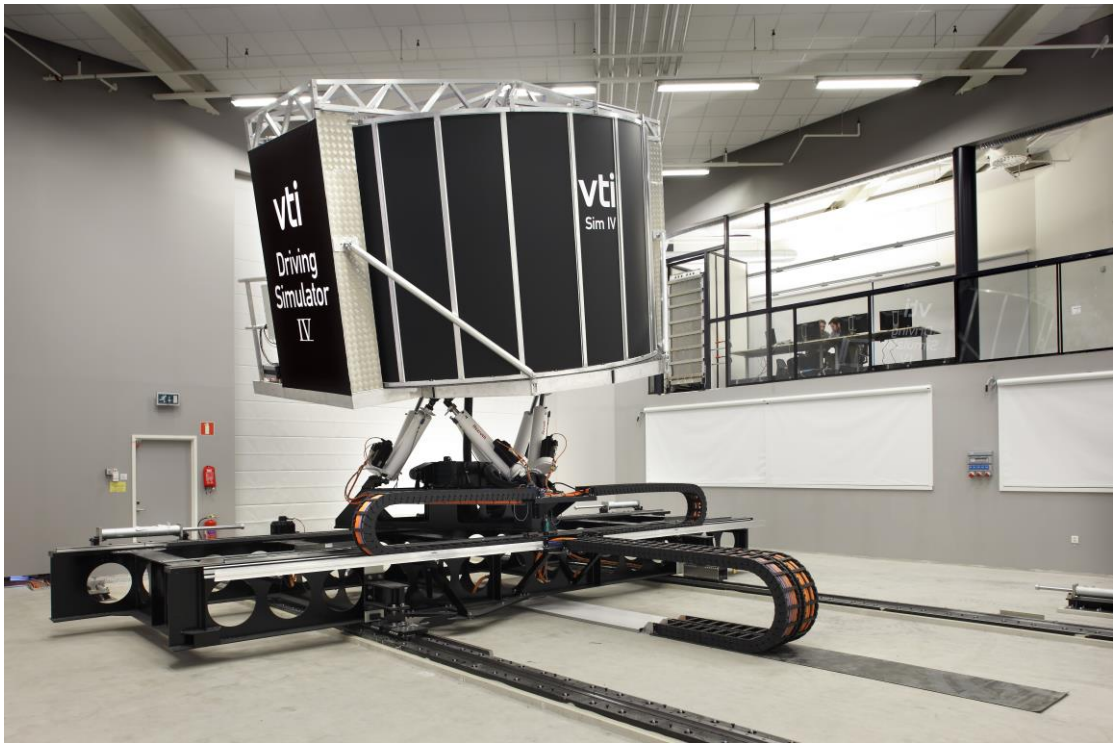

Figure 1.4 Sim IV with its rails and hexapod.

The vehicle dynamics model (VDM) calculates the motion of the simulated vehicle based on the inputs both from the driver (i.e. accelerator and brake pedals, steering wheel, gear clutch, cruise control selector, etc.) and from the environment (i.e. road profile, road-tire friction coefficient, wind, etc.). These inputs are received at each time step by the VDM, which uses them to calculate the vehicle accelerations and

rotations and other variables, which are sent through the coordinating software to the other simulator subsystems, i.e. to the graphic and sound systems and the motion system.

2 Model Description

In this Chapter, more details about the developed model are given. The chosen vehicle will be illustrated, together with the selected driving context. The context is of crucial importance for the modelling choices. Then, a brief description of the Volvo Trucks model, used as a reference, will be given. The last sections are dedicated to coordinate systems and other important aspects of the developed model.

2.1 Vehicle combination

The chosen vehicle combination for validation is an A-double (Figure 2.1). It consists of four units, i.e. a tractor, a semitrailer, a converter dolly and another semitrailer (Figure 2.2), for a total length of 31,5 m. This vehicle has not been allowed on real roads yet, at least in Europe. However, it is one of the most promising LCVs (Long Combination Vehicles) based on the European Modular System. In fact, there is a trend to increase the length of the combination vehicles for a reduced environmental impact and an increased productivity.

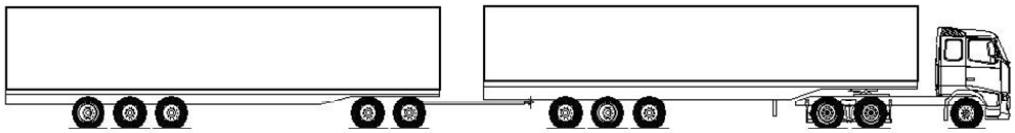

Figure 2.1 A-double combination.

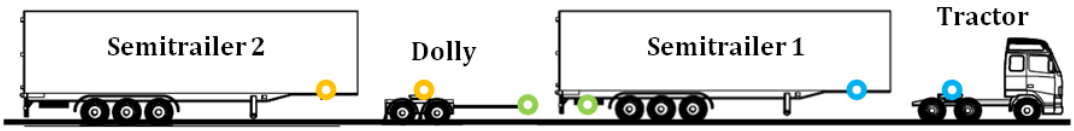

Figure 2.2 A-double combination divided into its four units. The connection points are highlighted with coloured spots.

In the modelled vehicle, the tractor has one steered front axle and two rear driven axles with twin tyres. Both semitrailers have three axles, whereas the dolly has only two.

2.2 Driving context

As already mentioned in Section 1.3, the model complexity needs to be defined in a context, i.e. a situation or a scenario. This is necessary to set the scope of the model and to delimit the work of comparison with the OEM model.
The chosen context was normal driving at almost constant speed on dry road, with small steering angles. This is the typical driving situation of the mentioned combination vehicle. This situation motivates a focus on vertical and lateral dynamics, rather than longitudinal. Therefore, the vehicle is supposed to accelerate slowly until cruise speed, perfome some maneuvers at almost constant speed (sufficiently far from a loss of lateral stability) and then decelerate gently.
A reference maneuver was chosen for the validation in the desktop simulations, i.e. a lane change maneuver, performed at a constant speed of 80 km/h (see Section 10.1). This is a common scenario used in the simulator when testing e.g. active safety

features and semi-autonomous driving, see e.g. Nilsson (2015). In fact, safety is one of the main concerns with such long vehicles.
The validating driving simulator experiment in this work comprised of lane changes at 50 and 80 km/h and straight driving on road banking, road slope and road holes (see Section 10.2).

2.3 Reference OEM model

The Volvo Trucks model, used as the reference, is implemented in the Simscape environment in Simulink. Simscape allows for modelling and simulating systems from many physical domains. Because Simscape components use physical connections, the models match the structure of the developed system. A vehicle is then modelled with many rigid bodies which interact with each other by means of the exchange of forces and moments at the points of connection.
The tractor sprung mass consists of the cabin and the chassis frame, which is split in two bodies to model the torsional flexibility (see Figure 2.3). The cabin and the front axle are connected to the front body, while the rear axles and the coupling to the semitrailer are connected to the rear body. They are linked via a one degree of freedom spring-damper system in roll. The chassis frame torsion angle is then defined as the difference between the roll angles of the two bodies. The cabin is suspended on the chassis in the heave, roll and pitch degrees of freedom, while it is fixed in all the others. The wheels are rigidly included in the axles, which can only heave and roll with respect to the sprung mass. The tyres are represented by Pacejka models (specifically PAC2002). The two semitrailers and the dolly consist of one rigid body for the sprung mass, to which a number of axles (3 for the semitrailers and 2 for the dolly) is connected.

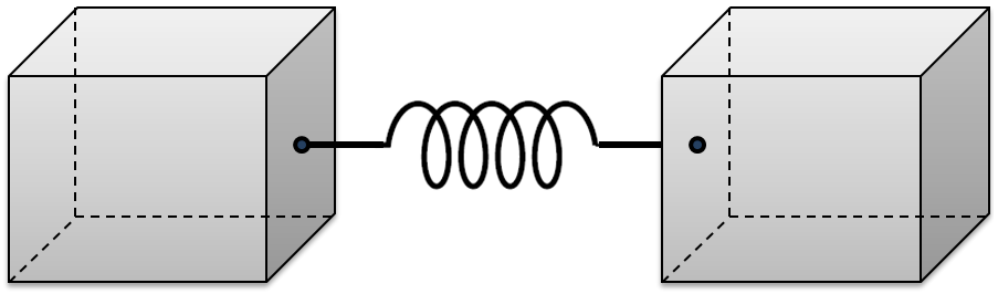

Figure 2.3 Sprung mass split into two bodies to implement the torsional flexibility of the chassis frame. The bodies are linked by a spring that allows their relative rotation about its axis, that is in the longitudinal direction of the chassis frame.

The inputs to the described system are the outputs of the steering, powertrain and braking systems. The inputs to these three systems are, in turn, the output of a block that controls their actuation based on the driver requests.
The Simulink file of the Volvo Trucks A-double model used as a reference for this project has a size of 4,059 KB.

2.4 The new VDM

2.4.1 Software choice and use

The model was written in the programming language Modelica, which is a non-proprietary, object-oriented, acasual and equation-based language developed by a non-profit organization, the Modelica Association, see Modelica Association (2012). There are different commercial Modelica simulation tools, such as CATIA systems, Dymola, AMESim, MapleSim, MathModelica and SimulationX. In this thesis the software Dymola 2013 was used, as it provides the feature to export the model in Matlab Simulink to run it in real-time. Simulink is, in fact, one of the most used software for real-time applications. It supports real-time computing via for example the XPC Target environment, which is available in Sim IV. However, its block-oriented programming language has limitations in terms of flexibility and readability. Therefore, the chosen alternative was to write the model in the Modelica language in the Dymola environment and using the Simulink interface for real-time implementation. This is the process currently used at VTI, even if the developed model does not set specific constraints for future utilization of an FMU Interface, which is a more adopted method nowadays for real-time applications.
The used Matlab version was the R2011b. The Modelica version was 2.2.2. The Modelica model is run with the "Explicit Euler" integration method and the "Euler" integration algorithm (fixed integration step of $1 \cdot 10^{-3}$ seconds). The solver is inlined with the code that is running in Simulink, which enables a more efficient use of the translator in Dymola.
Figure 2.4 shows a schematic representation of the necessary steps from the Dymola environment to the Simulink environment and, at last, to the XPC target.
The structure of the developed Modelica model is shown in Figure 2.6 and is further explained in Section 2.4.5. This model is exported to a Simulink file by means of a Dymola Block, as shown in Figure 2.5. The Dymola Block communicates with a block that represents the interface of the VDM with the the simulator coordinating software and thus with the other simulator subsystems (see Section 1.7). The inputs and outputs of the Dymola Block that allows for this communication are listed in Section 2.4.2.
Additionally, another Simulink file was created for performing desktop simulations in the same software as the OEM model. The same inputs, created in a Matlab script file, were fed to both models and a comparison was carried out, thanks to a plot generating script file (see Section 10.1).

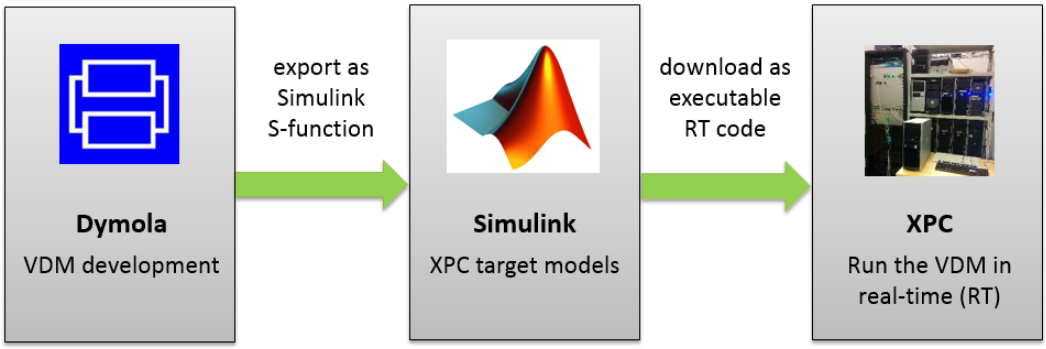

Figure 2.4 Process that brings from model development to real-time simulation.

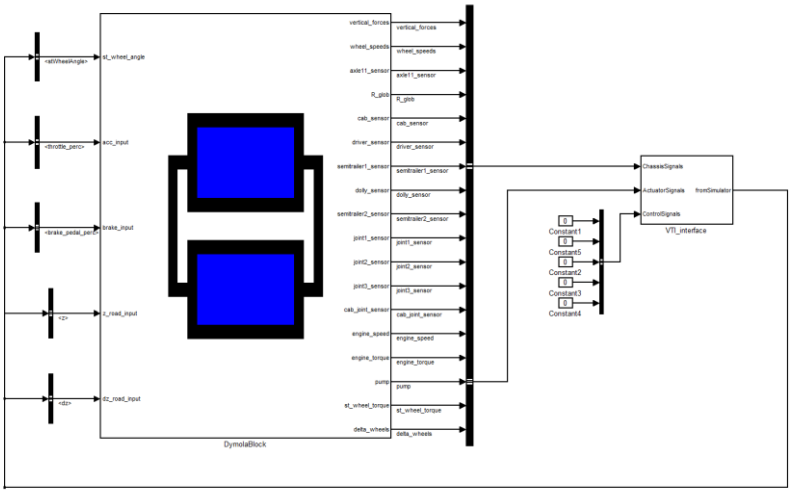

Figure 2.5 Screenshot of the structure of the Simulink file (middle step of Figure 2.4).

2.4.1.1 Programming language approach

Modelica can be used with two different approaches, i.e. with basic code or with libraries of predefined components. This choice may greatly affect different aspects of the way of working for both the developer and the future users of the model.

The first approach is with basic code, where all the parameters and variables and all the equations that define the system need to be formulated. This has the main disadvantage of requiring a large amount of workload; however, it allows a great readability and transparency, as the components are built for the particular application, therefore it is easy and straightforward to understand how each of them is working. This strategy does not necessarily implies a single level model, but a structure can be built, with a number of hierarchical levels tailored for the specific application. A further advantage is the possibility to run the model in the OpenModelica environment, which is an open source tool, see Fritzson (2005). The availability of a passenger car model developed a few years ago by two students at VTI using this approach contributes in favor of this choice, as its structure may be taken as a simpler example, see Gómez Fernández (2012), Obialero (2013) and Bruzelius (2013).

The second possible approach is to use the components of the available libraries: in this case, VTI has the license of the 2013 version of Dymola with the Vehicle Dynamics Library (VDL). This would allow for a relatively fast and easy generation of a model by putting together predefined components. In contrast, these components are designed to be general to allow for a high level of flexibility. This is significantly affecting the readability. This choice would also violate the openness of the model, due to the use of proprietary software.

Another way to proceed with this second approach is to use the standard component libraries (Modelica Standard Library): this could be seen as a trade-off between the transparency of the system modelled from scratch and the modelling easiness of the system built using the VDL; in addition, it could allow running on OpenModelica. On the other hand, this trade-off may be disadvantageous, as it may imply a significantly higher workload with respect to the VDL case, without producing a notable gain in terms of readability or even making it worse.

Table 2.1 Pros and cons of the available alternatives for the approach to Modelica.

Basic code	Libraries of predefined components	
	Vehicle Dynamics Library	**Modelica Standard Library**
+ readability + open + structure - high workload	+ low worklaod + flexibility - readability - not open	+ open +/- medium workload ? flexibility ? readability

The different aspects of the alternatives are summarised in Table 2.1. They were examined, together with the preferences of the main future users of the model, i.e. VTI's researchers. As the primary objective was to keep the model simple, readable and free of proprietary software, the final choice was the coded mode. The next decision of the most suitable number of levels is given in Section 2.4.5.

2.4.2 Model inputs and outputs

This Section summarises the inputs and outputs of the VDM of an A-double when performing real-time experiments on the driving simulator Sim IV. The mentioned coordinate systems are clarified in Section 2.6.

- INPUTS
  - Steering wheel angle
  - Accelerator pedal position
  - Brake pedal position
  - Vertical global coordinate of the wheel-road contact point for each wheel
  - Road inclination (in the road coordinates) at the wheel-road contact point of each wheel in the heading direction of the vehicle and in the direction perpendicular to it.

- OUTPUTS
  - Vertical forces on each wheel
  - Rotational speeds of each wheel
  - Global rotation matrix of the reference frame of the tractor chassis in the point where the cabin is attached to it
  - Values of velocities, accelerations, angles, angular rates and angular accelerations in the local reference frame of:
    - first axle of the tractor
    - cabin
    - driver (not used)
    - first semitrailer
    - dolly
    - second semitrailer

- Values of angles, angular rates, angular accelerations and torques of the following joints and in the following axes (in the local coordinate frame of the first mentioned unit of each joint):
  - joint of tractor to first semitrailer: y and z
  - joint of first semitrailer to dolly: x ,y and z
  - joint of dolly to second semitrailer: y and z
- Values of angles, angular rates, angular accelerations and torques in the x- and y-axes and values of position, velocity, acceleration and force in the z-axis (in the local coordinate frame of the tractor) of the joint of tractor to cabin
- Engine rotational speed
- Engine torque
- Fuel pump signal (not used)
- Steering torque
- Mean of the wheel steer angles of the right and left wheels of first axle of the tractor.

2.4.3 Vehicle model summary

This section summarizes the general characteristics of the developed Modelica model and the implications of the modelling choices. References are given to the parts of the thesis report where more details can be found.

- The tractor has a front axle with steerable wheels and two driven rear axles with twin tyres. Both semitrailers have three axles. The dolly has two axles.
- The sprung mass of each unit has the degrees of freedom (DOFs) of 3 displacements and 3 rotations in the space. The roll and pitch dynamics is performed with the roll and pitch axes analysis. In addition, the tractor hosts the cabin and its chassis frame is considered to have a torsional flexibility around the x-axis. See Chapter 3 for more details.
- The cabin is a rigid body suspended on the tractor frame with the DOFs of two rotations (roll and pitch) and one translation (heave) relative to the tractor frame. See Chapter 5 for more details.
- The first semitrailer is connected to the tractor frame through a fifth wheel connection, which allows for two relative rotations along the y- and z-axes of the tractor reference frame; the latter rotation is limited by a dry friction and a linear damping torques. The dolly is coupled to the first semitrailer through a spherical joint (i.e. three axes of relative rotation). Finally, the second semitrailer is attached to the fifth wheel on the dolly frame, which allows for two relative rotations along the y- and z-axes of the dolly reference frame. This connection is modelled in the same way as the first fifth wheel, except that here is no friction torque in the z direction. See Chapter 6 for more details.
- The axles are modelled as rigid and each of them has one rotation (roll) and one displacement (heave) degrees of freedom relative to the sprung body. In other words, the sprung mass can heave, roll and pitch with respect to the axles. The suspension elements for each axle are two springs (with constant stiffness coefficient), two dampers (with constant linear damping coefficient with the same value in both deformation directions) and an anti-roll bar (with constant stiffness coefficient). See Chapter 4 for more details.
- The tyres have a vertical flexibility and are modelled as springs. See Section 4.4 for more details.

- The rotational velocities of the wheels have a kinematic relationship with their translational velocities, that means that no relative motion (longitudinal slip) between the wheel and the road at the tyre-road contact is present. In addition to this, no limits are set to the tyre forces. The tyres have been implemented with a simple linear model, with infinite stiffness longitudinally and finite stiffness laterally. The cornering stiffness of each tyre is linearly variable with its vertical load. See Section 4.5 for more details.
- The steering system is a conventional hydraulic truck steering system. It receives the steering wheel angle from the driver and imposes the torque on the steering wheel as a feedback. Roll steer is included and the compliance of the steering torsion bar is considered. Fully Ackermann steering is used. No friction is considered. See Chapter 7 for more details.
- The powertrain uses an engine map for the torque-speed characteristics. The automatic gear shift is simply dependent on the engine speed. It does not take into account any transient behaviour of the engine. The retarder torque is not present. No delay from driver request to actuation is present. See Chapter 8 for more details.
- The braking system is designed in a basic way, i.e. the braking torque is set equal to the brake pedal input multiplied by a coefficient and it is the same for all wheels. No delay from driver request to actuation is present. See Chapter 9 for more details.
- The parameters representing the inertial data of the semitrailers include the kerb weight and the payload together.

2.4.4 Key numbers

This Section summarises the key numbers that can characterise the developed model and presents a comparison with the OEM model for the real-time performances. A comparison in other terms (size of files, number of variables, etc.) would appear difficult, because of the completely different environments of model development.

I. Size of library code:
   a. 83 KB
   b. 1581 lines
II. A-double model:
   a. 212 scalar parameters
   b. 86 state variables
III. Size of Simulink file: 370 KB.

The real-time performances of a VDM depend on the hardware of the simulator and on its performance, therefore the absolute numbers cannot characterise its value. On the contrary, a comparison between two VDMs can represent their difference. The integration time used in the simulator experiments was $1 \cdot 10^{-3}$ seconds. The average task execution time, i.e. the time to calculate the values of the outputs from the values of the inputs, and the percentage of time step utilisation (i.e. task execution time divided by integration time, with 100% meaning that the model is not able to finish the calculations in real-time) were:

- $6.7 \cdot 10^{-4}$ seconds (i.e. 67%) for the OEM model. Given the small execution time margin, problems of real-time performances sometimes arise.
- $7.4 \cdot 10^{-5}$ seconds (i.e. 7.4%) for the Modelica model, which is more or less 10 times faster than the OEM model, which, therefore, can be more stable.

2.4.5 Modelica model structure

The main requirements of the Modelica model were high readability and flexibility for future understanding and use. Its structure and implementation should guarantee a high degree of transparency and easy modifications.
The number of levels of the library structure and how the units and the vehicles are composed is a crucial point for the value of the model. Figure 2.6 shows a snapshot of the library in the Dymola environment.
First, the structure will be briefly described to show its main features and advantages; then, more details are provided, such as how the structure was used to form and simulate an A-double combination; moreover, some suggestions for future use of the model are here present. A theoretical explanation of the various parts of the model (*Components* and *Systems*) can be found in Chapters 3 to 9.

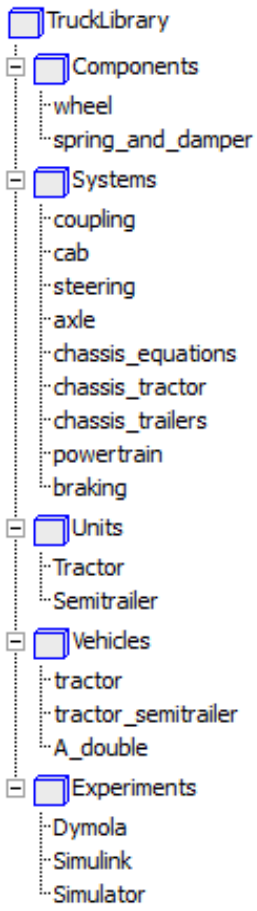

Figure 2.6 Modelica model structure, screenshot in Dymola environment.

The library *TruckLibrary* comprises of 5 packages, called *Components, Systems, Units, Vehicles* and *Experiments*, each of which is made of a number of models. In the *Experiments* there are models suited for simulations. At this level, a vehicle is defined (from the *Vehicles* package), together with the inputs and the outputs for simulation. In the *Vehicles* the vehicles are formed by using the models of the *Units* package to define the units of the specific combination and the *coupling* model (from the *Systems* package) to connect the units. Moreover, the connections of the braking system take place at this level, as the *braking* model (of the Systems package) is defined in the first unit of the combination vehicle. In the *Units* the units are formed by using the models in the *Systems* package, which are defined and connected to each other and the

parameters are assigned to them. Finally, the *axle* model of the *Systems* package makes use of the two models of the *Components* package.
The advantages of this structure are several. Some of them are listed here, while others will be mentioned in the rest of this Section:

1. The modifications need to be done in only one point of the library, as the equations are written only once: in case of an A-double, there is one *wheel* model for the 22 wheels, one *axle* for 11 axles, one *spring_and_damper* for the 22 springs and dampers, one *chassis_equations* for the 4 units, one *coupling* for the 3 couplings, one *Semitrailer* for the two semitrailers and the dolly.
2. A unit may be easily modified to represent different vehicles.
3. A unit may be easily connected to any other unit, so that any vehicle combination may be formed at the *Vehicles* level, provided that the necessary units are present in the *Units* package.
4. A unit may have any number of axles and they may be in any position with respect to the unit CG: everything is done at the *Units* level, i.e. the axles are defined, the proper distances and other parameters are assigned and the proper connections made.
5. Each axle may be made steerable and/or driven by making the proper connections with a steering/powertrain system at the *Units* level.
6. Different models may be created for the same system (e.g. the steering system) and a comparison may be easily carried out, thanks to a fast switch from one model to the other at the *Units* level.

The *Experiments* package comprises three models, which are ready for three different types of simulations. One allows simulating the model in the Dymola environment: the default maneuver consists of acceleration, lane change and braking, but others may be designed by changing the inputs to the steering wheel, accelerator pedal and brake pedal. Currently three different vehicles can be selected for simulation: an A-double combination, a tractor and semitrailer combination or a tractor alone. The second model in the *Experiment*s package allows exporting the model to Simulink for desktop simulation; this was used for comparisons with the OEM model. Finally, the *Simulator* model contains all the inputs and outputs for real-time simulation in the driving simulator. Simple modifications of the input and output vectors may allow to drive any type of combination, provided that it is first created in the *Vehicles* package, if not already present. Modifications of this model would also allow driving the truck on different driving simulators.
As already said, in the *Vehicles* package three vehicles are ready to be simulated. In particular, the *A_double* model is formed with a *Tractor* for the tractor and three *Semitrailer* models for the two semitrailers and the dolly. Three *coupling* models are defined for the connections between the four units. Furthermore, the braking connections from the *braking* model to the units (except the tractor) take place here.
Two types of units are present, the *Tractor* and the *Semitrailer*. The *Tractor* receives the inputs from the driver and from the road, whereas the *Semitrailer* only the ones from the road. The *Semitrailer* includes one *chassis_trailers* and three *axle* systems, but it features the possibility to have either two or three axles (by means of a parameter), which allows also for its use for the two-axle dolly. If a unit with either one or more than three axles is desirable, a fast choice is to duplicate the *Semitrailer* model and either add or remove the proper number of equations and of *axle* definitions and modify the equations and the sizes of vectors where the *axle* systems are used. Otherwise, it is possible to keep only one model and use a parameter in the

same way as for the selection of 2 or 3 axles. This is completely done within the *Semitrailer* model. The *Tractor* model has the following systems: one *chassis_tractor*, three *axle*, one *cab*, one *steering*, one *powertrain* and one *braking*. The modification of the number of axles of the *Tractor* is relatively easy and follows the same process as for the *Semitrailer* model with one or more than three axles. If also the number of driven wheels needs to be modified, also the proper adjustments in the *powertrain* system are needed. The parameters defined in the *Units* models can be easily modified to model vehicles with different characteristics. For instance, the *Tractor* can be used to model a rigid truck or the *Semitrailer* for a centre-axle trailer or a B-semitrailer, bearing in mind that the parameters representing the inertial data of the semitrailers include the kerb weight and the payload together (the same would occur for a rigid truck).

Some necessary adjustments need to be remembered whenever creating a new model in the *Vehicles* package (with a modified number of axles of some units or a different vehicle combination). All of them are at the *Vehicles* level, provided that the new models in the *Units* package have already been created, as explained in the previous. What need modifications are the sizes of the vectors of the road inputs and their connections, the braking connections and, if applicable, the *coupling* definition and connections. Exceptionally, the number of braking torques in the braking system also needs modifications in case of a new vehicle with more than 11 axles (this is done in the *braking* model in the *Systems* package).

The *Systems* package includes the following models: *coupling, cab, steering, axle, chassis_equations, chassis_tractor, chassis_trailers, powertrain* and *braking*. The *axle* system includes two *wheel* and two *spring_and_damper* from the *Components* package and it may have driven and/or steered wheels. The *wheel* in the *Components* package can model twin tyres. The *chassis_equations* define the general equations for a chassis (it may include a cabin, a front coupling and a rear coupling, an arbitrary number of axles and it may consider chassis frame torsion). The *chassis_tractor* and the *chassis_trailers* are an extension of this model (only a few equations are added). The frame torsion may be excluded from the model or, on the contrary, it may be included for any unit, setting the right parameters for the frame torsion. The coupling can be used in different ways to model different types of couplings: in particular, it may have either free or constrained relative roll; either free or limited by friction relative yaw.

More complex modifications can be thought. In the *steering* system, a torque may be added to the torque applied by the driver to model an active steering system. A new powertrain and/or steering system may be designed for the dolly in order to study a vehicle with driven and/or steerable wheels in the dolly. The designed system(s) can be defined in a *dolly* model, which can be an extension of the *Semitrailer* model.

2.5 Modelling steps

A relevant aspect of the model is how it was developed, as its complexity was gradually increased step-by-step, as stated in Section 1.6. In each step, the increment was determined by focusing on what was believed to be the main sources of error. The analysis is summarised in Section 10.1. The purpose of this method was to keep the complexity to a minimum.

The starting point was the simplest possible model, i.e. a linear single-track model with linear tyres, represented in Figure 2.7 (see Section 10.1.1). The parameters were determined to resemble the OEM model. The dry friction and linear damping torque

in the fifth wheel coupling between the tractor and the first semitrailer had a great impact on the trajectory and was hence included in this model (see Section 10.1.1.1). After this first model, complexity was increased as explained in the following.

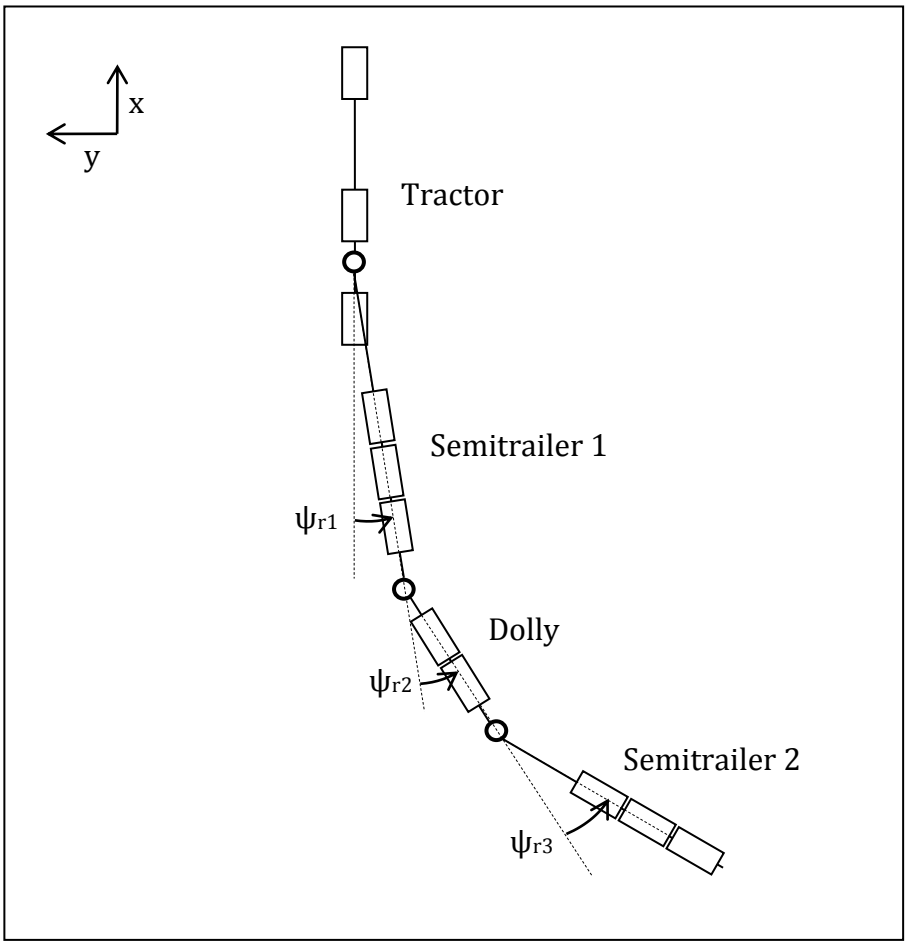

Figure 2.7 Schematic representation of a single-track A-double with the articulation angles between two consecutive units highlighted.

The single-track was extended to a double-track model, using an Ackermann steering, which means that nonlinearities are introduced. This model did not show a significant difference from the previous one, but this was a necessary intermediate step (see Section 10.1.2).

Roll, pitch and heave are the out-of-road-plane degrees of freedom. Each unit is now made of a sprung mass and a number of axles, each of which is free to move vertically and to roll with respect to the sprung mass. In the tractor, the chassis and the cab are considered as one rigid body. This addition to the model allowed including the roll steer contribution (see Section 10.1.3).

An important factor in the cornering dynamics of trucks is the torsional flexibility of the tractor chassis frame, which it also affects the roll steer term (see Section 10.1.4).

The cabin as a separate body from the tractor chassis had the main motivation of the final intended application of the model, which is a driving simulator (see Section 10.1.5).

The roll and heave of the axles were added by considering the vertical flexibility of the tyres (see Section 10.1.6).

A conventional truck steering system was modelled, which transforms the steering wheel angle to the steered wheels angles (see Section 10.1.7). The steering model also gives the driver a torque on the steering wheel as a feedback.
The powertrain and braking systems were the last missing parts to allow driving the model in the driving simulator (see Section 10.1.8).
Finally, the road input accounts for possible road slope, banking, holes, bumps and irregularities. This was useful for the simulator experiments (see Section 10.2).

2.6 Coordinate systems

The coordinate system adopted here is in accordance to ISO standards, as described in ISO 8855, which is a right-handed system and it is fixed on the sprung mass and centred in the centre of gravity (CG) so that the x is directed forward on the vehicle, y pointing left and z pointing upwards. A coordinate system is defined for each unit in the mentioned way, having that the tractor sprung mass does not include the cabin and that the semitrailers sprung masses include the payload.

Figure 2.8 Coordinate system of a unit (tractor in this case).

In addition, a global coordinate system is defined as being an inertial reference frame with the earth, with the vertical coordinate in the direction of the gravitational force, the longitudinal coordinate in the initial forward direction of the road and the lateral coordinate defined with the right-hand rule.
Each wheel has its own reference frame, which also follows the ISO standards (see Figure 2.9).
The longitudinal geometric distances for each unit are measured from the unit CG with positive direction rearward the CG (see Figure 2.8). This, for example, allows defining a unique *axle* component (see Section 2.4.5). In fact, the forces transmitted to the sprung mass are calculated with the same equations for each axle and the sign of its distance from the CG will define if it is forward or rearward the CG.
The origin for the vertical dimensions is on the ground.

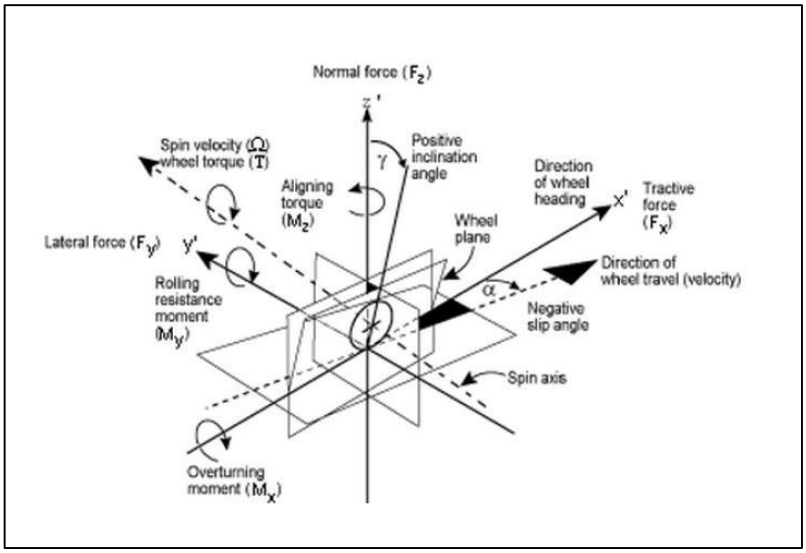

Figure 2.9 Wheel coordinate system.

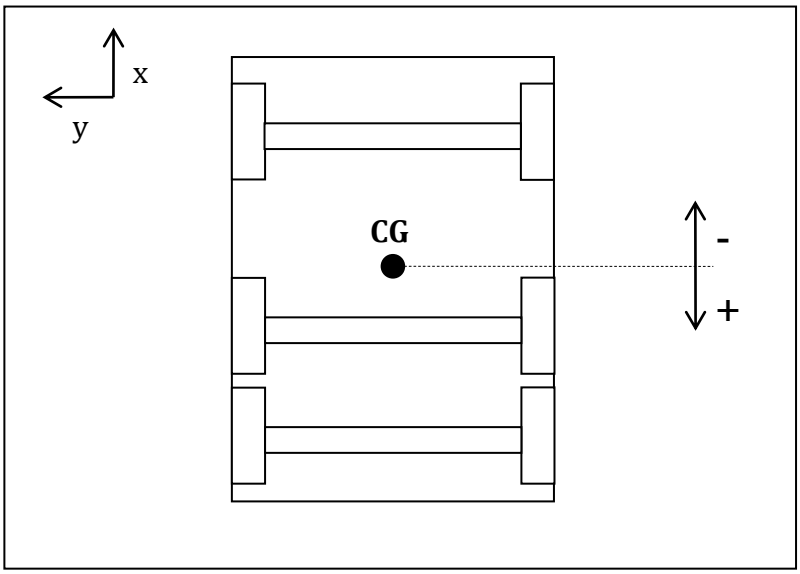

Figure 2.10 Definition of positive and negative distances in the longitudinal local coordinate of a unit (example of the tractor).

3 Chassis

The equations of motion are defined equally for all units. They include the forces (and moments) coming from the cabin, a front articulation joint, a rear articulation joint and an arbitrary number of axles. Depending on the particular unit, these forces may be set to zero or equal to the forces of the proper articulation joint of another unit. In particular, the tractor has a rear articulation joint and is obviously the only unit that has the cabin; both the first semitrailer and the dolly have a front and a rear articulation joints; finally, the second semitrailer has only a front articulation joint. See again Figure 2.2, which also clarifies the order of the units and hence the connections of the articulation joints.

In each equation of motion, the forces and moments coming from the cabin and the rear articulation joint are seen as "resisting", that means that they are defined in the negative directions of the axes. Whereas, axles and the front articulation joint are seen as "driving", hence with forces and moments in the positive directions.

Each unit is made by a sprung mass and a number of axles. The sprung mass can heave, roll and pitch with respect to the axles. The roll and pitch dynamics is studied with the corresponding axes analysis. Moreover, the chassis of the tractor is considered flexible in torsion, that means that an additional equation is present for this unit.

For the in-ground-plane degrees of freedom, the vehicle is seen as a rigid body consisting of the sprung mass and the axles. This implies that the computed x, y and ψ coordinates refers to the CG of the unit sprung mass plus axles, in other words the whole unit (except for the tractor, where the cabin is seen as a separated body). Consequently, the displacement of the sprung mass CG with respect to the axles in the x and y directions (due to roll and pitch) have to be considered in an indirect way. The same happens for the vertical displacement due to pitch motion.

On the contrary, the out-of-ground-plane degrees of freedom take into account the sprung mass only.

Consistently with this difference, each unit has two different centre of gravity positions: the CG of sprung mass plus axles and the CG_S of the sprung mass only. The same holds for the masses and the inertias used in the equations. Moreover, for the in-ground-plane degrees of freedom, the forces from the tyre-road contact enter directly the relevant chassis equations of motion; whereas, for the out-of-ground-plane degrees of freedom, they enter the axle equations of motion, from which the forces and moments transmitted to the chassis are derived.

3.1 Equations of motion

A Newtonian approach was used for the derivation of the equations of motion. The forces and moments coming from the axles, the cabin, the front and the rear articulation joints are considered. In particular, the moments coming from the axles and the cabin consist of a single term in each equation. In other words, these moments are such that the forces coming from these interfaces have been moved to the centre of gravity of the unit, as shown respectively in Sections 4.1 and 5.1. This is beneficial especially for the axles, as the calculations of these moments are concentrated in the *axle* system (see Section 2.4.5), avoiding to repeat them in the chassis equations as many times as the number of axles. However, for the sake of clarity, the figures of this Section show the forces coming from the cabin at the point of cabin-chassis interface, rather than passing through the centre of gravity of the unit. They are marked with a prime superscript (') to distinguish them from the moments used in the

chassis equations of motion. The definitions of the moments is then clarified for each equation.
The forces coming from the articulation joints are found in Section 6, specifically in Equations (6.3). The forces of the rear articulation joint of one unit (towing unit) will be equal to the forces of the front articulation joint of the successive unit (towed unit), having that the rear articulation joint of a unit is seen as "resisting", while the front as "driving".
It is worth to remember that the longitudinal distances are defined positive when rearward the CG or CG_S (see Section 2.6).
The external forces and moments $F_{x,ext}$, $F_{y,ext}$, $F_{z,ext}$, $M_{x,ext}$, $M_{y,ext}$ and $M_{z,ext}$, not represented in the schemes, are added to account for possible interactions with the external environment, such as aerodynamics forces. As the forces are applied at the centre of gravity, the moments may be used for external forces applied in a different point. In this model, only $F_{x,ext}$ is considered as being different from zero.

3.1.1 Longitudinal dynamics

Figure 3.1 shows the forces and moments for the in-ground-plane degrees of freedom. It is worth to remember that the axles are considered together with the sprung mass. This means that the forces $F_{x,axles}$, $F_{y,axles}$ and $M_{z,axles}$ are acting from the road to the unit. A generic unit is considered, so that the same equations can be used for all of the four units: hence, a front coupling point, a rear coupling point and a cabin are considered. Note that in the figure neither the external forces nor the fractions of gravitational force acting in the longitudinal and lateral equilibriums are shown.

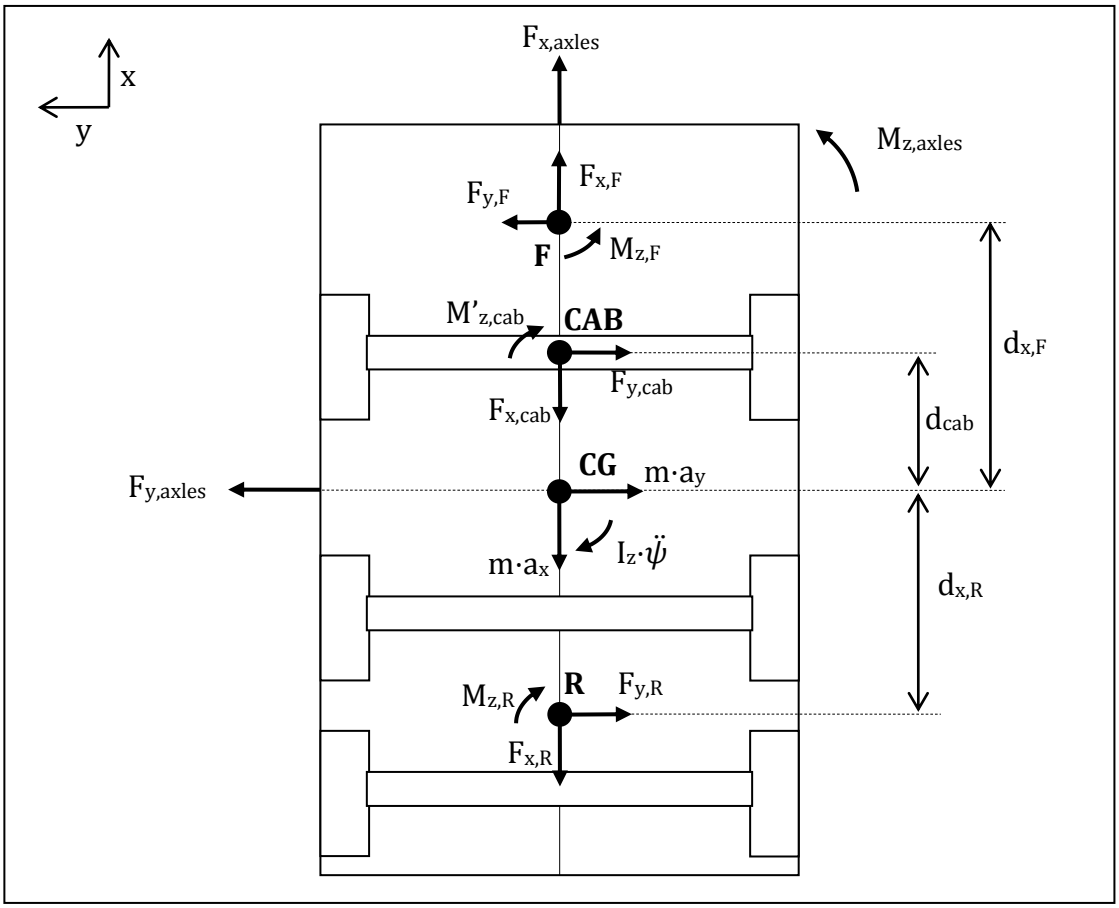

Figure 3.1 Forces and moments acting on a unit in the xy-plane.

The equilibrium along the x-axis is given by Equation (3.1).

$$m \cdot a_x = F_{x,axles} - F_{x,cab} + F_{x,F} - F_{x,R} + F_{x,ext} + m \cdot g \cdot slope\_road \quad (3.1)$$

The value of the road slope for each unit was found in an approximated way from the the road inputs of the wheels of the specific unit.
The longitudinal acceleration can be expressed by Equation (3.2).

$$a_x = \dot{V}_x - V_y \cdot \dot{\psi} \quad (3.2)$$

The force $F_{x,axles}$ is the sum of the forces $F_{x,axle}$ of each axle of the unit, which comes from Equation (4.1).

$$F_{x,axles} = \sum_{axles} F_{x,axle} \quad (3.3)$$

The longitudinal external force accounts for the aerodynamic drag, as expressed by Equation (3.4), and is acting only on the first unit.

$$F_{x,ext} = F_{aero} = -\frac{1}{2} \cdot \rho_{air} \cdot A \cdot C_d \cdot {V_x}^2 \cdot sign(V_x) \quad (3.4)$$

3.1.2 Lateral dynamics

The equilibrium along the y-axis is given by Equation (3.5).

$$m \cdot a_y = F_{y,axles} - F_{y,cab} + F_{y,F} - F_{y,R} + F_{y,ext} - m \cdot g \cdot bank\_road \quad (3.5)$$

The value of the road banking for each unit was found in an approximated way from the the road inputs of the wheels of the specific unit.
The lateral acceleration can be expressed by Equation (3.6).

$$a_y = \dot{V}_y + V_x \cdot \dot{\psi} \quad (3.6)$$

The force $F_{y,axles}$ is the sum of the forces $F_{y,axle}$ of each axle of the unit, which comes from Equation (4.2).

$$F_{y,axles} = \sum_{axles} F_{y,axle} \quad (3.7)$$

3.1.3 Vertical dynamics

The vertical equilibrium can be derived equivalently from Figure 3.4 or Figure 3.7 and it is given by Equation (3.8).

$$m_s \cdot a_z = F_{z,axles} - F_{z,cab} + F_{z,F} - F_{z,R} + F_{z,ext} - m_s \cdot g \quad (3.8)$$

The vertical acceleration is simply expressed by the derivative of the vertical velocity (Equation (3.9)), while the latter is the derivative of the z coordinate of the centre of gravity of the unit sprung mass (Equation (3.10)).

$$a_z = \dot{V}_z \tag{3.9}$$

$$V_z = \dot{z} \tag{3.10}$$

In particular, the pitch equilibrium is such that the vertical displacement z does not include the displacement due to pitch motion, but only due to pure heave.
The force $F_{z,axles}$ is the sum of the forces $F_{z,axle}$ of each axle of the unit, which comes from Equation (4.3).

$$F_{z,axles} = \sum_{axles} F_{z,axle} \tag{3.11}$$

3.1.4 Roll dynamics

In the OEM model, the sprung mass is a rigid body in the space, whose movement is determined by the forces and moments acting on it (see Section 2.3). The position of the connection points of the axles to the sprung mass, together with the terms (and their coefficients) of the suspension forces, will determine the roll and pitch dynamics.
In this thesis, a roll axis analysis is performed. Each unit is assumed to roll about a roll axis, which is found by the roll centres of the axles. In particular, the roll centre height of an axle is equal to its wheel centre height, except for the rear axles of the tractor, which have higher roll centres. This would imply an inclination of the roll axis with respect to the xy-plane, which is neglected. Therefore, the tractor sprung mass is assumed to roll about an axis parallel to the ground at a height which is found from the roll centres heights of the axles as explained in the following (with reference to Figure 3.2). The roll centre height of the rear axles was assumed to be the height of a point (RR) at the middle between the two rear axles. The line joining this point with the front axle roll centre (RC_1) defines the height of the roll axis, as well as the rear axles roll centres, as shown in Equations (3.12), (3.13), (3.14) and (3.15).

$$d_{2-3,S} = \frac{d_{2,S} + d_{3,S}}{2} \tag{3.12}$$

$$h_r = \frac{h_{rc,1} \cdot d_{2-3,S} + h_{rc,2-3} \cdot \left|d_{1,S}\right|}{\left|d_{1,S}\right| + d_{2-3,S}} \tag{3.13}$$

$$h_{rc,2} = h_r + \frac{h_{rc,2-3} - h_r}{d_{2-3,S}} \cdot d_{2,S} \tag{3.14}$$

$$h_{rc,3} = h_r + \frac{h_{rc,2-3} - h_r}{d_{2-3,S}} \cdot d_{3,S} \tag{3.15}$$

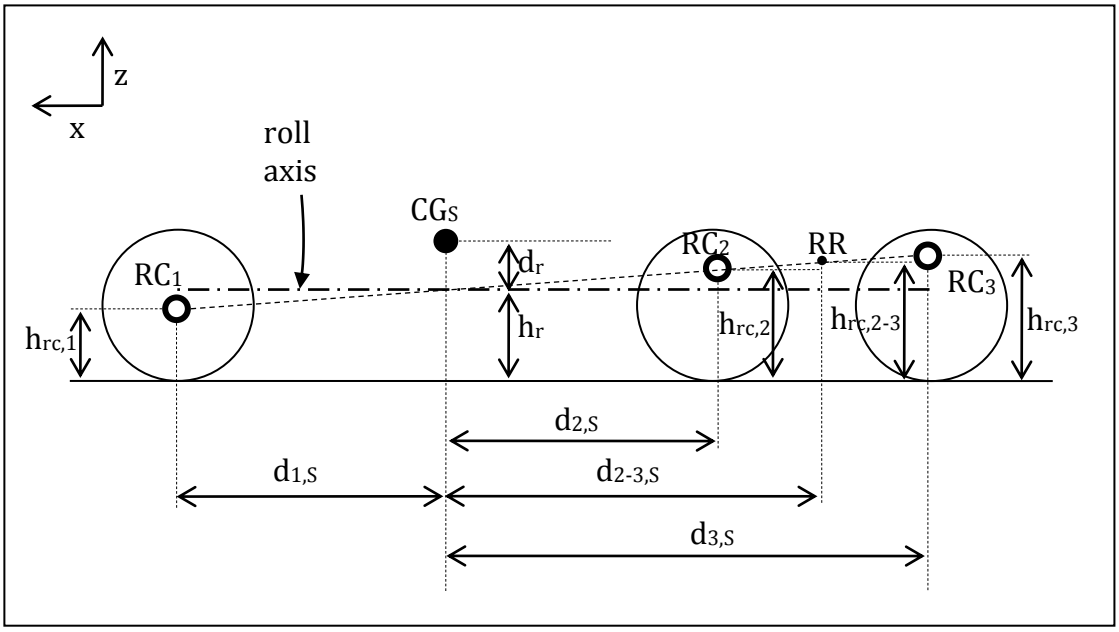

Figure 3.2 Roll axis calculation for the tractor.

Figure 3.3 shows the rolled configuration of the sprung mass of a generic unit in the yz-plane, with the displacements of the centre of gravity of the sprung mass (CG_S), of the point of cabin-chassis joint (CAB) and of the two coupling points (F and R). The grey points are prior to roll (at rest), while the black ones are after roll.

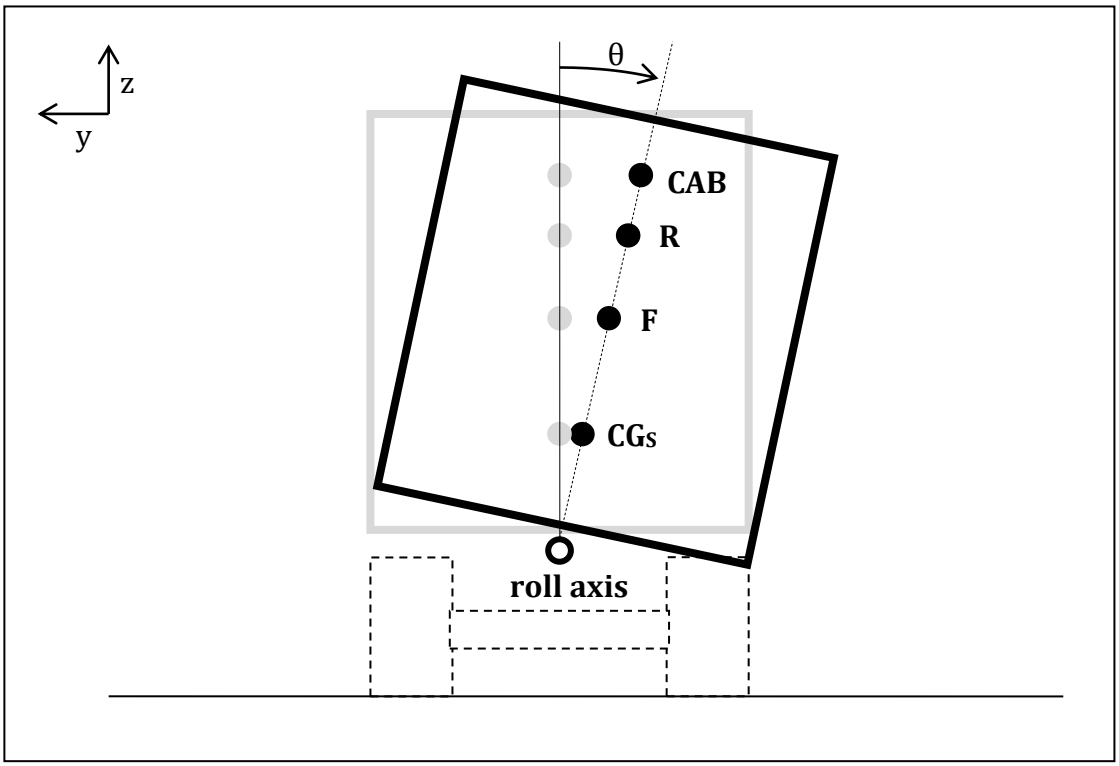

Figure 3.3 Sprung mass in the rolled configuration around the roll axis, with some highlighted relevant points.

Figure 3.4 shows the relevant distances and the forces acting on the sprung mass. It is worth to remember that for the out-of-ground plane degrees of freedom, only the sprung mass is considered. This means that the force $F_{z,axles}$ and the moment $M_{x,axles}$ are coming from the axles and not directly from the road. Moreover, it is important to

notice that the moment $M_{x,axles}$ coming from the axles is such that the line of action of the force $F_{z,axles}$ passes through the CG_S, even in the rolled configuration.

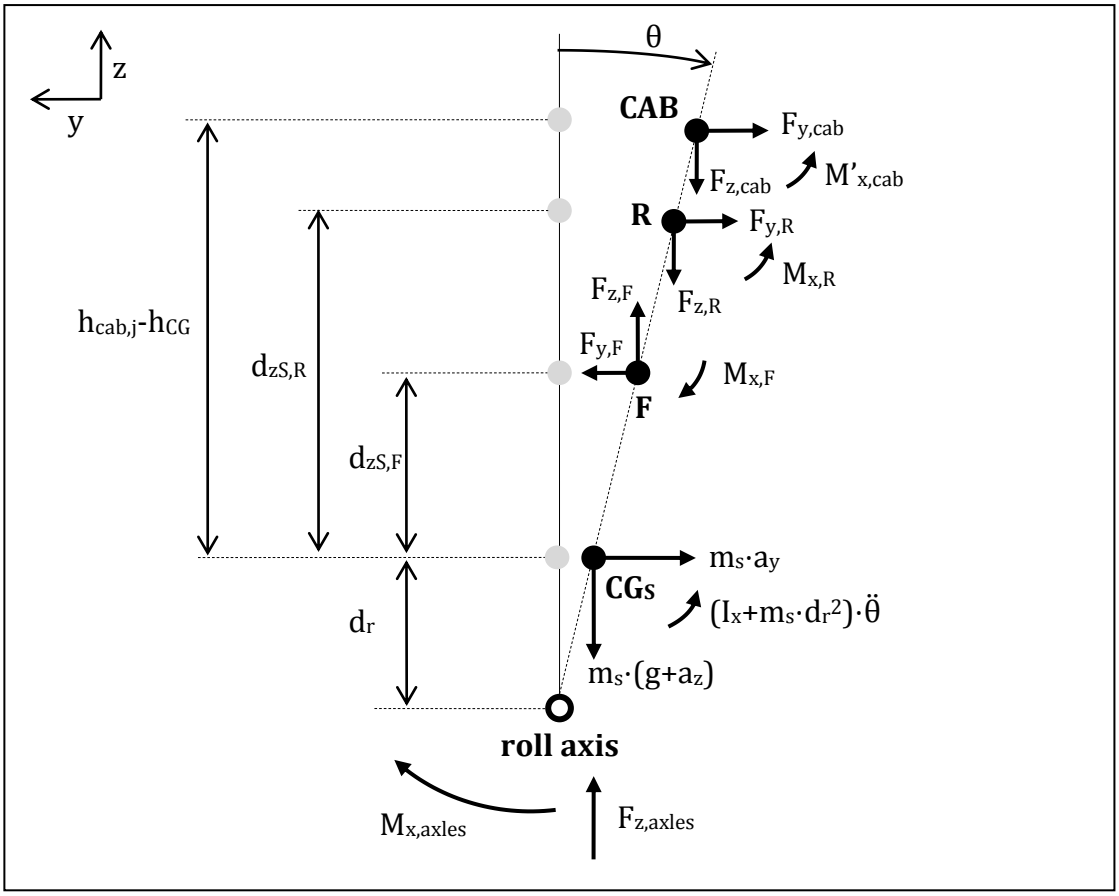

Figure 3.4 Forces and moments acting on a unit in the yz-plane.

The equilibrium around the CG_S is expressed by Equation (3.16). The equilibrium may be performed around the roll centre equivalently, but the moments around the CG_S can be used directly for the frame torsion calculation (Equation (3.26)). The axle free body diagram in section 4.2 shows how the forces coming from the road are transmitted through the axle to the sprung mass.

$$\begin{aligned}\left(I_x + m_s \cdot {d_r}^2\right) \cdot \ddot{\theta} = \\ M_{x,axles} - M_{x,cab} + M_{x,F} - F_{y,F} \cdot d_{zS,F} - F_{z,F} \cdot \theta \cdot d_{zS,F} + \\ -M_{x,R} + F_{y,R} \cdot d_{zS,R} + F_{z,R} \cdot \theta \cdot d_{zS,R} + M_{x,ext}\end{aligned} \tag{3.16}$$

The moment $M_{x,axles}$ is the sum of the moments $M_{x,axle}$ of each axle of the unit, which comes from Equation (4.4).

$$M_{x,axles} = \sum_{axles} M_{x,axle} \tag{3.17}$$

The moment $M_{x,cab}$ present in Equation (3.16) is the moment calculated in Equation (5.11), while Figure 3.4 shows the moment $M'_{x,cab}$, which is equal to the term ${}^{C}M_{x,j}$ in the same equation.

During roll rotations, the sprung mass rotates around the roll centre, describing an arc of circle. Consequently, the relative lateral position of the CG_S and the points CAB, F and R will change accordingly. This is taken into account in Equation (3.16). The vertical displacement can be neglected for small roll angles. The situation for the tractor is more complex, as a roll angle cannot be defined for the whole unit because of frame torsion. Consequently, the corresponding roll angles at the specific longitudinal positions of CAB, F and R are used for the calculations. This will be further presented in Section 3.2.

3.1.5 Pitch dynamics

With the pitch axis concept, the pitch motion is started by the longitudinal forces at the tyres, that are developed e.g. after an input from the powertrain or the brakes. This force acts on the sprung mass at the height of the pitch axis. This has as a consequence a pitch moment, that causes in turn a pitch acceleration. When a pitch rate and a pitch angle have been created, the springs and dampers of the suspensions come into play and generate a counteracting moment, which will eventually bring the system to a steady-state.
The longitudinal position of the pitch axis of each unit was found as the point around which a pure pitch rotation would cause a null net vertical force due to the compression of the springs. This means that for the semitrailers it will be at the middle axle and for the dolly at the middle point between the two axles. The vertical position was assumed equal to the centre of the wheels.
During pitch rotations, the sprung mass rotates around the pitch centre, similarly to the roll rotations around the roll axis. However, in this case the sprung mass will move both longitudinally and vertically of a not negligible amount, being the pitch axis at a different x coordinate with respect to the CG_S.

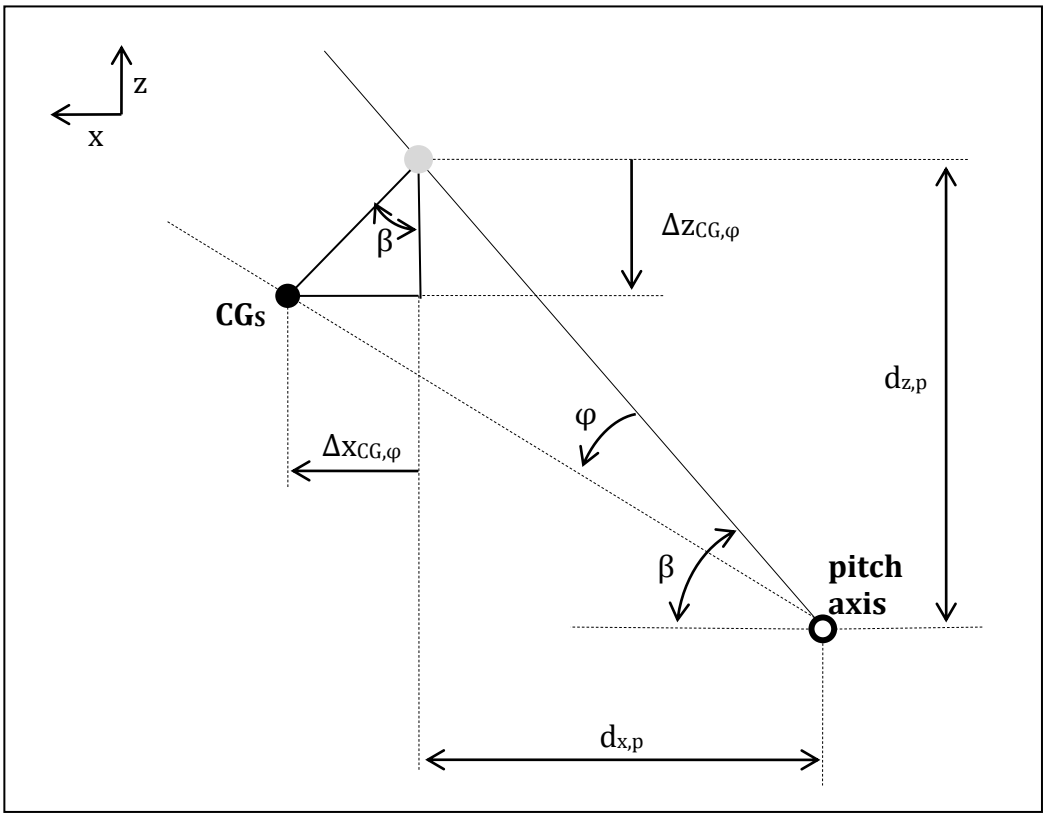

Figure 3.5 CG_S displacement in the xz-plane during pitch motion.

The distance of the CG_S from the pitch axis is found through the longitudinal and the vertical distances at rest, thanks to the Pythagorean theorem. Moreover, the angle with respect to the x-axis is found from the same distances.

$$d_p = \sqrt{\left({d_{x,p}}^2 + {d_{z,p}}^2\right)}$$
$$\beta = \tan^{-1}\left(\frac{d_{z,p}}{d_{x,p}}\right) \tag{3.18}$$

The distance variations of the CG_S relative to the axles are defined positive in the positive directions of the axes and are found by Equations (3.19). They are used in the calculations of the pitch moment of the axles (see Figure 4.2 and Equation (4.6)). On the contrary, the variations of the relative distances of the points CAB, F and R from the CG_S are not considered. The motivation is that these variations are smaller, as all these points rotate during pitch motion, even though with different arcs.

$$\Delta x_{CG,\varphi} = d_p \cdot \varphi \cdot \sin\beta$$
$$\Delta z_{CG,\varphi} = -d_p \cdot \varphi \cdot \cos\beta \tag{3.19}$$

Figure 3.6 shows the pitched configuration of the sprung mass of a unit, with the displacement of the centre of gravity of the sprung mass (CG_S), of the point of cabin-chassis joint (CAB) and of the two coupling points (F and R). The grey points are prior to pitch (at rest), while the black ones are after pitch.

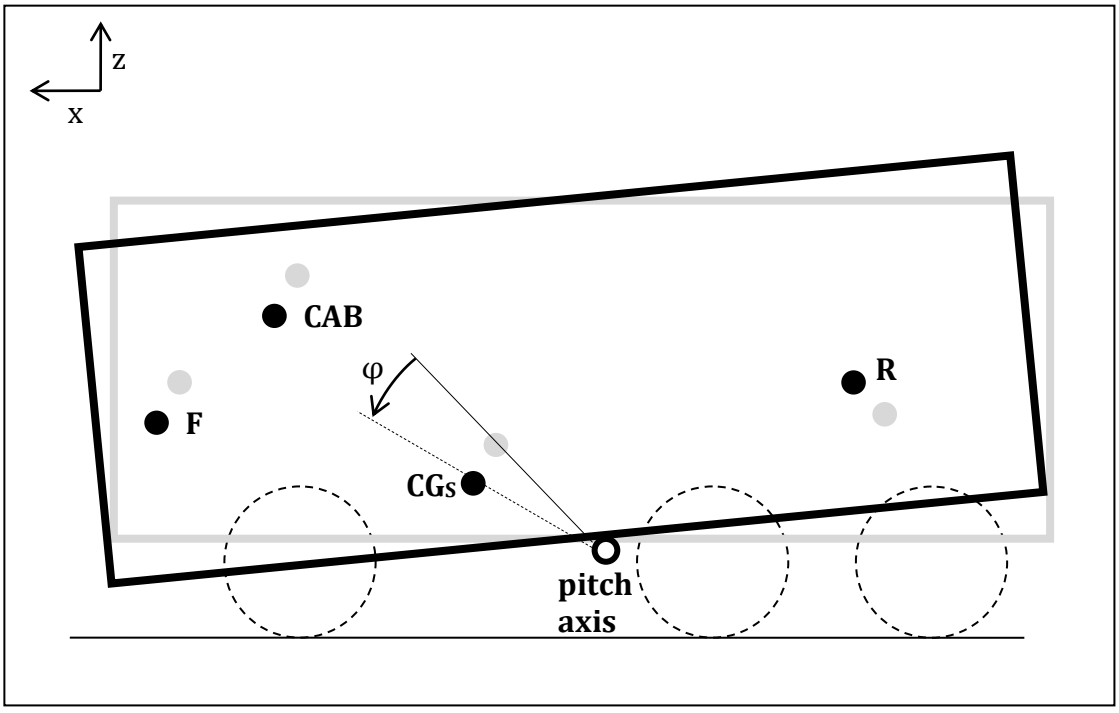

Figure 3.6 Sprung mass in the pitched configuration around the pitch axis, with some highlighted relevant points.

Figure 3.7 shows the relevant distances and the forces acting on the sprung mass. The considerations done for the roll about the force and moment from the axles holds here in an analogous way.

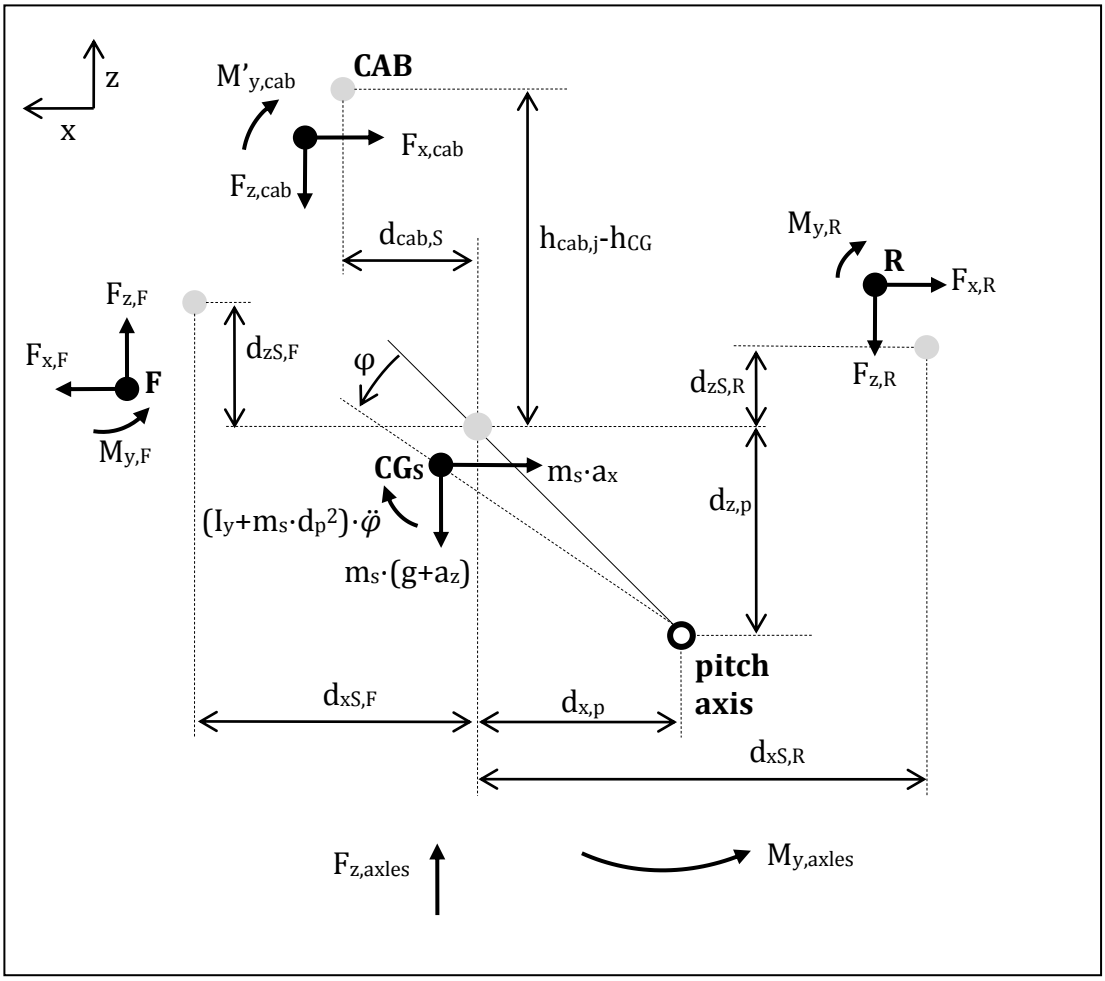

Figure 3.7 Forces and moments acting on a unit in the xz-plane.

The equilibrium around the CG_S is expressed by the Equation (3.20).

$$\begin{aligned}\left(I_y + m_s \cdot {d_p}^2\right) \cdot \ddot{\varphi} = \\ M_{y,axles} - M_{y,cab} + M_{y,F} + F_{x,F} \cdot d_{zS,F} + F_{z,F} \cdot d_{xS,F} + \\ -M_{y,R} - F_{x,R} \cdot d_{zS,R} - F_{z,R} \cdot d_{xS,R} + M_{y,ext}\end{aligned} \tag{3.20}$$

The moment $M_{y,axles}$ is the sum of the moments $M_{y,axle}$ of each axle of the unit, which comes from Equation (4.6).

$$M_{y,axles} = \sum_{axles} M_{y,axle} \tag{3.21}$$

The moment $M_{y,cab}$ is the moment calculated in Equation (5.11), while Figure 3.7 shows the moment $M'_{y,cab}$, which is equal to the term ${}^{C}M_{y,j}$ in the same equation.

3.1.6 Yaw dynamics

The yaw equilibrium around the CG can be expressed by Equation (3.22), which is derived from Figure 3.1. It is important to notice that the moment $M_{z,axles}$ coming from the road is such that the lines of action of the forces $F_{x,axles}$ and $F_{y,axles}$ pass through the CG.

$$I_z\ddot{\psi} = M_{z,axles} - M_{z,cab} + M_{z,F} - F_{y,F} \cdot d_{x,F} - M_{z,R} + F_{y,R} \cdot d_{x,R} + M_{z,ext} \quad (3.22)$$

The second order derivative of the yaw angle gives rise to two state variables, the yaw rate $\dot{\psi}$ and the yaw angle ψ.
The moment $M_{z,axles}$ is the sum of the moments $M_{z,axle}$ of each axle of the unit, which comes from Equation (4.7).

$$M_{z,axles} = \sum_{axles} M_{z,axle} \quad (3.23)$$

The moment $M_{z,cab}$ is the moment calculated in Equation (5.11), while Figure 3.1 shows the moment $M'_{z,cab}$, which is equal to the term ${}^{C}M_{z,j}$ in the same equation.

3.2 Frame torsion

The frame torsion is a fundamental aspect of trucks dynamics. Only the frame of the tractor unit is considered flexible, while for the other units it is considered as infinitely stiff. This is mainly because the effect of the frame flexibility of the other units is much lower to the vehicle trajectory and to the cabin motion.
The OEM model implements the frame flexibility by modelling two rigid bodies which are connected one to the other by means of a torsional spring, as already stated and illustrated in Section 2.3. This is the most obvious solution when working with multi-body simulation tools, as a solution with one single body would require it to be deformable. The various components (axles, cabin, rear articulation joint) are mechanically connected to either the front body or the rear body. These two bodies have two different roll angles, whose difference defines the torsion angle.
In order to follow the same approach in the Modelica model, two different roll equations should be formulated, one for the front body and one for the rear body. In this thesis, another approach is chosen: there is only one roll equation in the vehicle CG_S (Equation (3.16)), that means that it is the same equation as for the vehicle with infinitely stiff frame. As shown in Section 2.4.5 this is also the same equation as for the two semitrailers and the dolly. To this, a torsion equation is added, which will determine the roll angles at each longitudinal position of the vehicle other than the CG_S, as clarified in the following.
Even though the chassis is thought as one single body, we need to define two points along the frame that will define the length of the frame section that is subject to torsion. These points will be taken as the ideally unique points of application of torques. This is needed in order to have only one degree of freedom. More complex dynamics can be studied, considering the frame as composed by different sections, with each torsion angle defined by a different equation. Ideally, it would be necessary to put a point anywhere an external torque is applied.
The two reference points are taken at the front axle and at position of the fifth wheel, according to the OEM definition. The torques which are not applied at these points will be scaled by a coefficient to take it into account. By doing so, the approximation of having one degree of freedom is partially balanced. However, a good approximation requires that each torque is applied close to the reference points.
Figure 3.8 shows an industrial vehicle frame subject to a torsion test. It can be seen that both rails and crossmembers are subject to torsion, but not to bending, i.e. their

axes keep straight. When this is true, the torsion can be modelled by a single degree of freedom and linearity applies, which justifies using linear equations (Equation (3.25)).

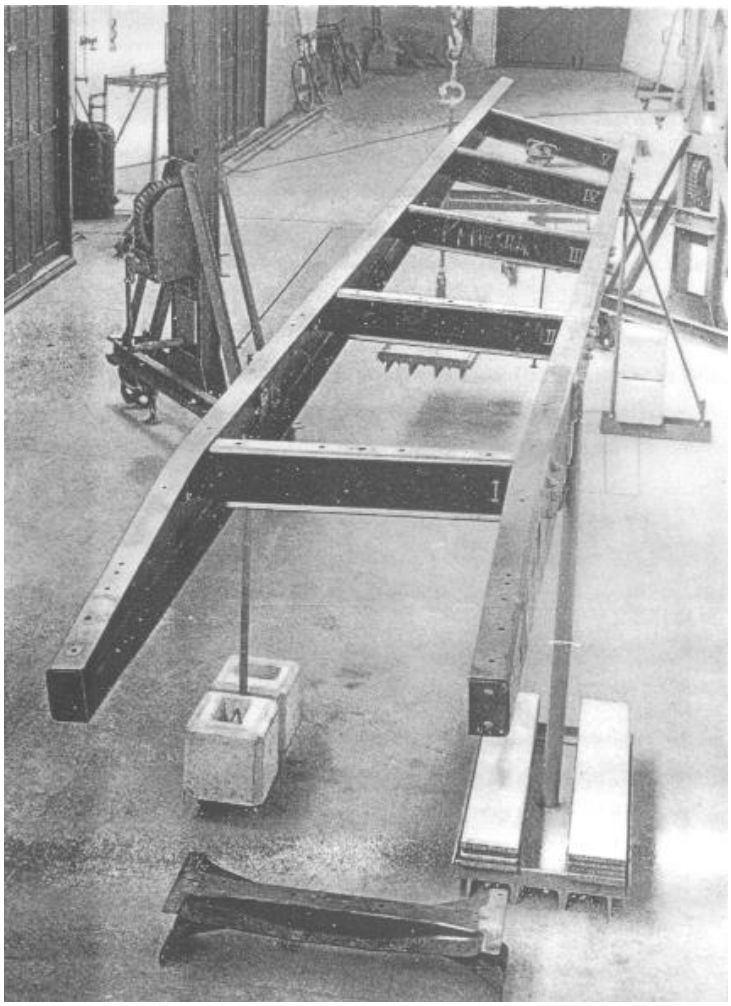

Figure 3.8 Ladder frame subject to a torsion test, from Morello (2001).

As already mentioned (Section 3.1.4), the torques used for the torsion equation are the same as the for the roll calculations. However, the torques applied at the front reference point will have opposite sign with respect to the torques at the rear reference point. This is because only a difference between the roll moments at the front and at the rear of the tractor would cause a frame torsion. It can be better understood thanks to the analogy of the interaction of roll or pitch moments with vertical forces: the suspensions act on the sprung mass with vertical forces and different combinations of them may cause either only pitch or only roll or only heave or a combination of them. In the same way, the roll moments may cause either only roll or only torsion or both of them.

Figure 3.9 shows a schematic representation of the chassis frame subject to both roll and torsion. For simplicity, the frame is represented by a longitudinal line (representing the two longitudinal rails) and three transversal lines showing the frame orientation at the positions of the CG_S and of the two reference points, called F_{ref} and R_{ref}. When torsion takes place, the roll angles at each of these three points are different, as shown in the scheme (the hatched transversal lines represent the orientation of the frame after roll and torsion).

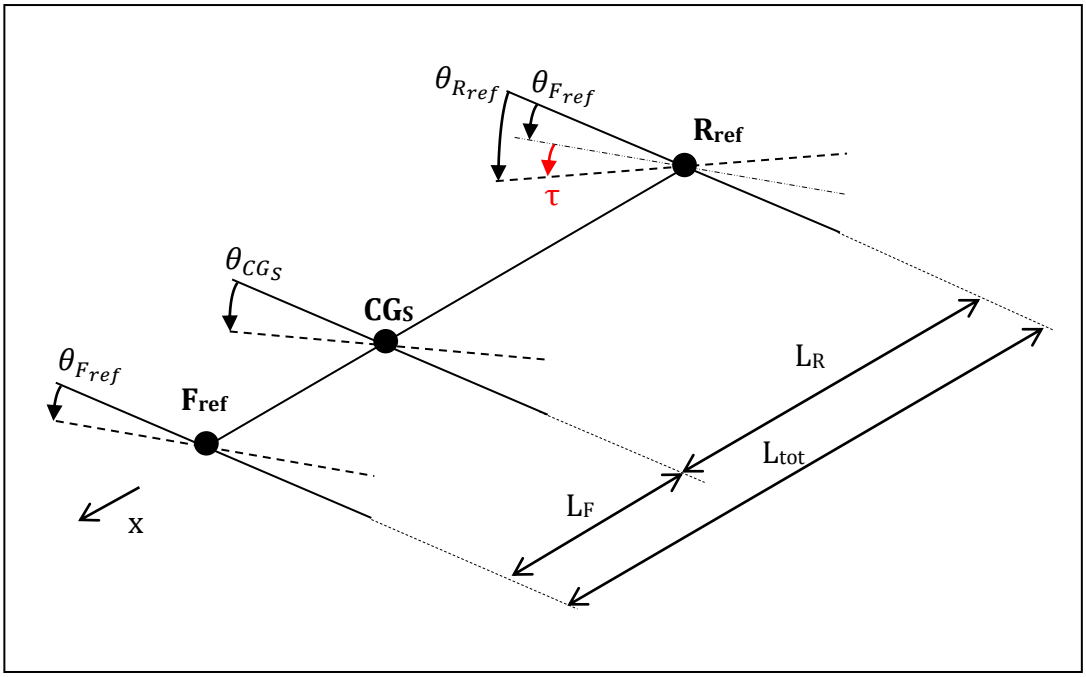

Figure 3.9 Coupled roll and torsion of frame, schematic representation.

The torsion angle τ is then defined as the difference between the roll angles at the two reference points. This is the same definition as for the OEM model.

$$\tau = \theta_{R_{ref}} - \theta_{F_{ref}} \tag{3.24}$$

However, differently from the OEM model, here the roll angle is defined at each longitudinal position of the frame. In accordance with the previously mentioned assumption, the roll angle is linearly increasing (or decreasing, depending on the sign of τ) along the whole frame.
As θ_{CG_S} is the known variable from the roll equilibrium (Equation (3.16)), it can be used to find all other roll angles by adding (or subtracting) a fraction of the torsion angle τ. For instance the roll angle at the front reference point is found by Equation (3.25). This angle, minus the roll angle of the steered axle, is used in the roll steer term of the tractor steering system (Equation (7.7)).

$$\theta_{F_{ref}} = \theta_{CG_S} - \tau \cdot \frac{L_F}{L_{tot}} \tag{3.25}$$

Moreover, all the roll angles and rates needed for calculations in the tractor need to take into account for the torsion and this affects the roll angle for: rear articulation joint, axles, roll steer, cabin. This is done using the same kind of linear equation.
In addition, the stabilisers of the axles are not in the same longitudinal position of their connections to the chassis. Therefore, the stabiliser moments need to use the roll angle at its actual position, which is different from the position of the axle which it belongs to.
The warp angle and warp rate are found by the Equation (3.26), where the moments applied to the two reference points are summed together (with opposite signs). To them, the contributions of the frame stiffness and damping are also added. The torsional stiffness k_t was found from the specific torsional stiffness $k_{t,s}$ which has units [N·m·m/rad]. To be specific, it had to be divided by the length of the frame

section subject to torsion, i.e. L_{tot}, which result in a torsional stiffness with units [N·m/rad]. In fact, the stiffness is inversely proportional to the length of the frame section subject to torsion.

$$-k_t \cdot \tau - c_t \cdot \dot{\tau} + \sum M_{x,R_{ref}} - \sum M_{x,F_{ref}} = 0 \tag{3.26}$$

Under the stated assumptions, the moments are supposed to be acting in the two reference points only. If this conditions is not satisfied, more degrees of freedom would be needed. However, moments applied close to the reference points can be taken into account with a scaling factor: moments will be reduced if applied closer to the other reference point or increased otherwise. This is an approximated way to take into consideration that the shorter the frame, the stiffer it is. An example is shown in the following, with reference to Figure 3.10.

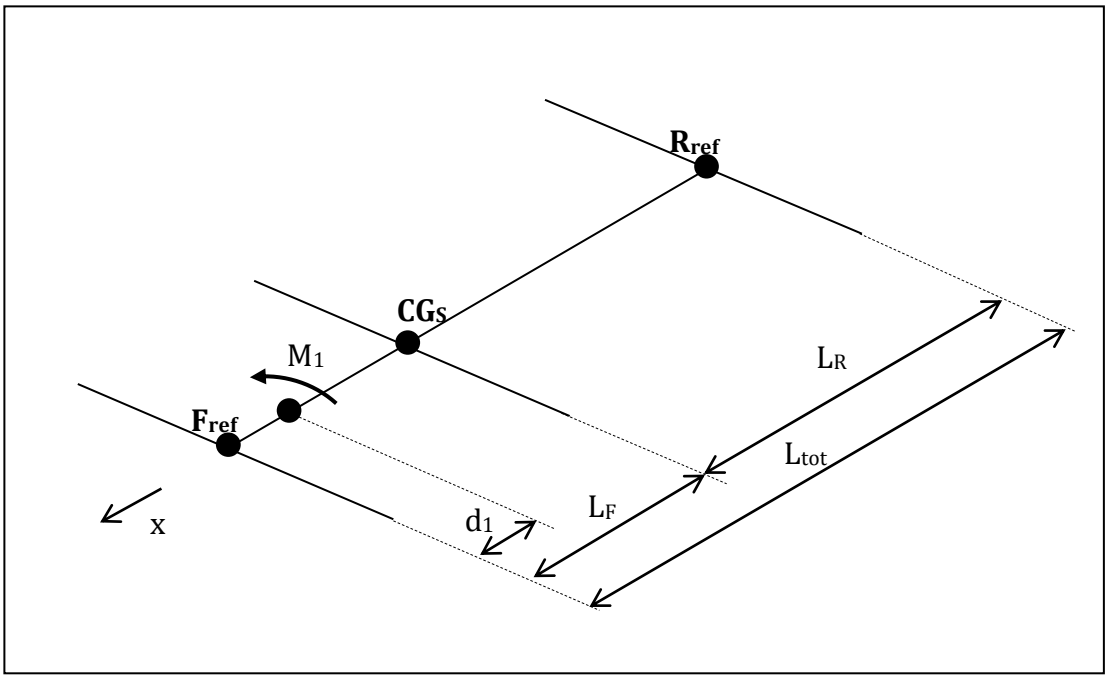

Figure 3.10 Example of a torque applied close to one of the two reference points.

The moment M_1 that is used in the roll equation will not be used with the same value in the torsion equation, but it will be scaled by the factor in Equation (3.27).

$$(1 - \frac{d_1}{L_{tot}}) \tag{3.27}$$

3.3 Velocities to articulation joints

The three components of velocity of the articulation joint points F and R are calculated by making use of the chassis variables. The velocities of the point R of one unit (towing unit) will be equal to the velocities of the point F of the successive unit (towed unit). This equality is handled within the *coupling* model (see Section 6, specifically Equations (6.3)).

$$\begin{pmatrix} V_{x,F} \\ V_{y,F} \\ V_{z,F} \end{pmatrix} = \begin{pmatrix} V_x \\ V_y - \dot{\psi} \cdot d_{x,F} - \dot{\theta} \cdot (h_F - h_r) \\ V_z + \dot{\varphi} \cdot d_{F,P} \end{pmatrix}$$
$$\begin{pmatrix} V_{x,R} \\ V_{y,R} \\ V_{z,R} \end{pmatrix} = \begin{pmatrix} V_x \\ V_y - \dot{\psi} \cdot d_{x,R} - \dot{\theta} \cdot (h_R - h_r) \\ V_z + \dot{\varphi} \cdot d_{R,P} \end{pmatrix} \quad (3.28)$$

4 Axles

This system represents a rigid axle, together with its two wheels and its suspension components, i.e. two springs, two dampers and a stabiliser (or anti-roll bar). It has two degrees of freedom with respect to the sprung mass, i.e. in roll and heave. According to previous statements in the previous Chapter, the forces and moments acting to the chassis coming from the road, directly or through the axles, are here computed. The difference between the in-road-plane and the out-of-road-plane degrees of freedom should be kept in mind. A generic axle is considered, so as to use the same equations for all of the axles of the vehicle.

4.1 Forces and moments to the sprung mass

The vertical force transmitted to the sprung mass (see Figure 3.4 and Figure 3.7 and Equations (3.8) and (3.11)) is made of the forces of the springs and the dampers, as shown in Figure 4.1. How these forces are computed is illustrated in Section 4.3.
The longitudinal and lateral forces (see Figure 3.1 and respectively Equations (3.1) and (3.3) for the longitudinal force and (3.5) and (3.7) for the lateral force) comprise only the tyre forces and can be computed by looking at Figure 4.3. The tyre forces calculations are illustrated in Section 4.5. The wheels steer angles are set by the steering system as shown in Section 7.

$$F_{x,axle} = F_{x,tyreL} \cdot \cos\delta_L + F_{x,tyreR} \cdot \cos\delta_R - F_{y,tyreL} \cdot \sin\delta_L - F_{y,tyreR} \cdot \sin\delta_R \tag{4.1}$$

$$F_{y,axle} = F_{y,tyreL} \cdot \cos\delta_L + F_{y,tyreR} \cdot \cos\delta_R + F_{x,tyreL} \cdot \sin\delta_L + F_{x,tyreR} \cdot \sin\delta_R \tag{4.2}$$

$$F_{z,axle} = F_{spring,L} + F_{spring,R} + F_{damp,L} + F_{damp,R} \tag{4.3}$$

Figure 4.1 shows the suspension forces in the yz-plane that an axle exchanges with the sprung mass for the rolled situation (see Figure 3.4 and Equations (3.16) and (3.17)). The lateral force $F_{y,axle}$ is assumed to be transmitted to the chassis at the axle roll centre, which is at a different height of the unit roll axis in the case of the tractor.
The chassis will react to the axle with the same forces, as shown in Figure 4.4.

$$\begin{aligned} M_{x,axle} = {} & F_{y,axle} \cdot d_r + M_{stab} + \\ & + F_{spring,L} \cdot \left(\frac{d_{springs}}{2} + \theta_{rel} \cdot d_r\right) - F_{spring,R} \cdot \left(\frac{d_{springs}}{2} - \theta_{rel} \cdot d_r\right) + \\ & + F_{damp,L} \cdot \left(\frac{d_{damps}}{2} + \theta_{rel} \cdot d_r\right) - F_{damp,R} \cdot \left(\frac{d_{damps}}{2} - \theta_{rel} \cdot d_r\right) \end{aligned} \tag{4.4}$$

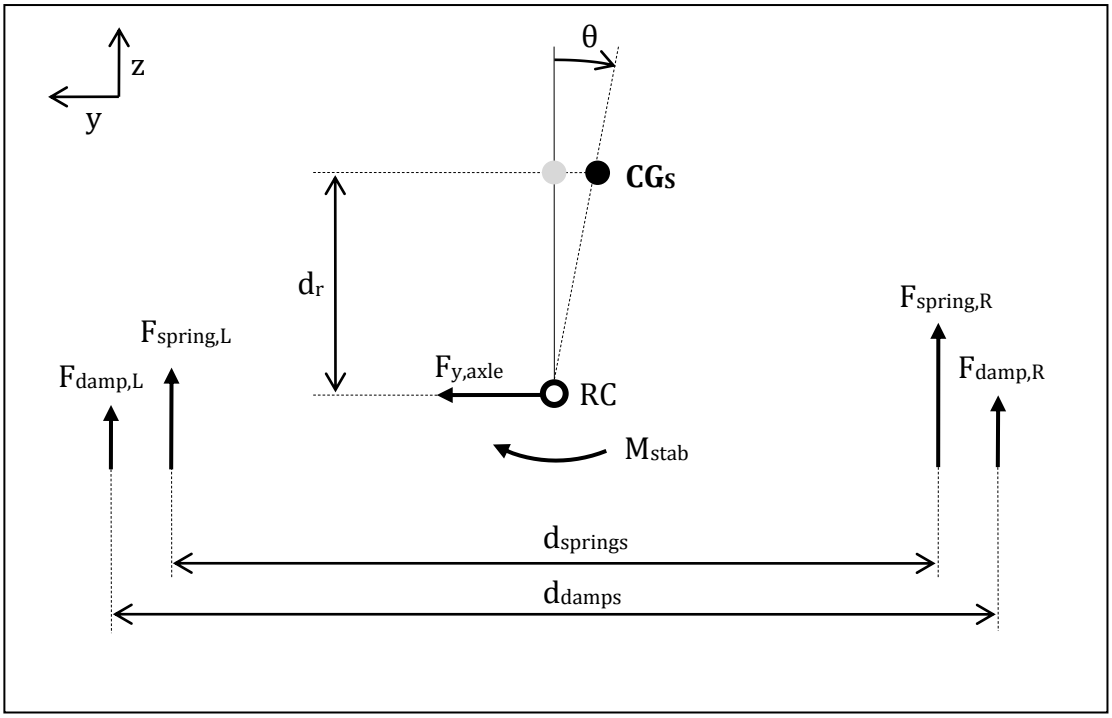

Figure 4.1 Forces and moments that an axle transmits to the sprung mass in the yz-plane.

The arms of the springs and dampers forces to the point CG_S vary due to roll dynamics, knowing that the lateral movement of the centre of gravity is assumed linear with the chassis roll angle and the suspension forces rotate with the axle roll angle (hence the use of the relative roll angle).

$$\theta_{rel} = \theta - \theta_{axle} \tag{4.5}$$

Figure 4.2 shows the sprung mass CG_S before (in grey) and after (in black) a pitch angle and the forces in the xz-plane that an axle exchanges with the sprung mass (see Figure 3.7 and Equations (3.20) and (3.21)). The force $F_{x,axle}$ is assumed to be transmitted to the chassis at the height of the pitch axis.

$$M_{y,axle} = -F_{x,axle} \cdot \left(d_{z,p} + \Delta z_{CG,\varphi}\right) + F_{z,axle} \cdot \left(d_{axle,S} + \Delta x_{CG,\varphi}\right) \tag{4.6}$$

Even though the figure shows an example of an axle rearward the CG_S, the equation holds as well for a forward axle, as the distance from the CG_S would be negative.

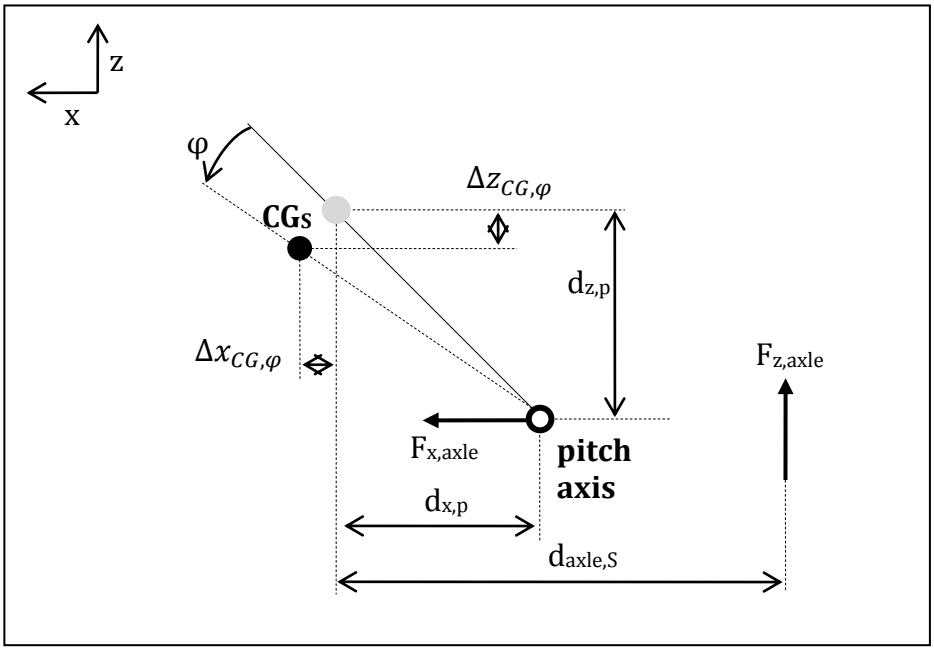

Figure 4.2 Forces and moments that an axle transmits to the sprung mass in the xz-plane.

Figure 4.3 shows the forces in the xy-plane that the road transmits to the vehicle (see Equations (3.22) and (3.23) for the yaw moments). The tyres aligning torques are found in Section 4.5 (Equation (4.24)). The shown scenario is for a steered axle, whereas in the other cases the steer angles are obviously null.

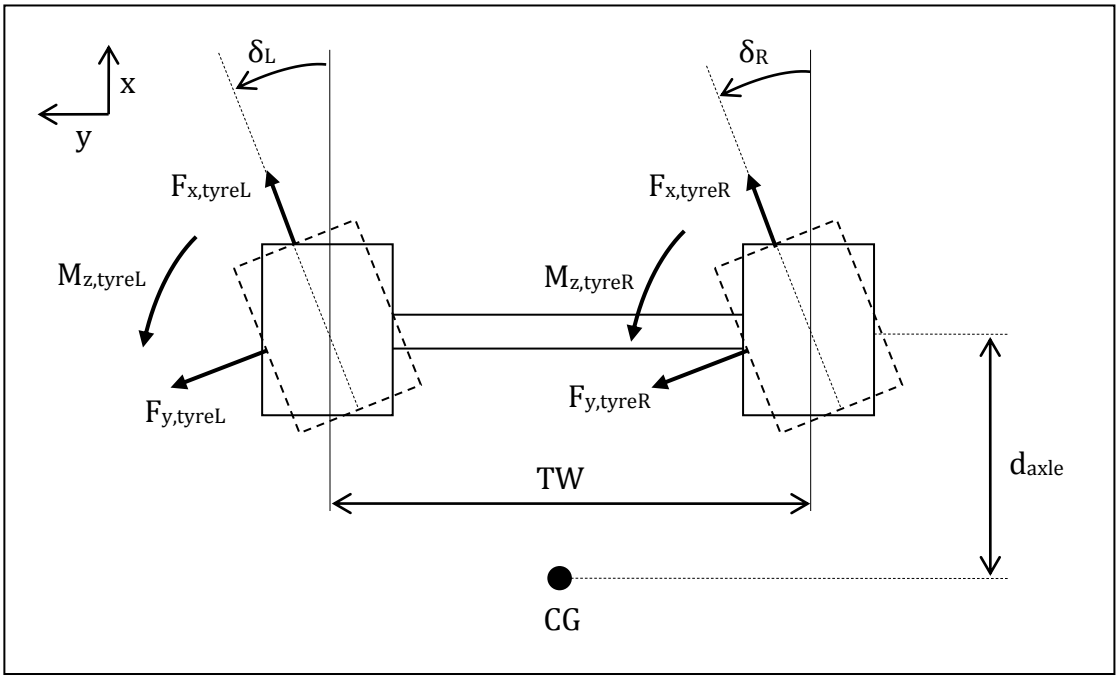

Figure 4.3 Forces and moments at the tyre-road contact for a steered axle.

$$M_{z,axle} = M_{z,tyreL} + M_{z,tyreR} - F_{y,axle} \cdot d_{axle} + (-F_{x,tyreL} \cdot \cos\delta_L + \\ +F_{x,tyreR} \cdot \cos\delta_R + F_{y,tyreL} \cdot \sin\delta_L - F_{y,tyreR} \cdot \sin\delta_R) \cdot \frac{TW}{2} \quad (4.7)$$

4.2 Axle dynamics

The free body diagram of the axle in the yz-plane is shown in Figure 4.4. The axle dynamics is represented in the unrolled configuration, as having the centre of gravity in the same position of the roll centre makes it equivalent to the rolled configuration.

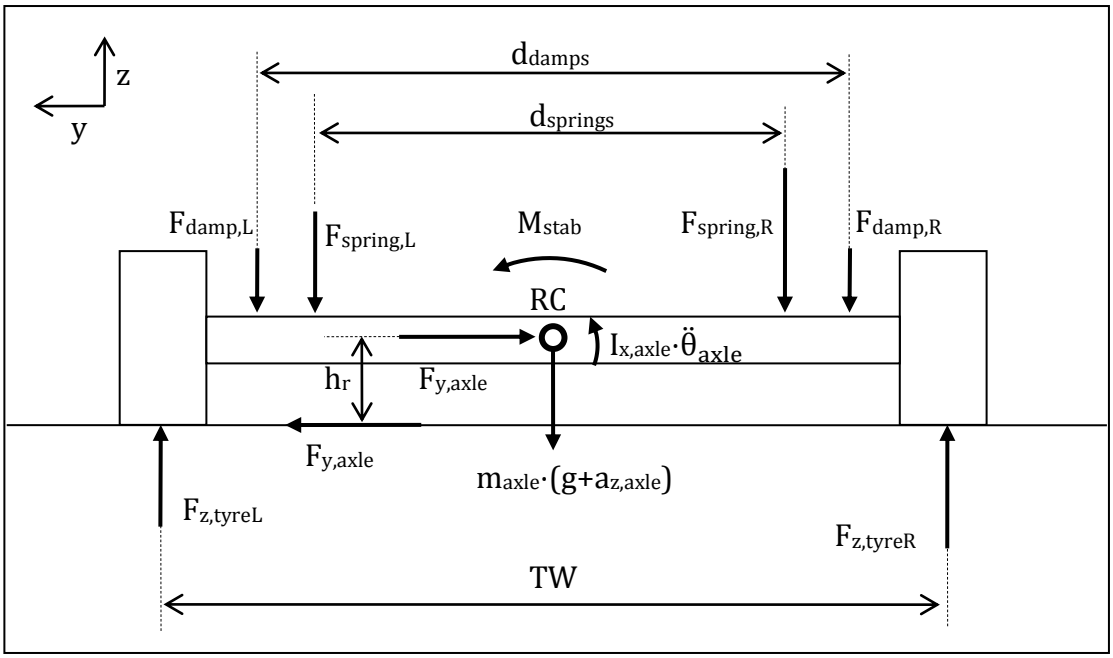

Figure 4.4 Free-body diagram of an axle in the yz-plane.

The shown forces determine the two equations of motion of the axle in heave (Equation (4.8)) and of roll (Equation (4.9)).

$$m_{axle} \cdot a_{z,axle} = F_{z,tyreL} + F_{z,tyreR} - F_{z,axle} - m_{axle} \cdot g \quad (4.8)$$

$$I_{x,axle} \cdot \ddot{\theta}_{axle} = \left(F_{z,tyreL} - F_{z,tyreR}\right) \cdot \frac{TW}{2} + F_{y,axle} \cdot h_r - M_{stab} + \\ -\left(F_{springL} - F_{springR}\right) \cdot \frac{d_{springs}}{2} - \left(F_{dampL} - F_{dampR}\right) \cdot \frac{d_{damps}}{2} \quad (4.9)$$

The axle is able to heave and roll relative to the ground thanks to the vertical compression of the tyres. Furthermore, being a rigid axle, this is completely determined by the wheel vertical displacements, as shown in Figure 4.5 and Equations (4.10) and (4.11). The vertical position of the axle z_{axle} is the second order derivative of the axle vertical acceleration $a_{z,axle}$, while $V_{z,axle}$is the first order derivative.

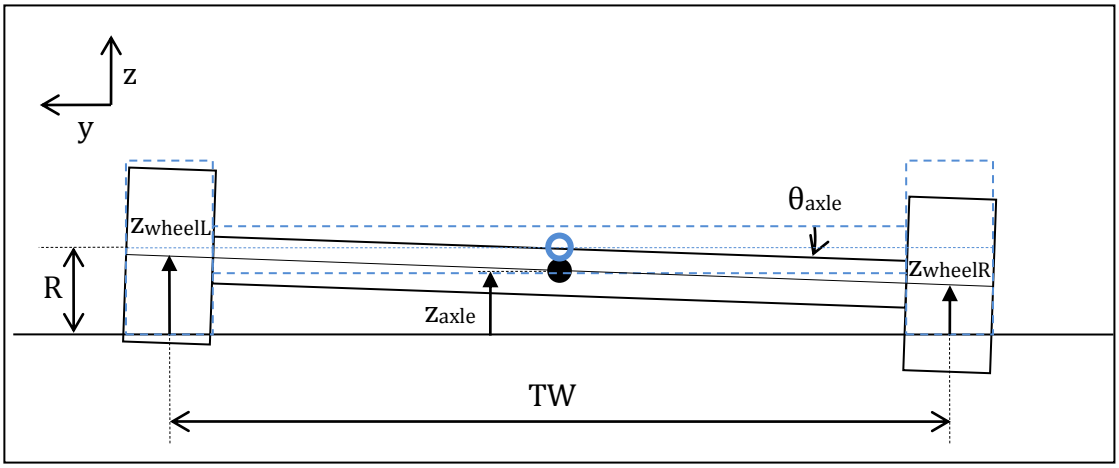

Figure 4.5 Axle shown in an exaggerated configuration of roll and heave, with the tyres intersecting the ground (as if they were not deformed).

$$z_{axle} = \frac{1}{2} \cdot (z_{wheelL} + z_{wheelR}) \tag{4.10}$$

$$\theta_{axle} = \frac{(z_{wheelL} - z_{wheelR})}{TW} \tag{4.11}$$

4.3 Springs, dampers and stabilisers

Both springs and dampers have constant linear coefficients. For each side of an axle, they are placed in two different positions; in particular, the springs are closer to the axle center (and thus further away from the wheels). This means that the derivative of the spring displacement is different from the velocity of the damper.
The stabilisers have longitudinal offsets from the axles. This has a consequence in the tractor, where frame torsion is present: the relative roll angle between the stabilisers and the chassis is different from the one between axle and chassis; moreover, the stabiliser moment will be multiplied by a factor as explained in section 3.2.
The spring displacement and damper rod velocity will be given by the Equations (4.12) and (4.13), which show the three contributions of heave, roll and pitch respectively. They are both defined positive when they are extensions. The heave terms of Equations (4.12) are the difference of variations from static conditions of the vertical positions of the sprung mass (see Equation (3.10)) and of the axle. The last term includes the distance of the axle from the pitch axis, which is found in a straightforward way from other geometrical parameters.

$$\begin{aligned} \Delta z_{springL} &= (\Delta z - \Delta z_{axle}) + \theta_{rel} \cdot \frac{d_{springs}}{2} + \varphi \cdot l_{axle,P} \\ \Delta z_{springR} &= (\Delta z - \Delta z_{axle}) - \theta_{rel} \cdot \frac{d_{springs}}{2} + \varphi \cdot l_{axle,P} \end{aligned} \tag{4.12}$$

$$v_{dampL} = \left(V_z - V_{z,axle}\right) + \dot{\theta}_{rel} \cdot \frac{d_{damps}}{2} + \dot{\varphi} \cdot l_{axle,P}$$
$$v_{dampR} = \left(V_z - V_{z,axle}\right) - \dot{\theta}_{rel} \cdot \frac{d_{damps}}{2} + \dot{\varphi} \cdot l_{axle,P} \quad (4.13)$$

Once that the spring displacements and dampers velocities are given, their forces are found by Equations (4.14) and (4.15), where *i* can be either *L* or *R*. Moreover, the stabiliser moment is proportional to the relative roll angle by means of a constant stiffness coefficient.

$$F_{spring,i} = -k_s \cdot \Delta z_{spring,i} + F_{static} \quad (4.14)$$

$$F_{damp,i} = -c_d \cdot v_{damp,i} \quad (4.15)$$

$$M_{stab} = -k_{stab} \cdot \theta_{rel} \quad (4.16)$$

In the Modelica model, the static force of the spring, or preload, is determined by the solution of the initialization problem. The motivation is that an analytical expression for the preload can be written only if the combination vehicle is known in advance, as the loads in the axles of one unit depend on the towed unit. Therefore, this modelling choice was done to allow for automatically finding the loads for any combination.

4.4 Wheels

The vertical tyre force is calculated assuming that the tyre behaves as a spring (with stiffness $n_W \cdot k_w$, where n_W is the number of wheels per axle side, i.e. 2 for twin tyres) when vertically compressed (Equation (4.17)(4.18)).

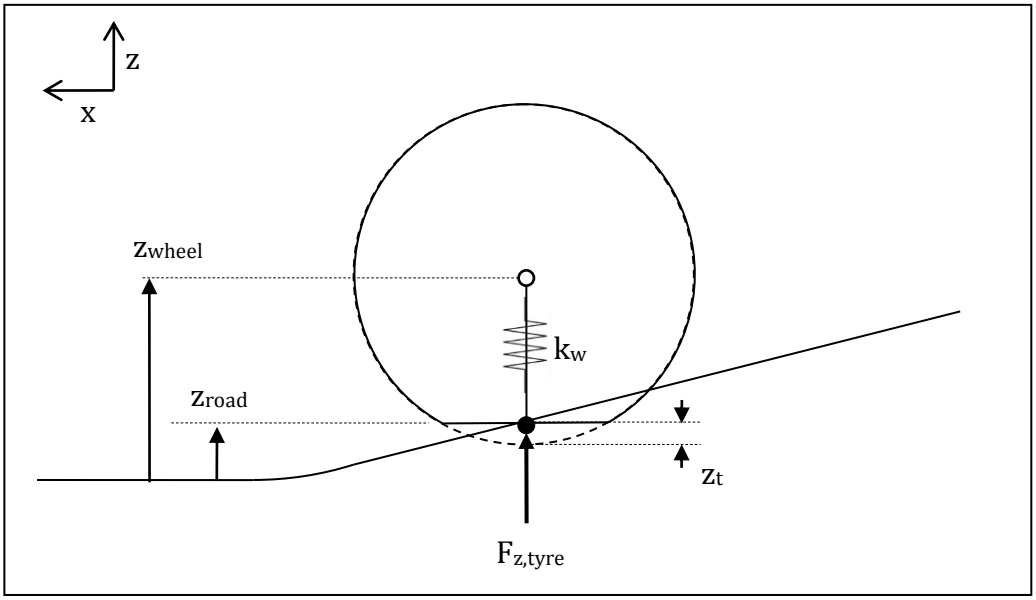

Figure 4.6 Scheme for the calculation of the vertical load on a tyre.

$$F_{z,tyre} = F_{z,static,tyre} + n_W \cdot k_w \cdot z_t \tag{4.17}$$

$$-z_t = (z_{wheel} - R) - z_{road} \tag{4.18}$$

The static force on the tyre will be found by the spring preload, which in turn comes from the solution of the initialization problem, as explained in the previous section.

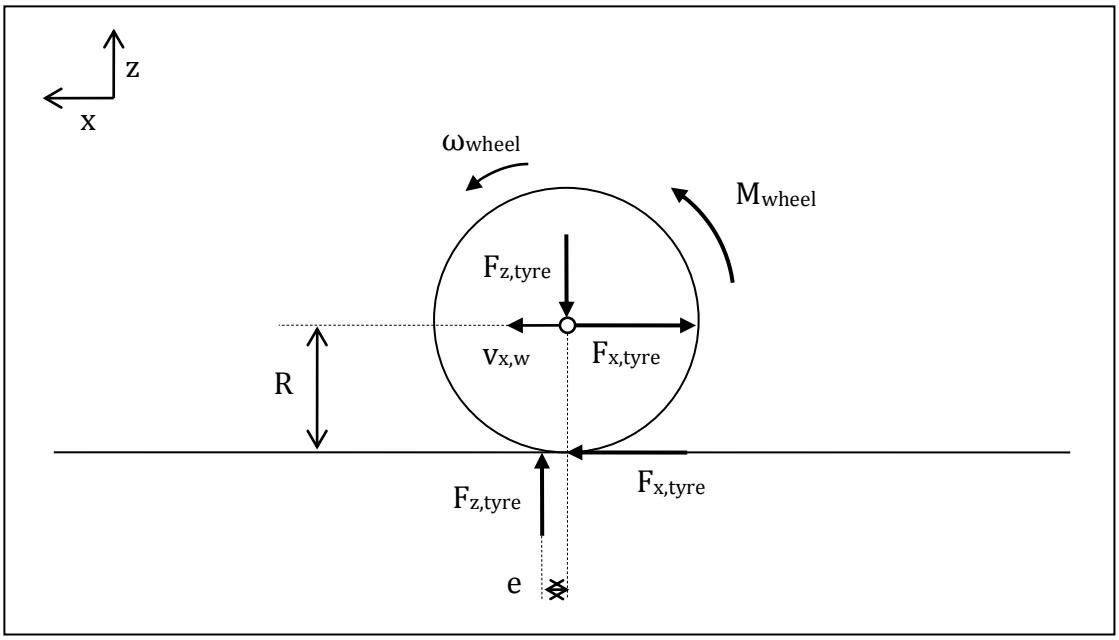

Figure 4.7 Equilibrium of a wheel in the xz-plane.

When the tyre is rolling, the resultant vertical load $F_{z,tyre}$ is applied forward the axis of rotation. This provokes what is called rolling resistance, as the longitudinal force transmitted to the wheel hub is decreased of the quantity $F_{z,tyre} \cdot \frac{e}{R}$ with respect to the ideal situation (i.e. $F_{z,tyre}$ applied at the axis of rotation).

$$F_{x,tyre} = \frac{M_{wheel}}{R} - F_{z,tyre} \cdot \frac{e}{R} \tag{4.19}$$

The coefficient $f_r = \frac{e}{R}$ is the coefficient of rolling resistance and for truck tyres can be assumed to be constant with speed and equal to 0.008.
The moment M_{wheel} is the sum of the drive torque of Equation (8.3) and of braking torque of Equation (9.1) for the driven wheels, whereas only the latter term is used for the non driven wheels.

4.5 Tyres

Simply linear tyre models are used, as it seemed to be sufficient for the chosen context (see Section 10.1). The slip angle is found from the velocities of the wheel hub and the steer angle, as in Equation (4.20).

$$\alpha = \frac{v_{x,w}}{v_{y,w}} - \delta \tag{4.20}$$

The cornering stiffness C is found by multiplying the cornering coefficient C_0 by the tyre vertical load. The slope at the origin of the tyre characteristic was used to calculate the cornering coefficient of the tyre.

$$C = C_0 \cdot F_{z,tyre} \tag{4.21}$$

$$F_{y,tyre} = -C \cdot \tan \alpha \tag{4.22}$$

The velocities are calculated from the unit yaw rate and velocities.

$$\begin{aligned} v_{x,wL} &= V_x - \psi \cdot \frac{TW}{2} \\ v_{x,wR} &= V_x + \psi \cdot \frac{TW}{2} \end{aligned} \tag{4.23}$$

$$\begin{aligned} v_{y,wL} &= V_y - \psi \cdot d_{axle} \\ v_{y,wR} &= V_y + \psi \cdot d_{axle} \end{aligned}$$

Finally, the aligning torque is the product of the lateral force times a constant pneumatic trail.

$$M_{z,tyre} = -F_{y,tyre} \cdot t \tag{4.24}$$

The tyre is assumed to roll without tangential deformation. This implies having a direct relationship between the longitudinal speed of the wheel hub and the wheel rotational speed.

$$v_{x,w} = \omega_{wheel} \cdot R \tag{4.25}$$

5 Cabin

The cabin is suspended on the tractor chassis at the same longitudinal position of the front axle and is allowed to move relative to the chassis in heave, roll and pitch. A unique point of joint to the chassis is assumed, which transfers 3 forces and 3 moments. In particular, the joint can be thought as two rotational springs in the x and y directions and a translational spring in the z direction (in the tractor reference frame). The motion of the cabin is always triggered by a movement of this point of connection to the tractor chassis. Therefore, the angles, angular rates and vertical displacement of this point are determined by the tractor chassis. The forces and moments transmitted to the chassis are, on the contrary, determined by the cabin equations of motion, which are calculated in its centre of gravity.
First, the relevant quantities of the point of cabin-chassis joint (marked with the subscript "j") are found. In the whole Chapter, the left-hand superscript of the variables shows if they are in the chassis reference frame ("C") or in the cab reference frame ("cab").

$$
\begin{gathered}
{}^{C}\Delta z_j = {}^{C}\left(\Delta z + \dot{\varphi}\cdot d_{cab,P}\right) \\
{}^{C}\begin{pmatrix} V_{x,j} \\ V_{y,j} \\ V_{z,j} \end{pmatrix} = {}^{C}\begin{pmatrix} V_x \\ V_y - \dot{\psi}\cdot d_{cab} - \dot{\theta}\cdot\left(h_{cab,j} - h_r\right) \\ V_z + \dot{\varphi}\cdot d_{cab,P} \end{pmatrix} \\
{}^{C}\begin{pmatrix} \theta_j \\ \varphi_j \\ \psi_j \end{pmatrix} = {}^{C}\begin{pmatrix} \theta \\ \varphi \\ \psi \end{pmatrix} \\
{}^{C}\begin{pmatrix} \dot{\theta}_J \\ \dot{\varphi}_J \\ \dot{\psi}_J \end{pmatrix} = {}^{C}\begin{pmatrix} \dot{\theta} \\ \dot{\varphi} \\ \dot{\psi} \end{pmatrix}
\end{gathered}
\tag{5.1}
$$

The rotation matrix between the tractor reference frame and the cabin reference frame is as defined in Equation (5.2) and the angles of relative rotation θ_r and φ_r are found thanks to Equation (5.3) (see the Appendix 14.1 for more details). This is according to the fact that these angles are defined in the chassis reference frame and the order of rotation is first about y and then about x.

$$
\mathbf{R} = \mathbf{R_x}(\theta_r)\cdot\mathbf{R_y}(\varphi_r) \tag{5.2}
$$

$$
{}^{C}\begin{pmatrix} \theta_j \\ \varphi_j \\ \psi_j \end{pmatrix} + \begin{pmatrix} \theta_r \\ \varphi_r \\ 0 \end{pmatrix} = \mathbf{R}\cdot {}^{cab}\begin{pmatrix} \theta_{cab} \\ \varphi_{cab} \\ \psi_{cab} \end{pmatrix} \tag{5.3}
$$

According to this definition, all the rotations of the relevant quantities are performed.

$$
\begin{aligned}
{}^{C}\begin{pmatrix}\theta_{cab}\\ \varphi_{cab}\\ \psi_{cab}\end{pmatrix} &= \mathbf{R}\cdot {}^{cab}\begin{pmatrix}\theta_{cab}\\ \varphi_{cab}\\ \psi_{cab}\end{pmatrix}\\
{}^{C}\begin{pmatrix}V_{x,j}\\ V_{y,j}\\ V_{z,j}\end{pmatrix} &= \mathbf{R}\cdot {}^{cab}\begin{pmatrix}V_{x,j}\\ V_{y,j}\\ V_{z,j}\end{pmatrix}\\
{}^{C}\begin{pmatrix}V_{x,cab}\\ V_{y,cab}\\ V_{z,cab}\end{pmatrix} &= \mathbf{R}\cdot {}^{cab}\begin{pmatrix}V_{x,cab}\\ V_{y,cab}\\ V_{z,cab}\end{pmatrix}\\
{}^{C}\begin{pmatrix}F_{x,j}\\ F_{y,j}\\ F_{z,j}\end{pmatrix} &= \mathbf{R}\cdot {}^{cab}\begin{pmatrix}F_{x,j}\\ F_{y,j}\\ F_{z,j}\end{pmatrix}\\
{}^{C}\begin{pmatrix}M_{x,j}\\ M_{y,j}\\ M_{z,j}\end{pmatrix} &= \mathbf{R}\cdot {}^{cab}\begin{pmatrix}M_{x,j}\\ M_{y,j}\\ M_{z,j}\end{pmatrix}
\end{aligned}
\tag{5.4}
$$

Afterwards, three kinematic relationships reduce the 6 degrees of freedom of the cabin as a rigid body in the space to the three degrees of freedom of the cabin attached to the chassis. The first two are the first two rows of Equation (5.5), which determine the longitudinal and lateral velocities of the cabin centre of gravity. The third one is the last row of Equation (5.3), which imposes that the relative yaw is zero.

$$
{}^{cab}\begin{pmatrix}V_{x,cab}\\ V_{y,cab}\\ V_{z,cab}\end{pmatrix} = {}^{cab}\begin{pmatrix}V_{x,j}+\dot{\varphi}_{cab}\cdot h\\ V_{y,j}-\dot{\theta}_{cab}\cdot h\\ V_{z,cab}\end{pmatrix} \tag{5.5}
$$

The quantity h in Equation (5.5) is defined as the distance from the cabin centre of gravity to the height of the point of connection to the chassis (Equation (5.6)). Its variation due to heave is neglected.

$$
h = h_{cabCG} - h_{cab,j} \tag{5.6}
$$

The translational motion and the rotational dynamics of the cabin are found through the Euler's equations (Equations (5.7)): they describe the dynamics of a rigid body, using a rotating reference frame with its axes fixed to the body and parallel to the body's principal axes of inertia.

$$
\begin{aligned}
\vec{F} &= m\cdot(\dot{\vec{V}} + \vec{\omega}\times\vec{V})\\
\vec{M} &= I\,\dot{\vec{\omega}} + \vec{\omega}\times(I\vec{\omega})
\end{aligned}
\tag{5.7}
$$

The development of the Equations (5.7) is shown in Equations (5.8).

$$^{cab}\left(m_{cab}\cdot a_{x,cab}\right)=\ ^{cab}\left(F_{x,j}+m_{cab}\cdot g\cdot\varphi_{cab}\right)$$

$$^{cab}\left(m_{cab}\cdot a_{y,cab}\right)=\ ^{cab}\left(F_{y,j}-m_{cab}\cdot g\cdot\theta_{cab}\right)$$

$$^{cab}\left(m_{cab}\cdot a_{z,cab}\right)=\ ^{cab}\left(F_{z,j}-m_{cab}\cdot g\right)$$

$$\begin{aligned}^{cab}\left(\left(I_{x,cab}+m_{cab}\cdot h^2\right)\cdot\ddot{\theta}_{cab}+\left(I_{z,cab}-I_{y,cab}\right)\cdot\dot{\varphi}_{cab}\cdot\dot{\psi}_{cab}\right)=\\ ^{cab}\left(m_{cab}\cdot a_{y,cab}\cdot h+m_{cab}\cdot g\cdot\theta_{cab}\cdot h+M_{x,j}\right)\end{aligned}\tag{5.8}$$

$$\begin{aligned}^{cab}\left(\left(I_{y,cab}+m_{cab}\cdot h^2\right)\cdot\ddot{\varphi}_{cab}+\left(I_{x,cab}-I_{z,cab}\right)\cdot\dot{\theta}_{cab}\cdot\dot{\psi}_{cab}\right)=\\ ^{cab}\left(-m_{cab}\cdot a_{x,cab}\cdot h+m_{cab}\cdot g\cdot\varphi_{cab}\cdot h+M_{y,j}\right)\end{aligned}$$

$$^{cab}\left(I_{z,cab}\cdot\ddot{\psi}_{cab}+\left(I_{y,cab}-I_{x,cab}\right)\cdot\dot{\varphi}_{cab}\cdot\dot{\theta}_{cab}\right)=\ ^{cab}\left(M_{z,j}\right)$$

The translational accelerations are defined as in Equations (5.9).

$$\begin{aligned}^{cab}a_{x,cab}&=\ ^{cab}\left(\dot{V}_{x,cab}-V_{y,cab}\cdot\dot{\psi}_{cab}+V_{z,cab}\cdot\dot{\varphi}_{cab}\right)\\ ^{cab}a_{y,cab}&=\ ^{cab}\left(\dot{V}_{y,cab}+V_{x,cab}\cdot\dot{\psi}_{cab}-V_{z,cab}\cdot\dot{\theta}_{cab}\right)\\ ^{cab}a_{z,cab}&=\ ^{cab}\left(\dot{V}_{z,cab}-V_{x,cab}\cdot\dot{\varphi}_{cab}+V_{y,cab}\cdot\dot{\theta}_{cab}\right)\end{aligned}\tag{5.9}$$

As already stated at the beginning of this Chapter, the joint can be thought as two rotational springs in the x and y directions, which allow respectively roll and pitch, and a translational spring in the z direction, which allows heave. In particular, the axes of this springs are considered to be aligned with the chassis reference frame. This is in accordance with the definition of the relative angles in Equation (5.3). Consequently, the suspension forces are defined in the chassis reference frame and they need a rotation to enter the cabin equations of motion. The suspension characteristics are defined by a constant stiffness and a constant damping coefficients in each of the three degrees of freedom.

$$\begin{aligned}^{c}F_{z,j}&=\ ^{c}\left(-k_{z,cab}\cdot\left(z_{cab}-h_{cabCG}-\Delta z_j\right)-c_{z,cab}\cdot\left(V_{z,cab}-V_{z,j}\right)\right)\\ ^{c}M_{x,j}&=\ ^{c}\left(-k_{r,cab}\cdot\theta_r-c_{r,cab}\cdot\dot{\theta}_r\right)\\ ^{c}M_{y,j}&=\ ^{c}\left(-k_{p,cab}\cdot\varphi_r-c_{p,cab}\cdot\dot{\varphi}_r\right)\end{aligned}\tag{5.10}$$

Finally, the variable $^{c}z_{cab}$ is the first order derivative of $^{c}V_{z,cab}$, which is found in Equation (5.4) from a rotation of the velocities of the cabin centre of gravity, which, in turn, are determined by the cabin equations of motion.

5.1 Forces and moments to the sprung mass

The forces coming from the cabin $F_{x,cab}$, $F_{y,cab}$ and $F_{z,cab}$ used in the Equations (3.1), (3.5) and (3.8) are equal to the forces ${}^{C}F_{x,j}$, ${}^{C}F_{y,j}$ and ${}^{C}F_{z,j}$. Whereas, the moments $M_{x,cab}$, $M_{y,cab}$ and $M_{z,cab}$ used in Equations (3.16), (3.20) and (3.22) take into account that those forces have been moved in the chassis centre of gravity. Consequently, they are given by Equations (5.11), which can be derived respectively from Figure 3.4, Figure 3.7 and Figure 3.1.

$$\begin{aligned} M_{x,cab} &= {}^{C}\left(M_{x,j} - F_{y,j}\cdot\left(h_{cab,j} - h_{CG}\right) - F_{z,j}\cdot\theta_j\cdot\left(h_{cab,j} - h_{CG}\right)\right) \\ M_{y,cab} &= {}^{C}\left(M_{y,j} + F_{z,j}\cdot d_{cab,S} + F_{x,j}\cdot\left(h_{cab,j} - h_{CG}\right)\right) \\ M_{z,cab} &= {}^{C}\left(M_{z,j} - F_{y,j}\cdot d_{cab}\right) \end{aligned} \tag{5.11}$$

6 Articulation Joints

In an A-double combination, there are three articulation joints between two consecutive units: a fifth wheel coupling between the tractor and the first semitrailer, a drawbar between the first semitrailer and the dolly and a fifth wheel on a turntable between the dolly and the second semitrailer.

Two consecutive units are ideally connected in one point. Hence, the velocity of that point in the space must be the same as seen by both units. In the same point, the exchange of forces and moments between the units will take place. They will be a consequence of the equations of motion of the two units. Specifically, the towing unit will determine the velocity of the point and the towed unit the forces and moments, in a similar way as the cabin joint to the tractor chassis of the previous Chapter.

However, the quantities calculated for each unit are in the respective reference frames, therefore a rotation needs to be applied. The rotation matrix between the towing unit reference frame ("TG") and the towed unit reference frame ("TD") is as defined in Equation (6.1) and the angles of relative rotation θ_r, φ_r and ψ_r are found thanks to Equation (6.2) (see the Appendix 14.1 for more details), where the angles θ, φ and ψ with subscript "TG" or "TD" come from the equations of motion of the respective unit. This is according to the fact that these angles are defined in the towing unit reference frame and the order of rotation is first about z, then y and finally about x. Also the forces and moments are always defined in the towing unit reference frame.

$$\mathbf{R} = \mathbf{R_x}(\theta_r) \cdot \mathbf{R_y}(\varphi_r) \cdot \mathbf{R_z}(\psi_r) \tag{6.1}$$

$$^{TG}\begin{pmatrix}\theta_{TG}\\ \varphi_{TG}\\ \psi_{TG}\end{pmatrix} + \begin{pmatrix}\theta_r\\ \varphi_r\\ \psi_r\end{pmatrix} = \mathbf{R} \cdot {}^{TD}\begin{pmatrix}\theta_{TD}\\ \varphi_{TD}\\ \psi_{TD}\end{pmatrix} \tag{6.2}$$

Based on this, all the necessary rotations are perfomed (Equations (6.3)). On the left-hand side of the equations we have the velocities, forces and moments of the rear articulation joint (subscript "R") of the towing unit in its reference frame (left-hand superscript "TG"), while on the right-hand side we have the variables of the front articulation joint (subscript "F") of the towed unit in its reference frame (left-hand superscript "TD"). The velocities come from Equations (3.28) of the respective unit and the forces and moments appear in Equations (3.1), (3.5), (3.8), (3.16), (3.20) and (3.22) of the respective unit.

In this model, the first and third coupling allow rotations in the yaw and the pitch directions and instead they constrain the roll rotation, that means that $\theta_r = 0$ is imposed; this is an usual approximation of the fifth wheel couplings. Whereas, the second coupling allows free rotations in all directions, i.e. like a spherical joint. This models the point where the drawbar eye of the dolly drawbar connects to the tow hitch of the first semitrailer. Besides, in the first coupling the yaw rotation is counteracted by a dry friction and linear damping torque, shown more in detail in the next Section. The presence of a turntable under the second fifth wheel, basically removes any friction in that coupling. In the directions where free rotations are allowed, the moments are imposed to be equal to zero. A summary of the imposed conditions for each coupling is illustrated in Figure 6.1.

$$
\begin{aligned}
{}^{TG}\begin{pmatrix} V_{x,R} \\ V_{y,R} \\ V_{z,R} \end{pmatrix} &= \mathbf{R} \cdot {}^{TD}\begin{pmatrix} V_{x,F} \\ V_{y,F} \\ V_{z,F} \end{pmatrix} \\
{}^{TG}\begin{pmatrix} F_{x,R} \\ F_{y,R} \\ F_{z,R} \end{pmatrix} &= \mathbf{R} \cdot {}^{TD}\begin{pmatrix} F_{x,F} \\ F_{y,F} \\ F_{z,F} \end{pmatrix} \\
{}^{TG}\begin{pmatrix} M_{x,R} \\ M_{y,R} \\ M_{z,R} \end{pmatrix} &= \mathbf{R} \cdot {}^{TD}\begin{pmatrix} M_{x,F} \\ M_{y,F} \\ M_{z,F} \end{pmatrix}
\end{aligned}
\tag{6.3}
$$

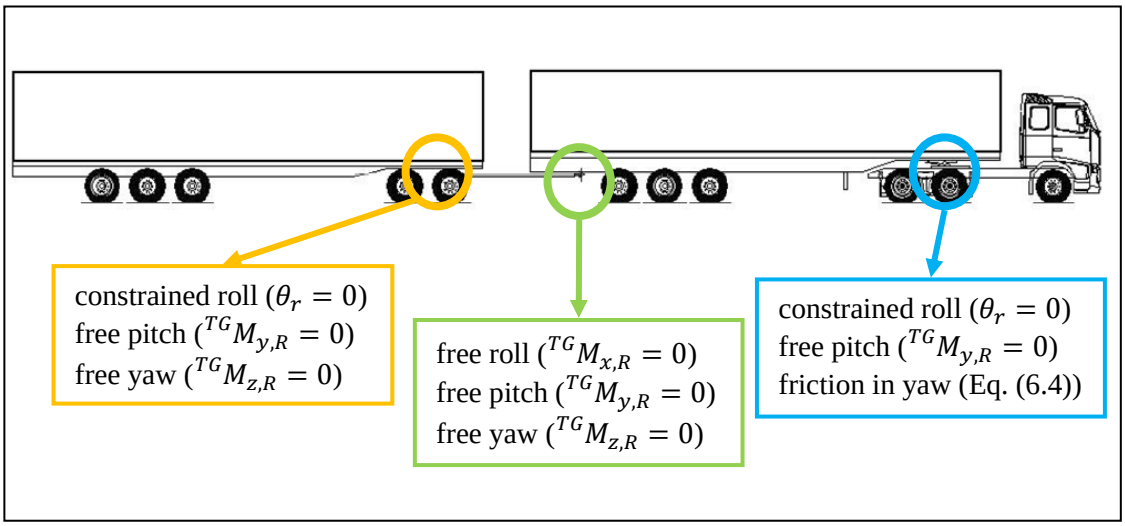

Figure 6.1 Definition of type of coupling for the three couplings of the A-double.

The type of coupling, i.e. if they have friction or not and if it is constrained in roll or not, is defined at the *Vehicles* level of the Modelica model structure (see Section 2.4.5). This allows defining the *coupling* model in a general way.

It is important to remember that the relative rotations are defined in the towed unit reference frame. This is relevant particularly for the fifth wheel couplings, where the two connected units are forced to have the same angle in the roll direction. However, they will have the same roll angle only when the other two relative angles are null. In the other cases, the roll angle of the towing unit is imposed equal to an angle which may be a combination of roll, pitch and yaw angles of the towed unit. In an extreme case, if $\varphi_r = 0$ and $\psi_r = -90°$, then $\theta_F = \varphi_R$, which means that the roll angle of the towing unit is equal to the pitch angle of the towed unit.

6.1 Friction in the fifth wheel coupling

As already mentioned, a dry friction and linear damping torque is present in the fifth wheel coupling between the tractor and the first semitrailer (Equation (6.4)).

$$
{}^{TG}\left(M_{z,R}\right) = M_{fr} + M_{damp} \tag{6.4}
$$

The damping torque is implemented by means of a constant coefficient (Equation (6.5)).

$$M_{damp} = -c_{5^{th}{}_w} \cdot \dot{\psi}_r \tag{6.5}$$

The friction torque was implemented in Modelica with a simple statement, which results in the plot in Figure 6.2 for the maneuver presented in Section 10.1.

$$\dot{M_{fr}} = \begin{cases} if M_{fr} < offset \; and \; \dot{\psi}_r > 0 \; or \; M_{fr} > -offset \; and \; \dot{\psi}_r < 0 \\ then \; 0 \; else \; k_{5^{th}{}_w} \cdot \dot{\psi}_r \end{cases} \tag{6.6}$$

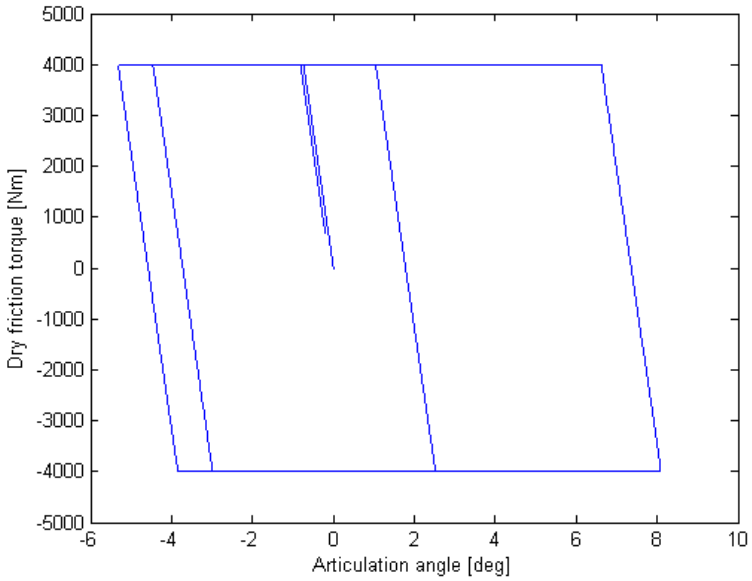

Figure 6.2 Dry friction torque M_{fr} versus articulation angle ψ_r.

7 Steering System

The steering system receives as input the steering wheel angle applied by the driver and the forces coming from the tyre-road contact. From those two, it calculates the steer angles at the wheels (to which a roll steer contribution is added) and the steering wheel torque that the driver must apply.

The modelled steering system was designed similar to the OEM model and it represents a conventionally steered front axle of a truck. The steering wheel is connected through the steering column and the steering shaft to the hydraulic steering gear. Here the steering wheel torque is amplified, while the steering wheel angle reduced. The rotation of the steering shaft causes the rotation of the torsion bar and of the worm gear (also called ballscrew). The latter causes the displacement of a nut, which meshes with a gear sector, causing, in turn, its rotation. An arm attached to the sector shaft moves the Pitman arm (or drop arm). This is connected via the steering linkage (or drag link) to the upper steering arm which rotates the steering knuckle around the kingpin bolt. Finally, the left and right wheels steer angles are made dependent via the track rod.

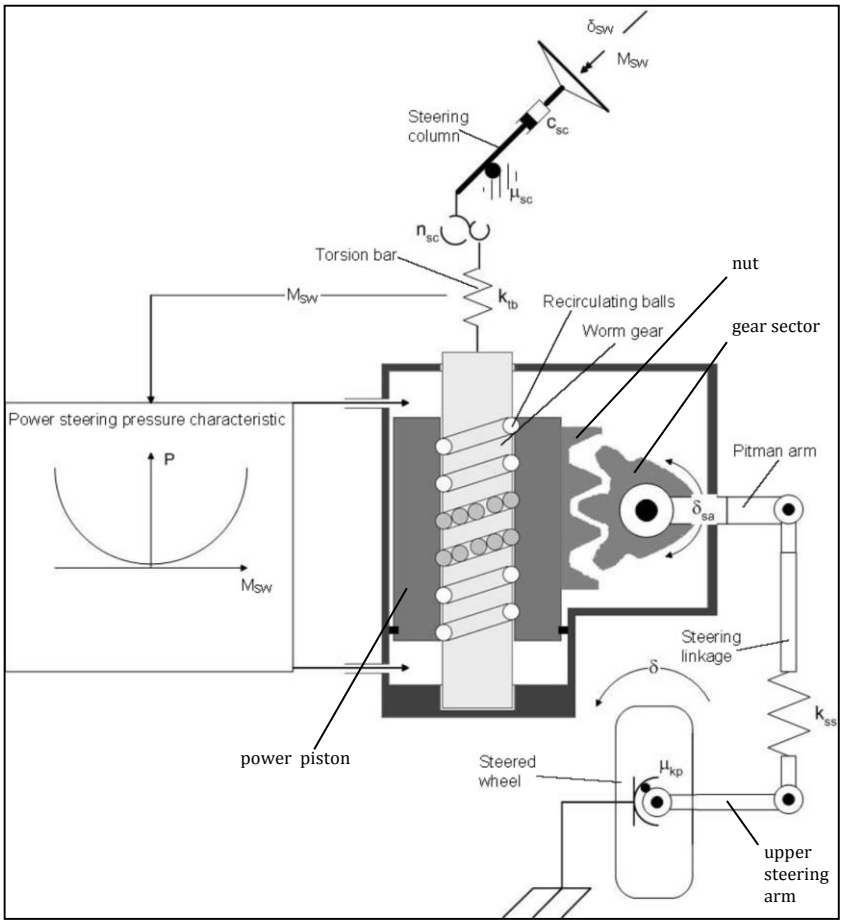

Figure 7.1 Example of a hydraulic power steering system of a truck, adapted from Rothhämel (2013).

The torsion bar produces the opening and closing of valves for the high pressure fluid, which is acting on one of the two sides of the power piston. Being the power piston integral with the nut, the fluid pressure helps its displacement and therefore the gear sector rotation, thus reducing the steering effort. The resultant torque, at the wheel

level, is the left-hand term of the Equation (7.1). This is the sum of the contribution of the steering wheel torque $M_{st.wheel}$ applied by the driver, multiplied by the total steering ratio i_{tot} (which will be explained in the following) and the torque given by the servo assistance pressure p_{servo}. This total torque must be equal to the torque around the kingpin axis M_{KP}, which is the outcome of the forces at the tyre-road contact (Equations (7.6)). Consequently, Equation (7.1) determines the steering wheel torque that the driver must apply.

$$M_{st.wheel} \cdot i_{tot} + p_{servo} \cdot A_{piston} \cdot r_p = M_{KP} \tag{7.1}$$

The product of the servo pressure with the area of the surface of the power piston which the pressure acts on (A_{piston}) gives a force that moves the piston itself, which in turn will make the gear sector rotate about its axis. The moment due to the servo pressure, then, is given by the product of this force with the coefficient r_p which is an equivalent radius, i.e. the distance of the force from the sector axis.
The servo pressure is a function of steering wheel torque, shown in figure Figure 7.2, and was implemented with a 5 degree polynomial, with an absolute maximum of 100 bar. The servo pressure expresses a relative pressure between the two sides of the power piston, hence the negative value for negative steering wheel torques.

$$p_{servo} = f(M_{st.wheel}) \tag{7.2}$$

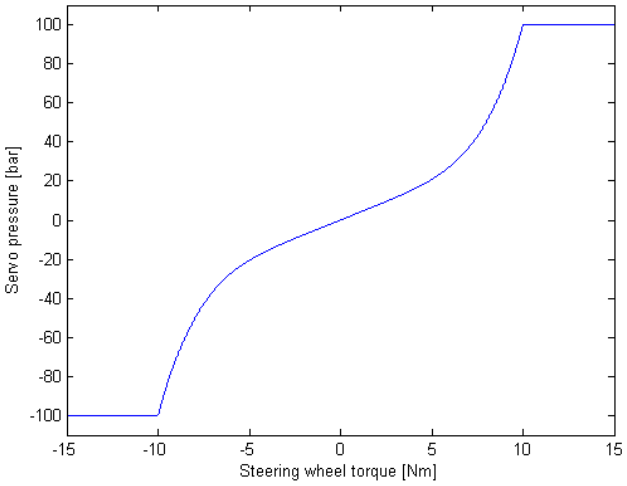

Figure 7.2 Servo characteristic.

The steering gear together with the linkage geometry produce the overall steering ratio i_{tot}, which is defined as the ratio between the steering wheel angle ($\delta_{st.wheel}$) and the mean of the two wheel steer angles (δ_{wheels}) when no load is applied to the steering system. The ratio i_{tot} is typically not constant and was implemented with a 3 degree polynomial of the absolute steering wheel angle (see Figure 7.3).

$$i_{tot} = f(|\delta_{st.wheel}|) \tag{7.3}$$

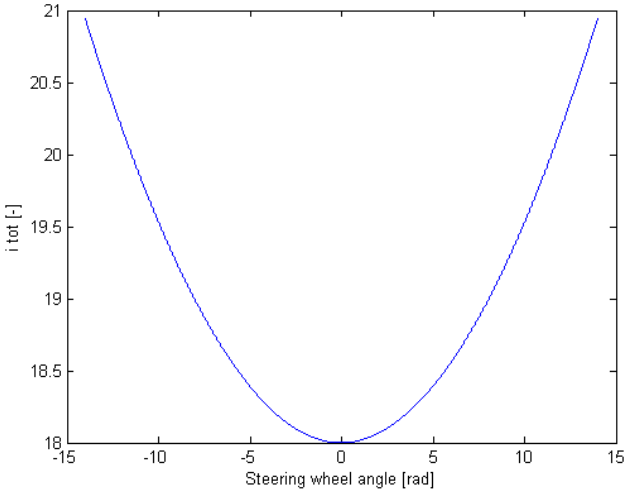

Figure 7.3 Overall steering ratio versus steering wheel angle.

When loading is added to the steering system, i.e. forces from the road, the actual ratio between $\delta_{st.wheel}$ and δ_{wheels} can deviate substantially from it, mainly due to the compliance of the torsion bar within the steering gear (the torsion bar contributes to around 50% of the stiffness in the entire steering system, according to Rothhämel (2013)). The Equation (7.4) relates $\delta_{st.wheel}$ with δ_{wheels} and with the torsion angle of the torsion bar $\varepsilon_{torsion}$, which will have opposite sign with respect to the other two terms. Consequently, a greater steering wheel angle must be applied by the driver to obtain the same steer angles at the wheels.

$$\frac{\delta_{st.wheel} + \varepsilon_{torsion}}{i_{tot}} = \delta_{wheels} \tag{7.4}$$

The torsion angle of the steering torsion bar is determined by the steering wheel torque (see Equation (7.5)), which comes from Equation (7.1). Then, the term $\varepsilon_{torsion}$ will enter the Equation (7.4), deciding δ_{wheels}.

$$M_{st.wheel} = k_{tb} \cdot \varepsilon_{torsion} \tag{7.5}$$

The moment around the kingpin axis M_{KP} can be computed from the tyre forces (the tyre forces of the steered axle, see Section 4) as in Equations (7.6). The kingpin axis (or steering axis) is the axis about which the wheel rotates relative to the chassis frame when steered. The moment about this axis is the moment that must be applied in order to steer the wheel. The meaning of the coefficients present in Equations (7.6) is clarified in the following, with reference to Figure 7.4.
The kingpin inclination angle σ is the angle between the steering axis and the z-axis on the yz-plane. The steering-axis offset at ground r_k (or scrub radius) is the component along y of the distance between the tyre-road contact centre and the intersection of the steering axis with the ground. Finally, the caster angle τ is the angle between the steering axis and the z-axis on the xz-plane.

$$
\begin{aligned}
M_{KP} &= M_{Fx} + M_{Fy} + M_{Fz} + M_{Mz} \\
M_{Fx} &= \left(F_{x,tyreR} - F_{x,tyreL}\right) \cdot r_k \\
M_{Fy} &= -(F_{y,tyreL} + F_{y,tyreR}) \cdot \tan\tau \cdot R \\
M_{Fz} &= -\left(F_{z,tyreL} + F_{z,tyreR}\right) \cdot r_k \cdot \sin\sigma \cdot \sin\delta + \\
&+ (F_{z,tyreR} - F_{z,tyreL}) \cdot r_k \cdot \sin\tau \cdot \cos\delta \\
M_{Mz} &= \left(M_{z,tyreL} + M_{z,tyreR}\right) \cdot \cos\sqrt{\sigma^2 + \tau^2}
\end{aligned}
\tag{7.6}
$$

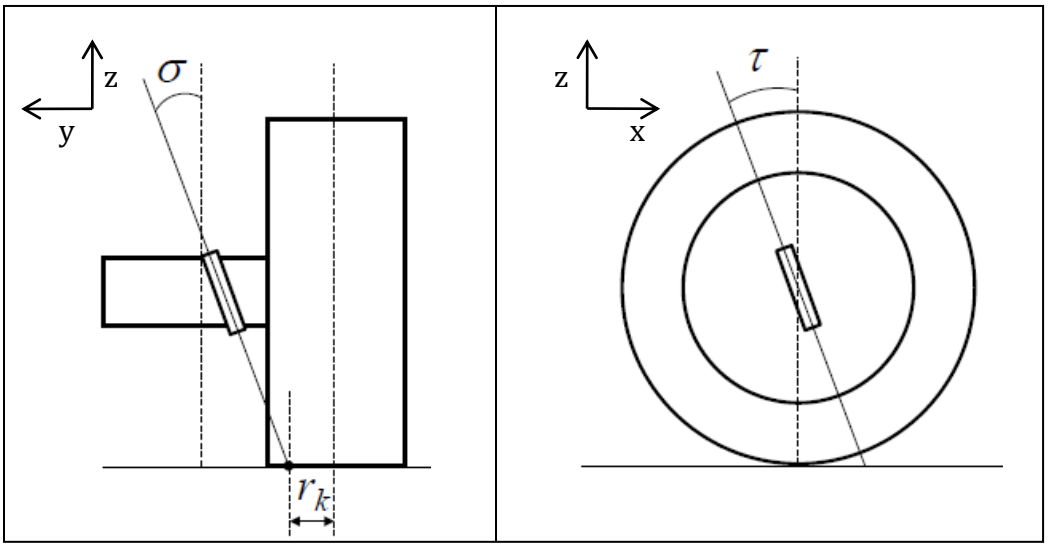

Figure 7.4 Kingpin inclination and caster angles, from Tagesson (2014).

A roll steer contribution is introduced, by adding a term which is the product of the roll angle of the tractor chassis at the steered axle (relative to the axle roll angle) with the roll steer coefficient (a positive E_r means roll right steer left).

$$\delta = \delta_{wheels} + E_r \cdot \theta_{rel} \tag{7.7}$$

The left and right wheels steer angles δ_L and δ_R are computed assuming an Ackermann steering geometry, which practically means more steer angle on the inner wheel in corners. On heavy trucks the steering geometry is in general closer to Ackermann than parallel (i.e. $\delta_L = \delta_R$). This is because of the importance of low speed manoeuvrability and of the relatively low average speed, see Tagesson (2014). The Equation (7.8) defines the two steer angles, bearing in mind that δ is the mean value of δ_L and δ_R.

$$\frac{1}{tan\delta_R} = \frac{1}{tan\delta_L} + \frac{TW}{l_{eq}} \tag{7.8}$$

For vehicles having more than one rear axle the equivalent wheelbase l_{eq} needs to be introduced for the calculation of the Ackermann steering geometry. The equivalent wheelbase describes the wheelbase of a two-axle vehicle with similar steady-state cornering behaviour as the multi-axle vehicle. It can be calculated as in Equations (7.9). L is, in this case, the distance from the front axle to the middle point between

the rear axles; C_F and C_R are front cornering stiffness and sum of rear cornering stiffnesses respectively; N is the number of rear axles; Δ_i is the longitudinal distance from the axle i to the middle point between the rear axles.

$$l_{eq} = L \cdot \left[1 + \frac{T}{L^2} \cdot \left(1 + \frac{C_R}{C_F}\right)\right]$$
$$T = \frac{\sum_{i=1}^{N} {\Delta_i}^2}{N} \tag{7.9}$$

8 Powertrain System

For the powertrain system, the car model used in the Vehicle dynamics model library for VTI (*vehlib2*, see Bruzelius (2013)) was used with the proper adjustments. The reason is that the longitudinal dynamics was outside the main focus of this thesis work (see Section 2.2).
The explained powertrain system holds for four driven wheels, however it can be easily adjusted to work with only two driven wheels.
The engine rotational speed is dependent on the mean speed of the driven wheels, with an imposed minimum (idle) and maximum engine speeds.

$$\omega_{eng} = \min(\omega_{eng,max}, \max(\omega_{eng,idle}, \omega_{mean,w} \cdot i_T) \tag{8.1}$$

The total transmission ratio i_T is the product of the final transmission ratio and the specific gear transmission ratio. The latter depends on the engaged gear, which is function of the engine speed, as the gear shift is automatic. Specifically, 12 gears are present.
The engine torque is found thanks to the accelerator pedal input acc_{input} which varies from 0 to 100 (Equation (8.2)).

$$T_{eng} = \frac{acc_{input}}{100} \cdot \left(T_{eng,max} - T_{eng,min}\right) + T_{eng,min} \tag{8.2}$$

The maximum and the minimum engine torques $T_{eng,max}$ and $T_{eng,min}$ are a third degree polynomial of the engine rotational speed. The coefficients of the polynomials were calculated by using the available engine map.
Finally, the drive torque at each wheel is found from the engine torque multiplied by the total transmission ratio and a transmission efficiency and it is set equal among the four driven wheels (hence the division by 4).

$$T_{drive} = \frac{\eta_T \cdot T_{eng} \cdot i_T}{4} \tag{8.3}$$

This torque, summed to the braking torque, enters the wheel equilibrium of the driven wheels (Equation (4.19)).

9 Braking System

The simplest possible braking system was designed for the same reasons mentioned in the previous Chapter. The braking force distribution between the axles is neglected, which is in accordance with the linear tyre model used, as no saturation of the tyre forces can occur.
The braking torque is set equal to the brake pedal input (which varies from 0 to 100) multiplied by a coefficient, which was chosen so to have a reasonable braking torque at maximum brake input, see Equation (9.1). The two additional terms were added to have a smooth braking at low speeds and prevent numerical instability (chattering). The expressions are taken from the same model library used for the powertrain system.

$$T_{brake} = -brake_{input} \cdot 120 \cdot \tanh(10 \cdot \omega_{wheel}) \cdot \tanh(2 \cdot abs(V_x)) \qquad (9.1)$$

The same torque was applied to every wheel of each axle of each unit. In fact, with the given tyre model, there was no interest in distributing the braking force according to the axle vertical load.
This torque, summed to the drive torque in case of the driven wheels, enters the wheel equilibrium (Equation (4.19)).

10 Model Validation

The model validation was first carried out with many desktop simulations in the Simulink environment. They compared each step of the developed model with the OEM model using an ISO lane change maneuver. When the level of detail was regarded as satisfactory, some experiments were carried out in the driving simulator. The purpose was both to prove functionality (real-time performance, etc.) and for subjective evaluation. The evaluation was based on a comparison with the OEM model.

10.1 Desktop experiments

The aim of this section is to show the comparison of the developed Modelica models with the validated OEM model and to show that the increase of accuracy reflects the progressive increase of complexity of the developed models, until the satisfactory level has been reached.

The progression goes from the single-track model to the last developed model (see Section 2.5), which has also been driven in the driving simulator (see Section 10.2). While the reference OEM model is denoted with the abbreviation OEM, the analysed models are the following, with their abbreviations in brackets: the single-track model (ST), the double-track model (DT), the model with roll, pitch and heave (T1), the model with frame flexibility (T2), the model with the cabin suspensions (T3), the model with the axle dynamics (T4) and the model with the steering system (T5). Obiouvsly, each of them is an improvement of the previous one. This analysis is focused on the lateral behaviour of the vehicle, with the purpose of making it similar to the OEM model in the chosen driving context (see Section 2.2). The gradual improvements were determined by focusing on what was believed to be the main sources of error. However, the final application of the model, i.e. a driving simulator, implies that the attention should be placed in what the driver may see and perceive. The driving simulator application also has the implication that the vehicle needs to be driven from standstill, should be accelerated to the cruise speed and, after the maneuver, it needs to be stopped. Therefore, a powertrain and braking systems are added to the last model in order to provide a reasonable longitudinal behaviour (T6).

One maneuver was chosen as representative of the selected driving context, i.e. an ISO lane change at 80km/h. When the vehicle is running at the test speed in a straight line, one full-period sinusoidal steering-wheel input is applied. The amplitude of the sine is chosen so that the value of the maximum lateral acceleration of the first unit is about 2 m/s^2. Figure 10.1 on the left shows the applied steering input, which is a single sine-wave of amplitude 40 degrees and period 3 seconds. On the right-hand side of the figure, the resulting lateral acceleration of the first unit (the tractor), according to the OEM model, can be seen to have the maximum close to 2 m/s^2. The longitudinal velocity was checked to keep more or less constant at 80 km/h during the entire maneuver.

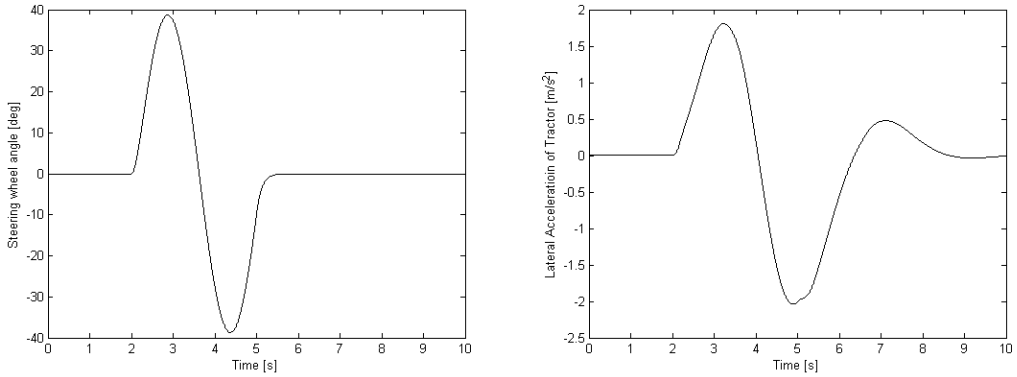

Figure 10.1 Steering wheel input and resulting lateral acceleration of tractor (according to OEM model).

The application of a single sine-wave steering input has the consequence that the vehicle trajectory might not be a perfect lane change. This is the case, mainly for three reasons. The first is related to the high oscillations of the towed units, which also causes a large oscillation in the tractor trajectory (of the order of 1 meter in this case), that is damped down only after several tens of meters after the steering input (see Figure 10.2). This may be explained with the excessively high values of yaw inertias of the two semitrailers. Typical values are around 500,000 kg·m^2, while the OEM values are approximately the double. To support this hypothesis, when the values of those inertias are halved, the mentioned oscillation almost completely disappears. Even though these values may affect the overall behaviour of the vehicle compared to the reality, they were used also in the Modelica model to keep a fair comparison with the OEM model. Additionally, the oscillations of the OEM model may be further amplified by the fact that the tyres of the last two units reach nonlinearity.

The second reason is a residual friction torque in the first fifth wheel coupling, true especially for the Modelica model, which exhibit a considerable non-zero yaw rate after the maneuver (see Section 10.1.1.1 for more details). When the friction is removed, this non-zero yaw rate vanishes.

The last reason is the roll steer contribution, which may have a net steering effect when applying a perfect sine-wave steering input. However, this is considerably reduced if the inertias of the semitrailers are halved.

A driver model should be implemented in order to have a perfect lane change. But in that case, the "driver" reaction would be different between the two models and the aim of comparing their lateral responses would be partially missed, as they would have different inputs.

In order to perform a desktop simulation in Simulink, the inputs to the models have to be designed, as they substitute the inputs originating from the driver and the environment in a driving simulator experiment. As already mentioned, the purpose is to obtain a lateral behaviour similar to the OEM model, hence a fair comparison was achieved in the following way.

The accelerator and brake inputs are null inputs fed to the OEM model. This is started at 80km/h and the cruise control function is used to keep the speed constant. The longitudinal speed signal is used as input to the Dymola block, so that the same speed can be maintained. This is to exclude the effect of the longitudinal dynamics.

In the same way, the steering input is applied to the OEM model. The steering input to the Dymola block is the output of the OEM steering system (in order to exclude its effect). Therefore, this signal is the wheel steer angle as decided by the steering

system, i.e. roll steer contribution is not included. This contribution can be taken into account in the Modelica model only from the model T1.
When the steering system has been modelled (T5), the input to the Dymola block can be the same as the OEM, i.e. the steering wheel angle.
Finally, when a powertrain and a braking systems have been modelled as well (T6), an experiment consisting of acceleration from standstill to 80km/h, lane change while keeping an approximately constant speed, and braking to standstill can be performed. Now the inputs to the Dymola block are the same as the ones to the OEM.
The last decision to take related to the desktop experiments was about the outputs, i.e. what needs to be plotted and compared. This depends also on the complexity of the models, as e.g. the first two models do not take roll into account. In these cases, the trajectory of the tractor and the yaw rates of the four units were examined. When the complexity of the models allowed, mainly the following variables were added in the analysis: the roll angles of the four units and the cabin roll angle and lateral acceleration.

10.1.1 Single-track model (ST)

This is the first model compared with the OEM model and thus the simplest one. As already said, it includes the friction (dry friction and linear damping) torque of the first fifth wheel coupling. This decision was based on the analysis shown in Section 10.1.1.1.

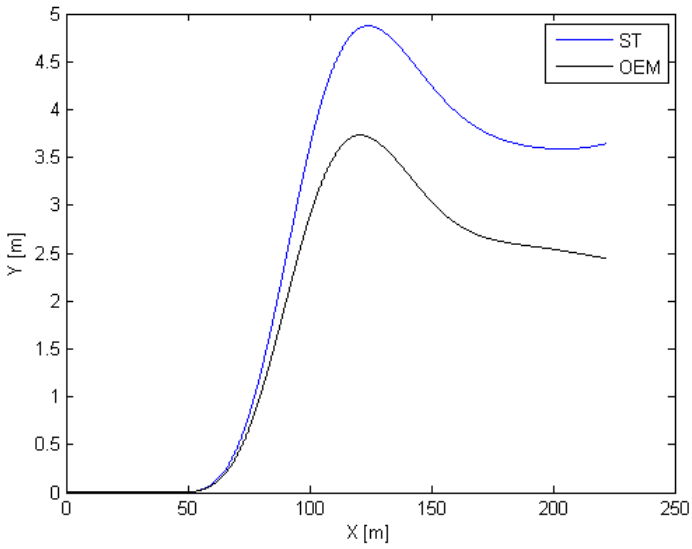

Figure 10.2 Tracjectory of tractor CG, ST vs. OEM.

Three main considerations can be done from Figure 10.2. Firstly, there is a considerable difference (about 1 meter) in lateral displacement of the tractor, which will be solved in the next developments of the model. Secondly, the tractor does not follow a path of perfect lane change, for the reasons already explained. At last, the final heading direction is different for the two models, as better illustrated in Section 10.1.1.1.

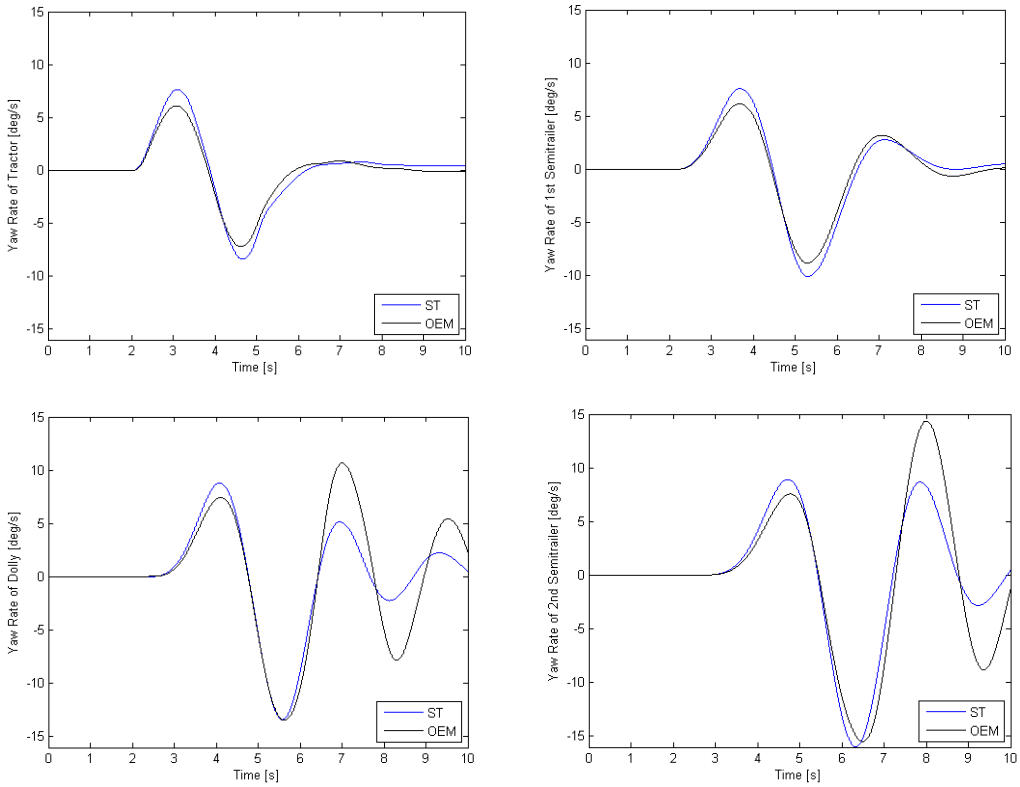

Figure 10.3 Yaw rates of the four units, ST vs. OEM..

From the plots of the yaw rates, it is interesting to note the different timings, amplitudes and number of peaks of the oscillations of the four units of the A-double.
The single-track model shows greater amplitudes with respect to the OEM model in a similar way for the four units, except for the last oscillations of the dolly and the second semitrailer. This can be explained by the fact that their tyres reach the nonlinear region of their lateral force-slip angle characteristics in the OEM model. Nevertheless, this does not seem to have a clearly noticeable influence on the first two units.

10.1.1.1 Fifth wheel friction torque

Two considerations were done about the friction torque in the fifth wheel coupling between the tractor and the first semitrailer (see Section 6.1).
First of all, its importance was assessed by removing it from the single-track model and checking the difference. The left part of Figure 10.4 shows the yaw rate of the tractor, equivalently as in Figure 10.3 on the left-top corner, but without friction of the fifth wheel coupling in the ST model. It is clear that the difference between the OEM and the ST models has highly increased, as the ST shows oscillations with large amplitude and several peaks. According to what previously said about the inertias of the semitrailers, their values were halved in both models. The result of the simulation is shown in the right part of Figure 10.4. Here the oscillations of the ST model without the fifth wheel friction torque are much lower and the difference from the ST model with this torque is greatly reduced, even if it is still noticeable.

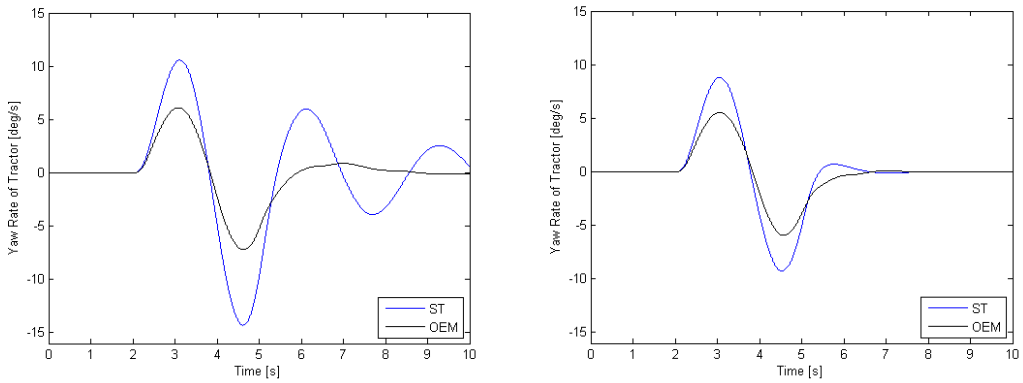

Figure 10.4 Yaw rate of tractor, ST vs. OEM. ST is without fifth wheel friction torque in both plots. Both models are with halved semitrailers inertias in the right-hand plot.

From this analysis, we can conclude the importance of this friction torque in damping down the oscillations, but also the fact that it is particularly relevant when the vehicle is close to a loss of lateral stability. This highly oscillatory behaviour (present also in the OEM model if the fifth wheel friction is removed) can be motivated by the excessively large values of the iniertias of the semitrailers.
A second consideration concerns a residual non-zero friction torque at steady-state, which has a considerable influence in the yaw equilibrium. The effect on the tractor yaw rate can be seen in the left-top corner of Figure 10.3: after the oscillations have ceased, the yaw rate value is not null. The trajectory of the tractor clearly shows this phenomenon (Figure 10.5). This can be demonstrated by removing the friction torque: in this case, this residual yaw rate disappears.

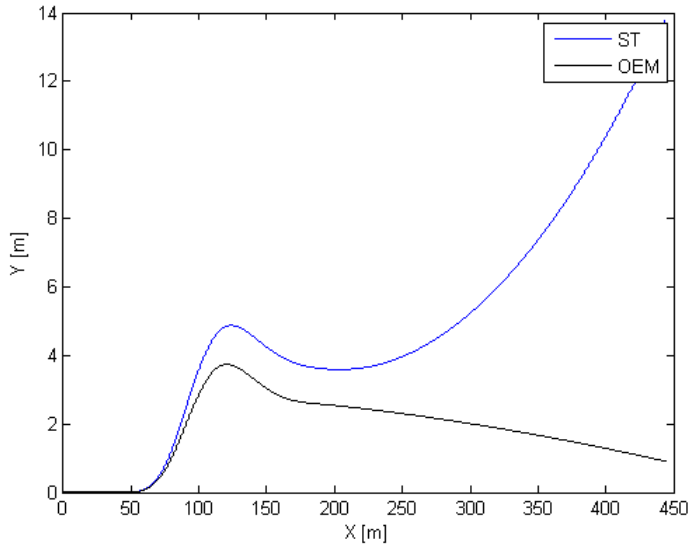

Figure 10.5 Trajectory of tractor CG, ST vs. OEM, same as Figure 10.2.

Figure 10.5 (which is simply an extension of Figure 10.2) shows how both models have a residual yaw rate, in opposite directions and higher for ST.

10.1.2 Double-track model (DT)

The double-track model did not bring important improvements to the previous model and this can be noticed from the tractor trajectory (Figure 10.6) and from the yaw rates of the four units.

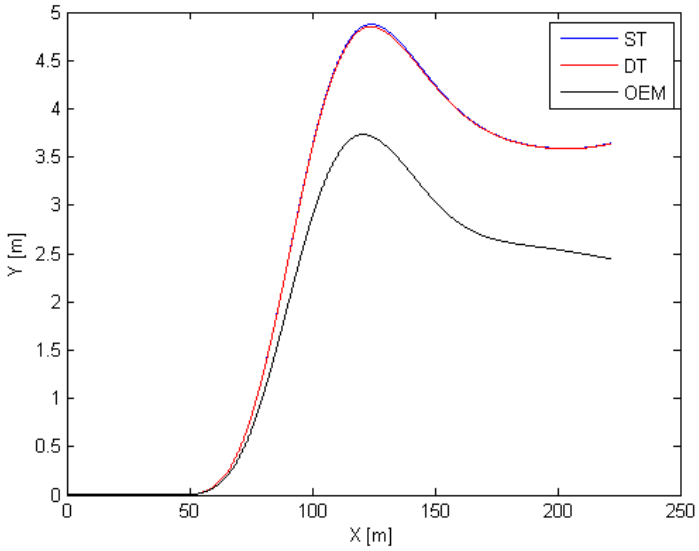

Figure 10.6 Trajectory of tractor CG, DT vs. ST vs. OEM.

10.1.3 Model with roll, pitch and heave (T1)

T1 is the first model that can include a roll steer contribution. The improvement from the previous two models is clear (Figure 10.7). The same improvement occur for the yaw rates.

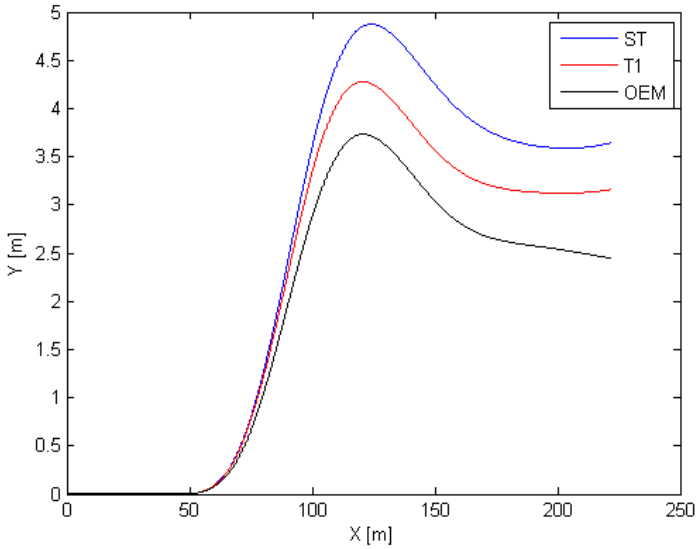

Figure 10.7 Trajectory of tractor CG, T1 vs. ST vs. OEM.

10.1.4 Model with frame flexibility (T2)

To the T1 model the torsional flexibility of the tractor chassis frame was added. The improvement in the trajectory is clear and this can be explained with a more accurate roll steer contribution.

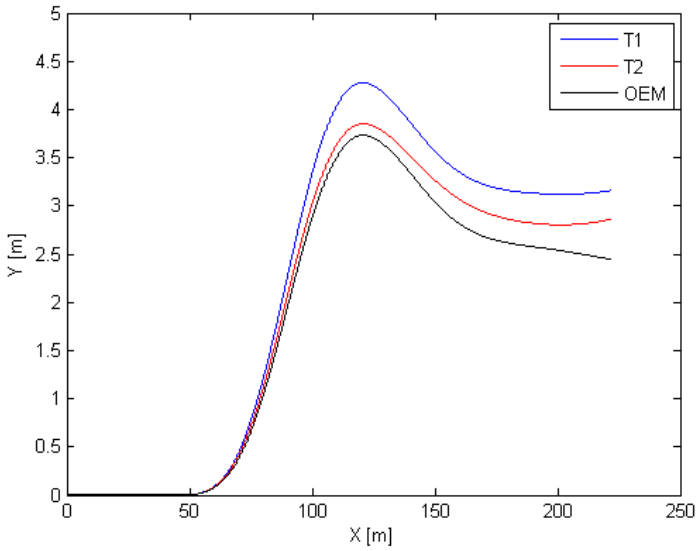

Figure 10.8 Trajectory of tractor CG, T2 vs. T1 vs. OEM.

Figure 10.9 shows how the roll angle at the front part of the tractor is different from the roll angle at the rear part (respectively the roll angles at the two reference points F_{ref} and R_{ref} defined for frame torsion, see Figure 3.9) due to frame torsion (compare with Figure 10.10). This difference was not modelled by the model T1. It is particularly relevant to compare the roll angle at the front part, which shows the greatest difference. Its relevance has two main reasons: it is the angle used for the roll steer term and it is the angle directly affecting the cabin. It is also possible to notice that the timings of the two roll angles are different, as the roll at the front part (i.e. at the steered axle) is the first that rolls.

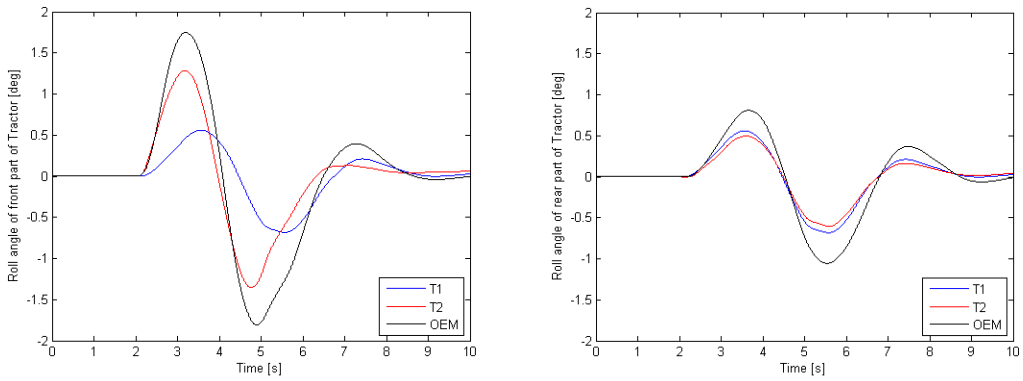

Figure 10.9 Roll angle of the front and rear part of the tractor, T2 vs. T1 vs. OEM.

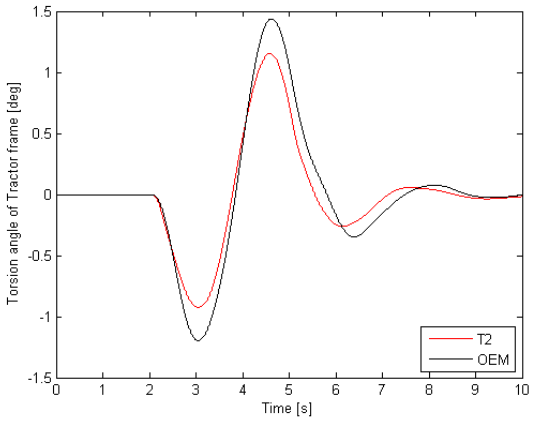

Figure 10.10 Frame torsion angle, T2 vs. OEM.

10.1.5 Model with cab suspensions (T3)

This model considers the cabin as a body suspended on the chassis frame. This seems to have a small, yet noticeable effect on the trajectory. This, again, can be justified by a modified roll steer contribution because of the cabin motion. However, the main motivation for this step was the final application of the model. i.e. a driving simulator.

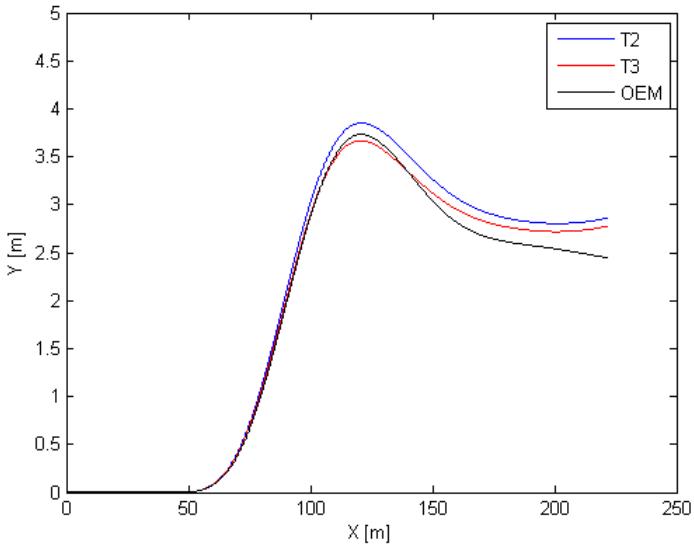

Figure 10.11 Trajectory of tractor CG, T3 vs. T2 vs. OEM.

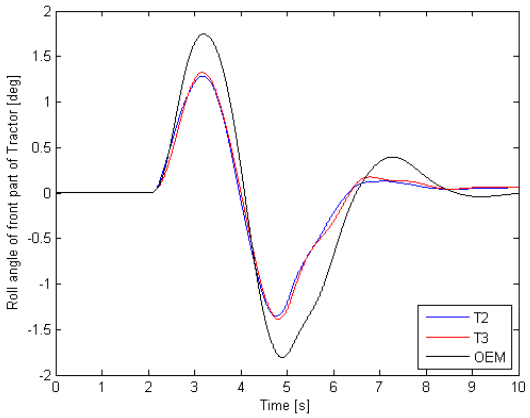

Figure 10.12 Roll angle of the front part of the tractor, T3 vs. T2 vs. OEM.

10.1.6 Model with axle dynamics (T4)

When the axle dynamics is added, the trajectory is not greatly modified (Figure 10.13), even though the increment in the roll angle of the front part of the tractor is important (top-left corner of Figure 10.14). This may sound contradictory with what said in the previous. However, the angle used in the roll steer term is the relative angle between the front part of the tractor and its first axle. This relative angle was coincident with the former in previous models, as the axles could not roll. When this degree of freedom is added, the roll angle of the tractor becomes the sum of the axle roll angle and their relative roll angle. This relative angle does not apparently change much, being the trajectory similar as before. However, the total roll angles does, and so does the cabin roll angle. This is of course of great interest for driving simulators purposes.

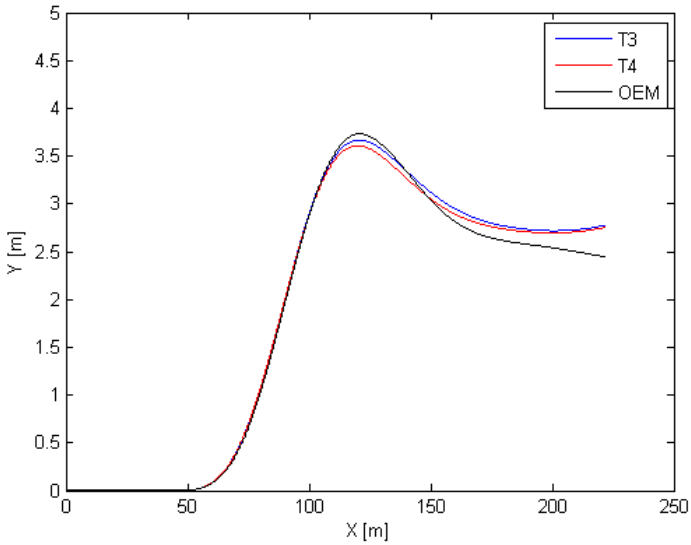

Figure 10.13 Trajectory of tractor CG, T4 vs. T3 vs. OEM.

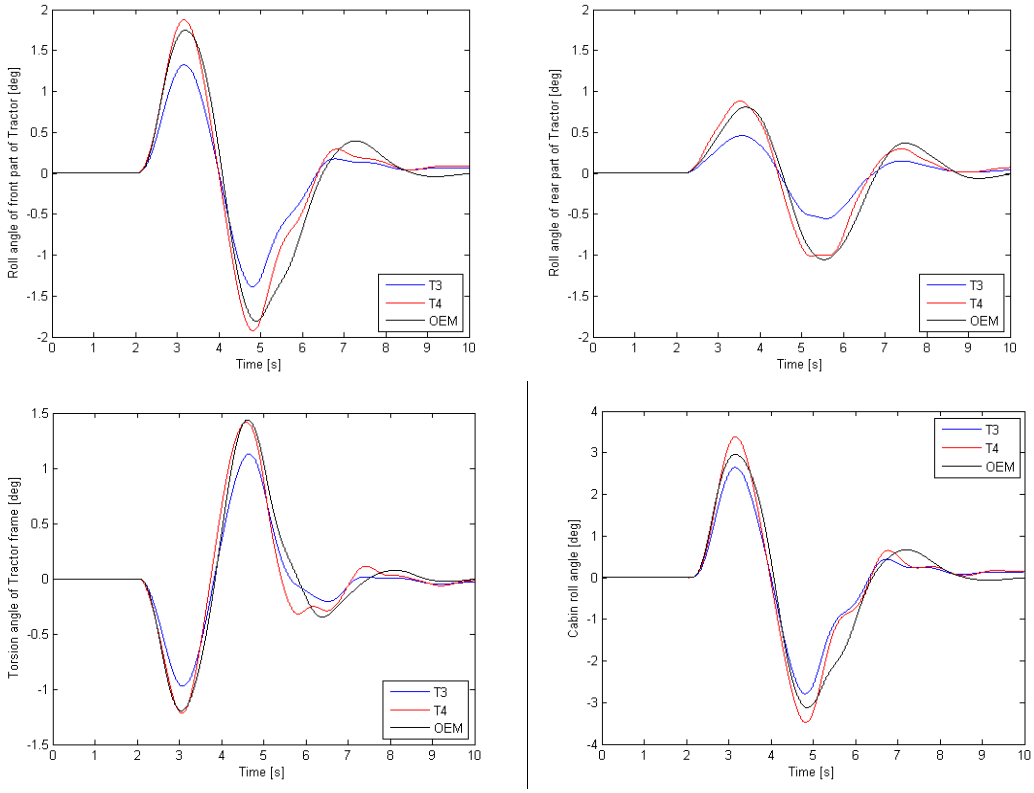

Figure 10.14 Roll angles of front and rear part of the tractor, frame torsion angle and cabin roll angle, T4 vs. T3 vs. OEM.

10.1.7 Model with steering system (T5)

The steering system allows a complete comparison of the lateral dynamics, starting from driver input, with the OEM model. However, the steer angles at the wheels were very similar, so no particular difference exists between the models T4 and T5.

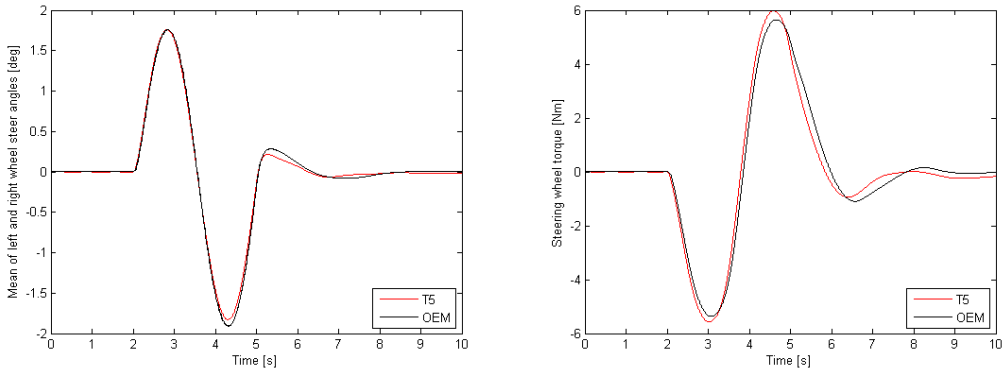

Figure 10.15 Mean value of wheel steer angles and steering wheel torque, T5 vs. OEM.

The trajectory of the tractor CG (Figure 10.16) is very close between the Modelica model and the OEM model, with a difference in the final heading direction due to the fifth wheel friction torque (as said in Section 10.1.1.1). Also the yaw rates are really close (Figure 10.17), with a difference in the last oscillations of the last two units due to the nonlinearity of tyres. Moreover, the articulation angles show a difference consistently with the yaw rates (Figure 10.18).

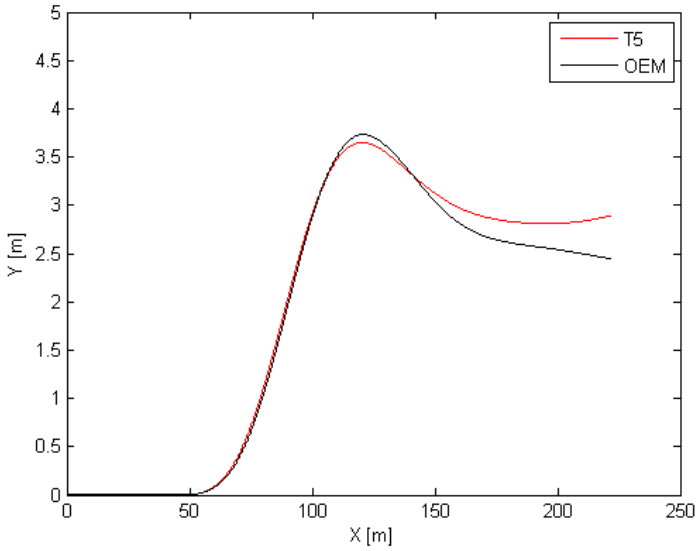

Figure 10.16 Trajectory of tractor CG, T5 vs. OEM.

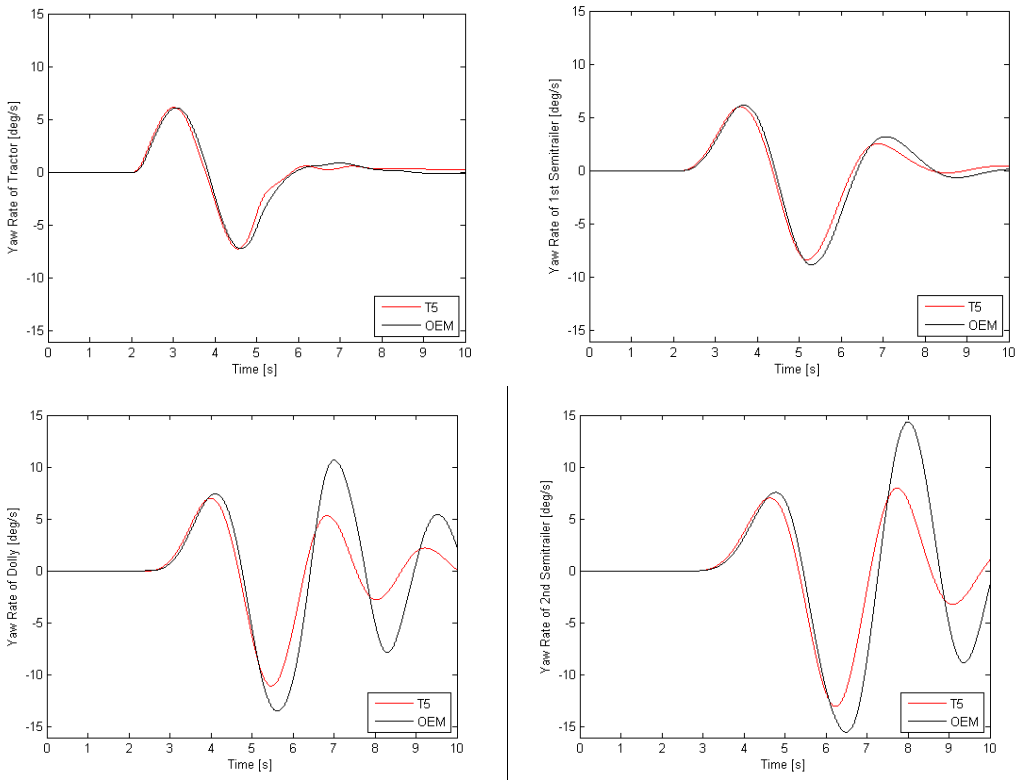

Figure 10.17 Yaw rates of the four units, T5 vs. OEM.

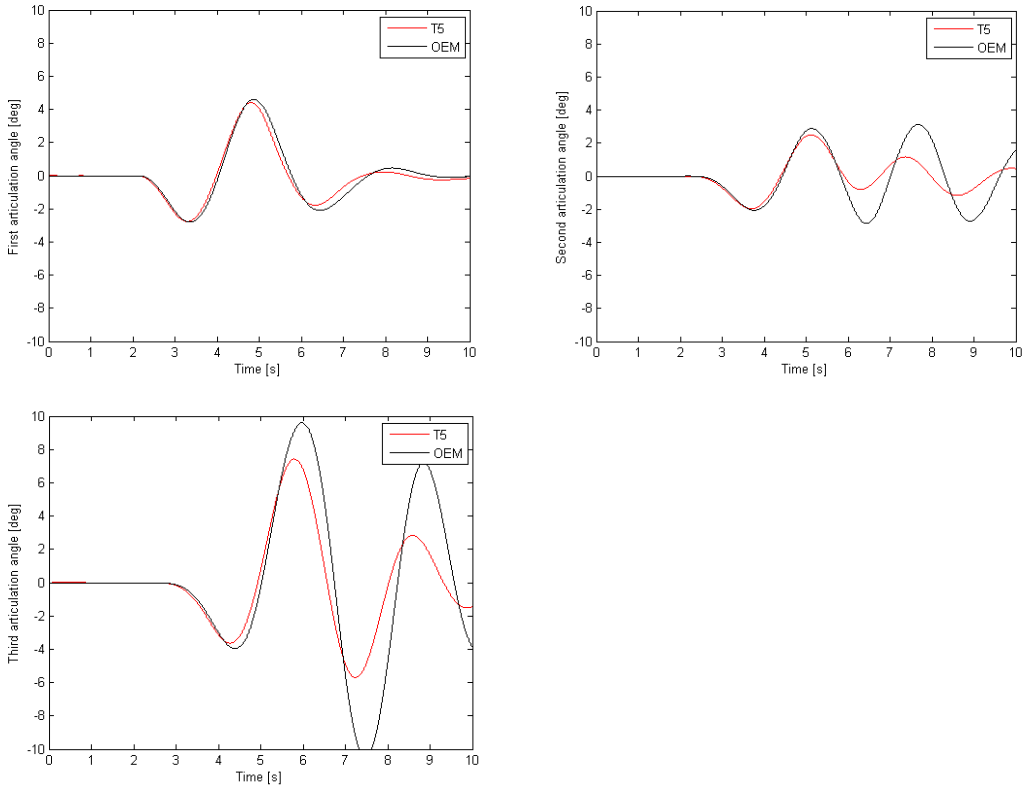

Figure 10.18 Articulation angles, T5 vs. OEM.

The roll angles of the units and the tractor frame torsion angle are very similar. It should be remembered that the fifth wheel couplings impose that the two connected units are constrained to have the same roll angle (in the towing unit reference frame). Therefore, having relatively small values of articulation angles, we can say that the roll angle of the first semitrailer is almost equal to the roll angle of the rear part of the tractor and it is therefore not shown. The same holds for the roll angles of the second semitrailer and the dolly. The roll angle of these two units displays a greater peak in the OEM model, for the same reason as for the yaw rates and articulation angles (the nonlinearity of their tyres).
The similarity of the roll angles is transmitted also to the cabin roll angle and lateral acceleration.

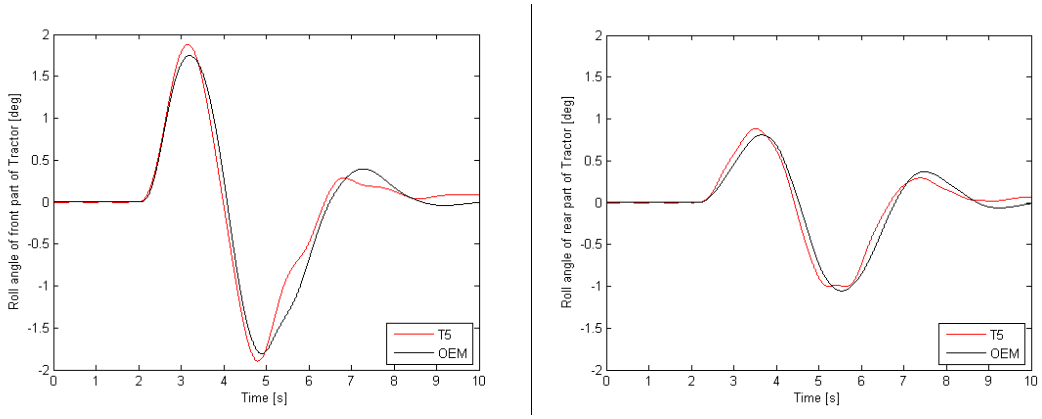

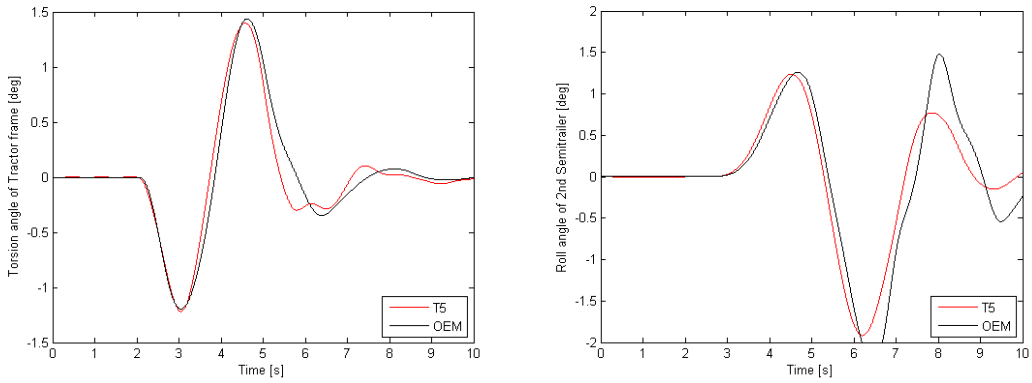

Figure 10.19 Roll angles of the front and rear part of the tractor, frame torsion and roll angle of the second semitrailer, T5 vs. OEM.

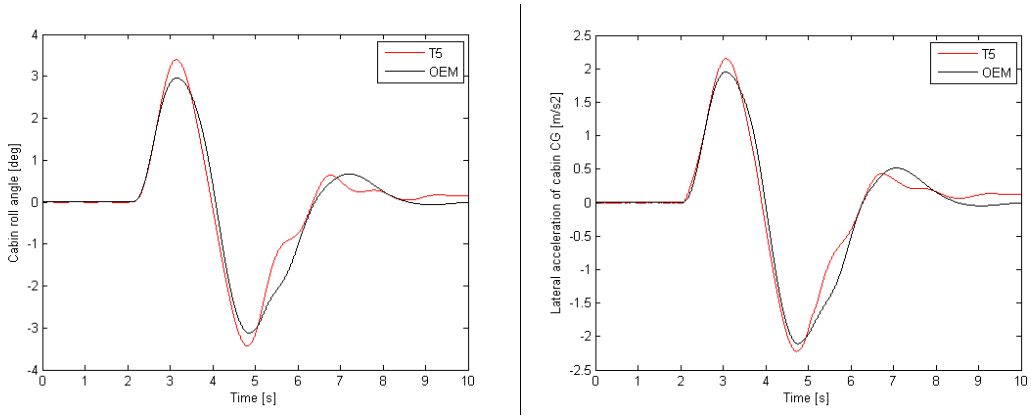

Figure 10.20 Cabin roll angle and lateral acceleration, T5 vs. OEM.

10.1.8 Model with powertrain and braking systems (T6)

When a powertrain and a braking systems have been modelled, a full experiment could be performed, which consisted of: acceleration from standstill to approximately 80 km/h, lane change and braking to standstill. This was mainly done to provide a reasonable longitudinal behaviour, therefore only a brief analysis is presented here. The inputs of the accelerator and brake pedals are shown in Figure 10.21, with the consequent longitudinal speed of the two models in Figure 10.22.

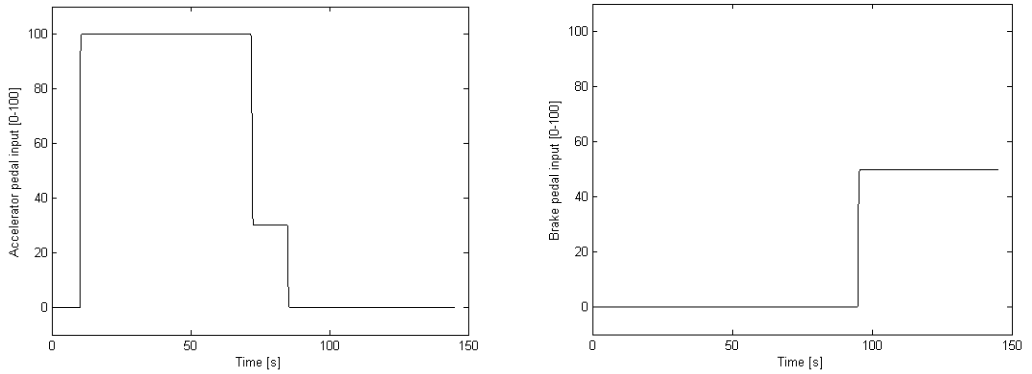

Figure 10.21 Accelerator and brake pedal inputs.

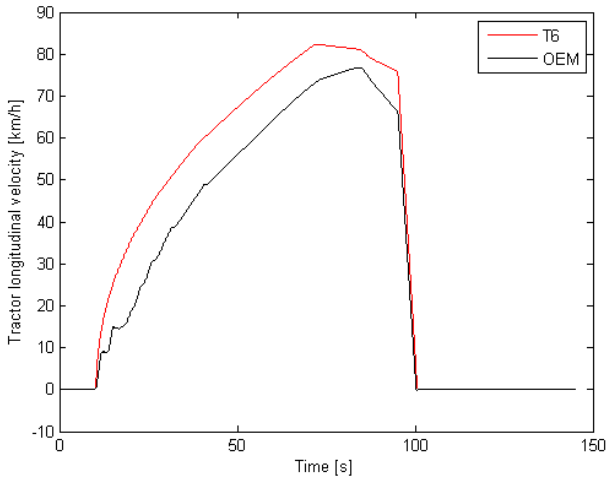

Figure 10.22 Tractor longitudinal speed, T6 vs. OEM.

The pitch angle of the tractor of the model T6 approximately follows the shape of the OEM model, with smoother variations during acceleration (because of smoother gear shifts), except for the first peak (as in T6 the longitudinal force generation is instantaneous). The reason for a different static pitch angle was not investigated.

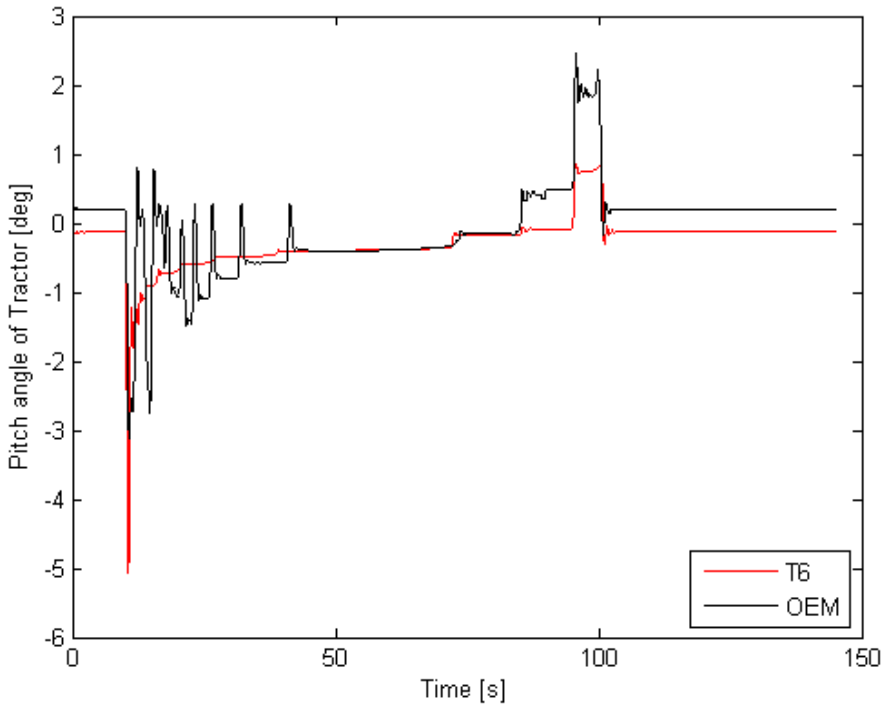

Figure 10.23 Pitch angle of tractor, T6 vs. OEM.

A similar behaviour is shown in the cabin longitudinal and vertical acceleration and pitch angle.

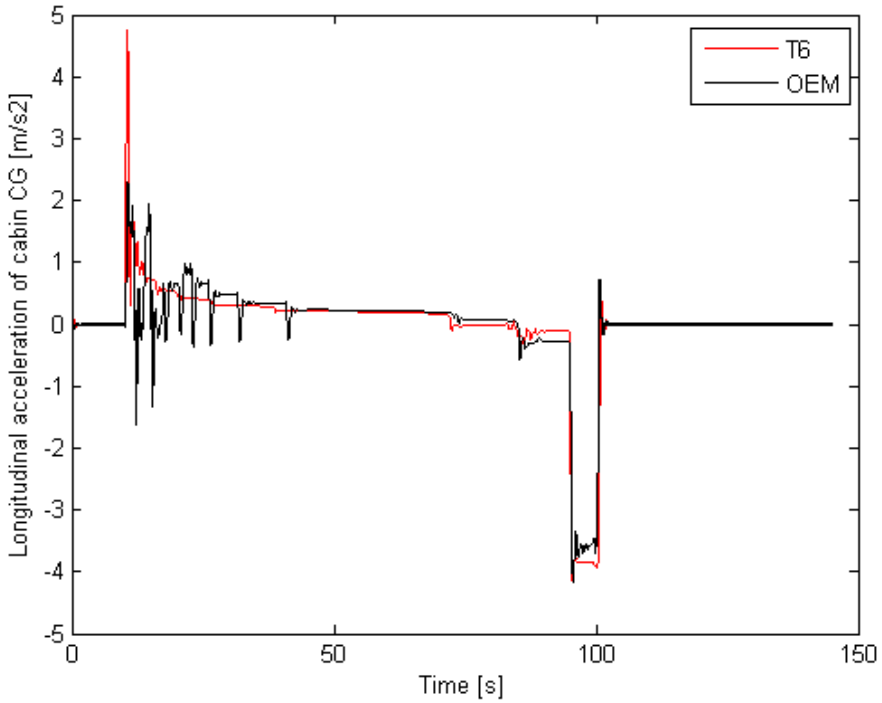

Figure 10.24 Longitudinal acceleration of cabin CG, T6 vs. OEM.

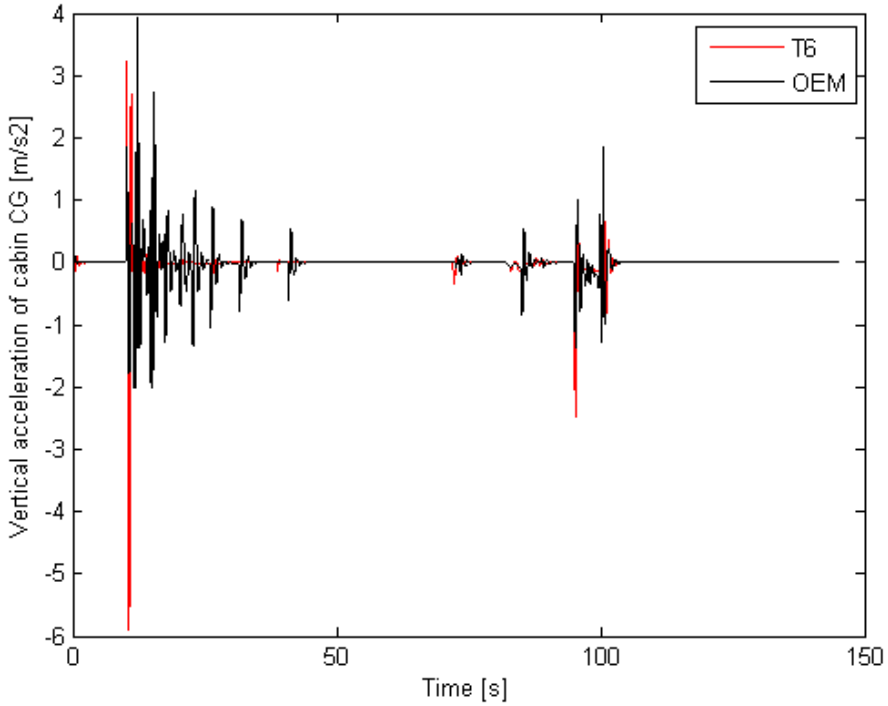

Figure 10.25 Vertical acceleration of cabin CG, T6 vs. OEM.

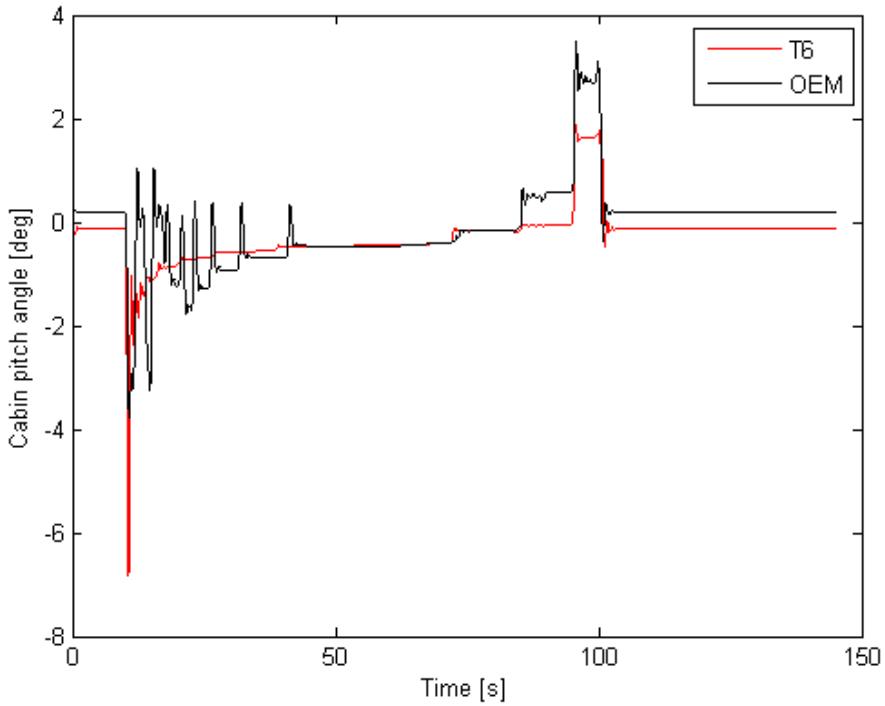

Figure 10.26 Cabin pitch angle, T6 vs. OEM.

10.2 Simulator experiments

The first experiments on the driving simulator Sim IV had the purpose of proving the functioning of the developed VDM, with no problem for real-time simulation and with a reasonable behaviour. Afterwards, an experiment with some test drivers was organised and performed.

One fundamental element of the performed experiments should be mentioned regarding the test drivers. Driving a truck is a different experience from driving a car for many reasons: different dimensions, presence of a cabin suspended on the chassis, different steering system, presence of trailers (at least in this case), etc. Therefore, the requirement of holding a truck driving license was asked to the test drivers, so that they had an experience on a real road to compare with the simulator experience. This resulted in a limited number of drivers that could be found on short notice. Five drivers participated to the experiment, of which only two of them have a driving license for truck combinations and only one had driven an A-double (on a test track).

One consideration needs to be done when performing driving simulator experiments. The VDM and the motion cueing algorithm interact in the way explained in Section 1.7. However, this interaction cannot be seen by the driver, who only perceives its result. In other words, even if the VDM perfectly calculates the motion of the vehicle, but the motion cueing algorithm is unable to reproduce the motion correctly, the driver would just report that the experience was not realistic and one may think that the problem lies in the VDM. There might has been a problem with the motion cueing algorithm that potentially can affect the outcome of this experiment.

The test consisted of driving the developed truck model and the OEM model to subjectively evaluate the behaviour compared to reality and between themselves. Each volunteer drove both models, without knowing the order. The order was chosen

to balance possible learning and order effects. In fact, a driver may drive the two models in two different ways and after the first experiment he may have "learned" something and taken more confidence with the simulator and the vehicle.
After each test, the volunteers were asked to fill in a questionnaire. Given the low number of drivers participating to the experiment, a statistical analysis of the results would not be meaningful. For this reason, they were also asked to give comments to give some details of their perception. The instructions and questionnaire given to the volunteers can be found in the Appendix 14.2.
The experiment focused on the lateral and vertical dynamics rather than longitudinal. The road consisted of the following sections. The first section was straight and without any inclination. Here the drivers were requested to perform several single lane changes at two different speeds, i.e. 50 and 80 km/h. After that, the road was still straight but included the following: road banking in both directions, road slope (uphill and downhill) and at last several road holes. Here the drivers were just asked to drive straight, without exceeding 20 km/h on the road holes. The reason is that, as some holes were particularly harsh, wheel lift may occur and safety features of the simulator would stop the simualtion if wheel lift is close.
The drivers were asked to give ratings (from 1 to 7) and comments on five aspects:

- the behavior of the vehicle during lane changes
- the behavior of the vehicle during road banking, road slope and road holes
- the effect of the trailers on the vehicle motion and on the steering wheel
- the overall steering wheel feeling
- the overall motion

Before presenting the results, additional considerations for their analysis should be done. At first, the OEM model that was used in the experiment was not exactly the same towards which the developed Modelica model was tuned. However, it was not investigated which parameters had different values. The second regards the consideration already done previously. When the last volunteer drove the models, he noticed a highly unrealistic lateral behaviour of the vehicle, as it was "*over-reacting in quick steering motions, even of small amplitudes*". Something similar was reported by other two drivers, but only for the Modelica model: "*Unrealistic jerks when small steering wheel angle pulses",* "*Cab roll 'tics' feel sharp*". After investigation of the problem, a bug was found in the motion cueing algorithm. The last volunteer had the opportunity to try again the models and he reported that the problem had disappeared for both of them and he decided to modify his ratings. This fact should be taken into account in the analysis of results.
The average ratings of the two models are shown in Figure 10.27, even though it should be kept in mind that the available data consisted of 5 samples only. The standard deviations are also shown in the figure.
An analysis of the results was performed with the purpose of getting an idea of the main differences of the two models and what should be improved to make it more realistic. However, because of the low number of test drivers it seems difficult to shape a clear idea. Moreover, the average ratings of the two models are very similar, making this even more difficult. In particular, one driver said "*I think the models were behaving very similar to each other. Can't feel any difference*". The opinions of the other drivers were that both models have a quite realistic behaviour, even though the OEM model was generally regarded slightly better.

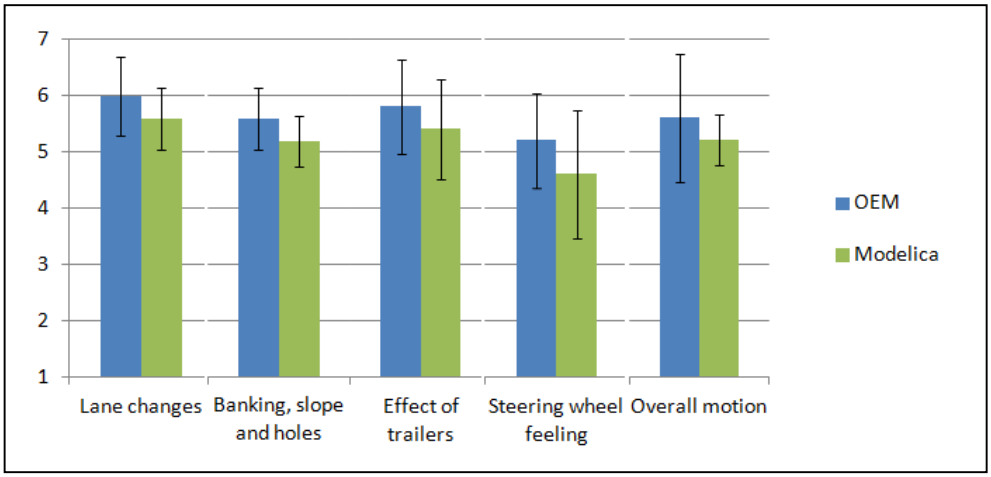

Figure 10.27 Average ratings of the two models with standard deviations.

It is worth to mention the comments about the behaviour during lane changes, which highlight some differences. Nevertheless, the quotes from three drivers seem to be contradictory. As an example, a comment about the Modelica model was "*it felt a bit exaggerated with the inertia of the trailers*" from one test driver, while "*jerks from trailers felt very clear*" and "*I felt more for less steering input and the vehicle oscillated for longer afterwards*" were stated from other drivers of the OEM model.
Some additional comments were reported about the unrealistic behaviour of the powertrain system of both models.

10.3 Discussion of results

The comparison of the gradual steps of the Modelica model showed how the increase of model complexity is reflected in the ability to mimic the OEM model. The largest source of discrepancy in the first model (ST) was the un-modeled roll steer contribution. When this contribution was added, the resulting output got much closer to the OEM model. The frame torsion was a fundamental element in this view. The cabin resulted in small differences, even if not negligible. Finally, the axle dynamics had a considerable effect, especially for the absolute values of the roll angles.
The final results from the desktop simulations show a good match with the OEM model and this confirms how the chosen modelling process was successful.
Specifically, the friction model for the fifth wheel coupling seems to be a good approximation, except for the steady-state value. Moreover, it seems to have relevance for damping down the trailers oscillations, especially for maneuvers close to the loss of lateral stability.
One relevant outcome is that the nonlinearity of tyres that is reached in the last two units of the vehicle does not considerably affect the motion of the first two units and therefore may not be necessary in the selected driving context for the final application of the model of a driving simulator. However, it may be argued that the graphic system of a driving simulator may allow the driver to notice the motion of the trailers on the side-view mirrors and larger trailer oscillations may affect the driver perception of the vehicle lateral stability.
In relation to what just said, the consideration about the values of the yaw inertias of the semitrailers must be remembered, as more realistic values would change the situation.

Also the results from the simulator experiment are overall positive. The developed model was considered slightly less realistic than the OEM model, but the difference is within the range of the uncertainty. The low number of test subjects and the problem detected in the motion cueing algorithm would suggest that more tests are necessary to obtain a more refined assessment.

11 Conclusions

This Chapter draws the conclusions of the thesis project:

- A truck dynamics model was created in the Modelica programming language.
- It is an open model and its structure gives a high level of readability and flexibility.
- The model was successfully implemented in the driving simulator Sim IV and run in real-time with a great execution time margin.
- The model was compared to the reference OEM model and it proved to represent adequately the modelled vehicle in the selected driving context. Moreover, the presented modelling process allowed obtaining a good approximation, while keeping the model complexity to a minimum.
- The model is a solid base for future developments of a library of truck dynamics models.
- The model will be used by VTI´s researchers and will be distributed as an open model, as it may be used both in other driving simulators and in desktop simulations.

12 Future work

The author gives the following suggestions for future developments:

- The Modelica model can be extended to represents more vehicle combinations.
- Investigate the influence of a more detailed friction model for the fifth wheel coupling.
- Create a more detailed tyre model, that can represent the nonlinear behaviour both longitudinally and laterally. This may be the first step to extend the previously selected driving context.
- Add the tyre-road friction coefficient as input to the model, possibly with one input for each wheel.
- Model a more detailed powertrain and braking systems in order to allow studying the vehicle longitudinal dynamics.
- Some functions may be added, as ABS, ESC and Cruise Control.

13 References

Jansson J., Sandin J., Augusto B., and Fischer M. (2014) , *Design and performance of the VTI Sim IV*, Driving simulation conference, Paris, France.

Fischer M., Sehammar H. and Palmkvist G. (2011), *Applied Motion Cueing Strategies for Three Different Types of Motion Systems*, ASME. J. Comput. Inf. Sci. Eng.

Nilsson P. (2015), *On traffic situation predictions for automated driving of long vehicle combinations*, Licentiate thesis, Chalmers University of Technology.

Aurell J. and Wadman T., *Vehicle combinations based on the modular concept. Background and analysis*, Volvo Trucks, Report no. 1/2007, Committee 54: Vehicles and Transports.

ISO (2002), *Road vehicles – Heavy commercial vehicle combinations and articulated buses – Lateral stability test methods*, Swedish Standard Institute SS-ISO 14791.

Modelica Association (2012), *Modelica Language Specification, Version 3.3*, May 2012, Available at https://www.modelica.org/documents/ModelicaSpec33.pdf.

Dynasim (2009): *Dymola Multi-Engineering Modeling Laboratory. User Manual*, Vol I & II, Dynasim AB, Lund, Sweden.

Fritzson P., Aronsson P., Lundvall H., Nyström K., Pop A., Saldamli L. and Broman D. (2005), *The OpenModelica Modeling, Simulation, and Software Development Environment*, Simulation News Europe, 44(45), December 2005.

Sundström P., Jacobson B.and Laine L. (2014), *Vectorized single-track model in Modelica for articulated vehicles with arbitrary number of units and axles*, Proceedings of the 10th International ModelicaConference, pp. 265-271.

Ellis J.R. (1994), *Vehicle handling dynamics*.

Balkwill J. (2014), *Advanced Chassis Engineering - P04731 – Student Handbook*, Version 8, Oxford Brookes University, Oxford, UK.

Jacobson B. (2012), *Vehicle Dynamics – Compendium for Course MMF062*, Chalmers University of Technology, Göteborg, Sweden.

Genta G. and Morello L. (2009), *The Automotive chassis*, Vol 1 & 2, Springer.

Morello L., Rossini L. R., Pia G., Tonoli A. (2001), *The Automotive Body*, Vol II, Springer.

Tagesson K. (2014), *Truck steering system and driver interaction*, Thesis for the degree of licentiate of engineering, Chalmers University of Technology, Göteborg, Sweden.

Rothhämel M. (2013), *Characterisation and utilisation of steering feel in heavy trucks*, Doctoral thesis in Vehicle Engineering, Royal Institute of Technology, Stockholm, Sweden.

Gómez Fernández J. (2012), *A vehicle dynamics model for driving simulators*, Master's thesis, Chalmers University of Technology, Göteborg, Sweden.

Obialero E. (2013), *A refined vehicle dynamic model for driving simulators*, Master's thesis, Chalmers University of Technology, Göteborg, Sweden.

Bruzelius F., Gómez Fernández J., Augusto B. (2013), *A Basic Vehicle Dynamics Model for Driving Simulators*, International Journal of Vehicle Systems Modelling and Testing, Vol. 8, No. 4, pp 364–385.

Luijten M.F.J. (2010), *Lateral dynamic behaviour of articulated commercial vehicles*, Master's thesis, Eindhoven University of Technology, Eindhoven, Netherlands.

Stoerkle J. (2013), *Lateral dynamics of multiaxle vehicles*, Master thesis, Institute for Dynamic Systems and Control, Swiss Federal Institute of Technology, Zürich, Switzerland.

14 Appendices

14.1 Rotation matrices

The orientation of the body-fixed reference frame of a rigid body with respect to the global reference frame (an inertial reference frame with the earth) is defined by its roll, pitch and yaw angles. When two rigid bodies with their respective body-fixed reference frames are considered, the orientation of one reference frame with respect to the other is defined by the relative roll, pitch and yaw angles between them. However, these relative angles needs to be defined in one of the two reference frames, as for example the roll angle of one body may be not about the same global axis as the roll angle of the other body. Therefore, the angles of the second body need to be rotated in the reference frame of the first body and then their difference will give the relative angles (defined in the reference frame of the first body).
The rotation matrix from one reference frame to the other depends both on the order of rotation and on the definition of the rotation angles, i.e. if they are about an axis in the global reference frame or in the body reference frame. The Equation (14.1) shows the case of the order of rotation about z, then about y and finally about x, with all of the axes of the global reference frame (the pre-multiplication is used).

$$\mathbf{R} = \mathbf{R_x}(\theta_r) \cdot \mathbf{R_y}(\varphi_r) \cdot \mathbf{R_z}(\psi_r) \tag{14.1}$$

The matrices for the rotations by θ_r around the x-axis, φ_r around the y-axis, and ψ_r around the z-axis are shown in Equations (14.2).

$$\begin{aligned} \mathbf{R_x}(\theta_r) &= \begin{bmatrix} 1 & 0 & 0 \\ 0 & \cos\theta_r & -\sin\theta_r \\ 0 & \sin\theta_r & \cos\theta_r \end{bmatrix} \\ \mathbf{R_y}(\varphi_r) &= \begin{bmatrix} \cos\varphi_r & 0 & \sin\varphi_r \\ 0 & 1 & 0 \\ -\sin\varphi_r & 0 & \cos\varphi_r \end{bmatrix} \\ \mathbf{R_z}(\psi_r) &= \begin{bmatrix} \cos\psi_r & -\sin\psi_r & 0 \\ \sin\psi_r & \cos\psi_r & 0 \\ 0 & 0 & 1 \end{bmatrix} \end{aligned} \tag{14.2}$$

Having these definitions, the relative angles can be computed from the roll, pitch and yaw angles of the two bodies with the Equation (14.3), which implies that the angles θ_r, φ_r and ψ_r are defined in the reference frame 1.

$$^1\begin{pmatrix} \theta_1 \\ \varphi_1 \\ \psi_1 \end{pmatrix} + \begin{pmatrix} \theta_r \\ \varphi_r \\ \psi_r \end{pmatrix} = \mathbf{R} \cdot \, ^2\begin{pmatrix} \theta_2 \\ \varphi_2 \\ \psi_2 \end{pmatrix} \tag{14.3}$$

In accordance to the previous definitions, the relation between a vector v_1 in the reference frame 1 and a vector v_2 in the reference frame 2 will be through the rotation matrix as shown in Equation (14.4).

$$v_1 = \mathbf{R} \cdot v_2 \tag{14.4}$$

14.2 Questionnaire for the driving simulator experiment

SIMULATOR DRIVING EXPERIMENT

Experiment to evaluate a truck dynamics model for a driving simulator

ABOUT THE TEST

The test will consist of driving a truck model in the VTI driving simulator Sim IV in order to give a subjective evaluation of how it behaves compared to reality.

Two different models of the same truck will be compared. You will drive one after the other, without being told in which order.

After each test, you will be asked to fill in a questionnaire to give your evaluation of the model. You are suggested to read the questions before the test. The questions that require a rating also have some space for comments so that you can give some details of what was your perception.

Bear in mind that the focus of the experiment is on the lateral and vertical dynamics rather than longitudinal.

INSTRUCTIONS

You will be driving an A-double combination, therefore additional care must be given. You will be able to check the motion of the trailers on the side-view mirrors. Please keep a safety margin from possible vehicle rollover. The simulation will stop if wheel lift is close.

The first road section is straight and without any inclination. You are requested to perform several single lane changes at two different speeds, i.e. 50 and 80 km/h. You should try the maneuver applying a slow steering input first and then you can repeat it faster.

After the first section, the road is still straight but includes the following: road banking in both directions, road slope (uphill and downhill) and at last several holes. The maximum allowed speed for driving on the bumps is 20 km/h.

You do not need to remember this sequence of instructions, as you will be informed of what you need to do while driving.

Questionnaire

PERSONAL INFORMATION

Name (optional):

Gender	□ Male □ Female
How many times did you use a simulator before?	□ Never □ 1-3 □ More than 3
How many times did you drive a truck on a simulator before?	□ Never □ 1-3 □ More than 3
Do you have a truck driving license?	□ Yes □ No
If yes, which one(s)?	□ C1 □ C1E □ C □ CE
How often in average do you drive a truck?	□ Rarely □ Monthly □ Weekly □ Daily

MODELS COMPARISON

1) Model 1

1	How realistic would you rate the behavior of the vehicle during lane changes?						
	1 (very poor) □	2 □	3 □	4 □	5 □	6 □	7 (very good) □
	Comments: _____ _____ _____						
2	How realistic would you rate the behavior of the vehicle during road banking, road slope and road bumps?						
	1 (very poor) □	2 □	3 □	4 □	5 □	6 □	7 (very good) □
	Comments: _____ _____ _____						

3	How realistic would you rate the effect of the trailers on the vehicle motion and on the steering wheel?						
	1 (very poor) ☐	2 ☐	3 ☐	4 ☐	5 ☐	6 ☐	7 (very good) ☐
	Comments: _____ _____ _____						
4	How would you rate the overall steering wheel feeling?						
	1 (very poor) ☐	2 ☐	3 ☐	4 ☐	5 ☐	6 ☐	7 (very good) ☐
	Comments: _____ _____ _____						
5	How realistic would you rate the overall motion?						
	1 (very poor) ☐	2 ☐	3 ☐	4 ☐	5 ☐	6 ☐	7 (very good) ☐
	Comments: _____ _____ _____						

Do you have other comments on the model? What should be improved, in your opinion?

_____
_____
_____
_____
_____
_____
_____

Additional comments:

_____
_____
_____
_____

2) Model 2

1	How realistic would you rate the behavior of the vehicle during lane changes?						
	1 (very poor) ☐	2 ☐	3 ☐	4 ☐	5 ☐	6 ☐	7 (very good) ☐
	Comments: _____ _____ _____						
2	How realistic would you rate the behavior of the vehicle during road banking, road slope and road bumps?						
	1 (very poor) ☐	2 ☐	3 ☐	4 ☐	5 ☐	6 ☐	7 (very good) ☐
	Comments: _____ _____ _____						
3	How realistic would you rate the effect of the trailers on the vehicle motion and on the steering wheel?						
	1 (very poor) ☐	2 ☐	3 ☐	4 ☐	5 ☐	6 ☐	7 (very good) ☐
	Comments: _____ _____ _____						
4	How would you rate the overall steering wheel feeling?						
	1 (very poor) ☐	2 ☐	3 ☐	4 ☐	5 ☐	6 ☐	7 (very good) ☐
	Comments: _____ _____ _____						
5	How realistic would you rate the overall motion?						
	1 (very poor) ☐	2 ☐	3 ☐	4 ☐	5 ☐	6 ☐	7 (very good) ☐
	Comments: _____ _____ _____						

Do you have other comments on the model? What should be improved, in your opinion?

_____
_____
_____
_____
_____
_____
_____

Additional comments:

_____
_____
_____
_____